

# **Dynamics of DNA Methylation in Differentiating Hematopoietic Cells**

Dissertation zur Erlangung des Doktorgrades  
der Naturwissenschaften (Dr. rer. nat.) der Naturwissenschaftlichen  
Fakultät III - Biologie und vorklinische Medizin der Universität  
Regensburg



vorgelegt von  
Maja Klug aus Steinau  
Juli 2009

The work presented in this thesis was carried out in the Department of Hematology and Oncology at the University Hospital Regensburg from June 2005 to July 2009.

Die vorliegende Arbeit entstand in der Zeit von Juni 2005 bis Juli 2009 in der Abteilung für Hämatologie und internistische Onkologie des Klinikums der Universität Regensburg.

.

Promotionsgesuch eingereicht am: 20. Juli 2009

Die Arbeit wurde angeleitet von: PD Dr. Michael Rehli, Prof. Dr. Herbert Tschochner.

Prüfungsausschuss:

- |                             |                              |
|-----------------------------|------------------------------|
| Vorsitzender:               | Prof. Dr. Armin Kurtz        |
| 1. Prüfer (Erstgutachten):  | Prof. Dr. Herbert Tschochner |
| 2. Prüfer (Zweitgutachten): | PD. Dr. Michael Rehli        |
| 3. Prüfer:                  | Prof. Dr. Ernst Tamm         |

Ever tried, ever failed, no matter,  
Try again, fail again, fail better.

*Samuel Beckett*

# Table of Contents

<b>1</b>	<b>INTRODUCTION</b>	<b>- 1 -</b>
<b>1.1</b>	<b>Epigenetics</b>	<b>- 1 -</b>
1.1.1	Molecular Building Blocks of Epigenetics	- 1 -
1.1.1.1	Histone Modifications	- 1 -
1.1.1.2	DNA Methylation	- 7 -
1.1.1.3	Non-Coding RNA	- 11 -
<b>1.2</b>	<b>Epigenetics in Hematopoiesis</b>	<b>- 12 -</b>
1.2.1	Hematopoiesis	- 12 -
1.2.2	The Mononuclear Phagocyte System	- 13 -
1.2.2.1	Macrophages in the Immune Response	- 13 -
1.2.2.2	Dendritic Cells in the Immune Response	- 14 -
1.2.3	The Lymphoid Lineage	- 15 -
1.2.4	Role of Epigenetic Modifications for Lineage Commitment	- 15 -
<b>2</b>	<b>RESEARCH OBJECTIVES</b>	<b>- 17 -</b>
<b>3</b>	<b>MATERIAL AND EQUIPMENT</b>	<b>- 18 -</b>
<b>3.1</b>	<b>Equipment</b>	<b>- 18 -</b>
<b>3.2</b>	<b>Consumables</b>	<b>- 19 -</b>
<b>3.3</b>	<b>Chemicals</b>	<b>- 20 -</b>
<b>3.4</b>	<b>Enzymes and Kits</b>	<b>- 20 -</b>
<b>3.5</b>	<b>Oligonucleotides</b>	<b>- 21 -</b>
3.5.1	cDNA Primer	- 21 -
3.5.2	ChIP/MCIP Primer	- 22 -
3.5.3	Primer for <i>in vivo</i> Footprinting	- 22 -
3.5.4	Primer for Cloning Experiments	- 23 -
3.5.5	Bisulfite Amplicon Generation (Nested PCR)	- 23 -
3.5.6	Bisulfite Amplicon Generation (MassARRAY)	- 23 -
<b>3.6</b>	<b>Antibiotics</b>	<b>- 25 -</b>
<b>3.7</b>	<b>Plasmids</b>	<b>- 25 -</b>

<b>3.8</b>	<b>E.coli Strains</b> .....	<b>- 26 -</b>
<b>3.9</b>	<b>Antibodies</b> .....	<b>- 26 -</b>
<b>3.10</b>	<b>Cell Lines</b> .....	<b>- 27 -</b>
<b>3.11</b>	<b>Databases and Software</b> .....	<b>- 27 -</b>
<b>4</b>	<b>METHODS</b> .....	<b>- 28 -</b>
<b>4.1</b>	<b>General Cell Culture Methods</b> .....	<b>- 28 -</b>
4.1.1	Cell Line Culture .....	- 28 -
4.1.1.1	Culture Conditions and Passaging .....	- 28 -
4.1.1.2	Culturing of Stably Transfected Drosophila S2 Cells and Production of MBD-Fc.....	- 29 -
4.1.1.3	Assessing Cell Number and Vitality .....	- 30 -
4.1.1.4	Freezing and Thawing Cells .....	- 30 -
4.1.1.5	Mycoplasma Assay.....	- 30 -
4.1.2	Transient Transfection of Mammalian Cells .....	- 31 -
4.1.2.1	Lipofectamine Transfection .....	- 31 -
4.1.2.2	Transfection Using DEAE Dextran .....	- 31 -
4.1.2.3	Measuring Luciferase Activity.....	- 32 -
4.1.3	Primary Cells .....	- 32 -
4.1.3.1	Isolation of Monocytes.....	- 32 -
4.1.3.2	Cultivation of Monocytes .....	- 33 -
<b>4.2</b>	<b>General Molecular Biology</b> .....	<b>- 34 -</b>
4.2.1	Bacterial Culture .....	- 34 -
4.2.1.1	Bacterial Growth Medium .....	- 34 -
4.2.1.2	Transformation of Chemically Competent <i>E.coli</i> .....	- 34 -
4.2.1.3	Glycerol Stock .....	- 35 -
4.2.2	Plasmid Isolation from <i>E.coli</i> .....	- 35 -
4.2.3	Molecular Cloning.....	- 35 -
4.2.3.1	Construction of the pCpGL-basic Vector.....	- 35 -
4.2.3.2	Cloning of Reporter Vectors .....	- 36 -
4.2.4	<i>In Vitro</i> Methylation of Plasmid DNA .....	- 37 -
4.2.5	Preparation and Analysis of DNA.....	- 37 -
4.2.5.1	Isolation and Quality Control of Genomic DNA .....	- 37 -
4.2.5.2	Precipitation of DNA Using PEG (Polyethylene Glycol).....	- 37 -
4.2.5.3	Purification of DNA with Phenol Chloroform Extraction .....	- 38 -
4.2.5.4	Agarose Gel Electrophoresis.....	- 38 -
4.2.5.5	Restriction Endonuclease Digestion.....	- 39 -

4.2.5.6	Dephosphorylation of DNA with Alkaline Phosphatase.....	- 39 -
4.2.5.7	Fill in 5'-Overhangs with Klenow-DNA-Polymerase .....	- 39 -
4.2.5.8	Generation of Blunt Ends with T4 DNA Polymerase .....	- 40 -
4.2.5.9	Purification of DNA Fragments by Gel Extraction .....	- 40 -
4.2.5.10	Polymerase Chain Reaction (PCR).....	- 40 -
4.2.5.11	Bisulfite Sequencing.....	- 42 -
4.2.5.12	DNA Sequencing and Sequence Analysis .....	- 43 -
4.2.5.13	Methyl-CpG-Immunoprecipitation (MCIp).....	- 43 -
4.2.5.14	DNA Microarray Handling and Analysis .....	- 44 -
4.2.5.15	Quantitative DNA Methylation Analysis Using the MassARRAY System .....	- 44 -
4.2.6	Preparation and Analysis of RNA.....	- 46 -
4.2.6.1	Isolation of Total RNA.....	- 46 -
4.2.6.2	Formaldehyde Agarose Gel .....	- 46 -
4.2.6.3	Reverse Transcription PCR (RT-PCR).....	- 47 -
4.2.6.4	Whole Genome Expression Analysis .....	- 47 -
4.2.7	<i>In Vivo</i> Genomic Footprinting with DMS.....	- 48 -
4.2.8	Chromatin Immunoprecipitation (ChIP).....	- 49 -
<b>4.3</b>	<b>General Protein Biochemical Methods.....</b>	<b>- 51 -</b>
4.3.1	Purification of the Recombinant Protein MBD-Fc.....	- 51 -
4.3.1.1	Dialysis .....	- 51 -
4.3.1.2	Affinity Chromatography .....	- 51 -
4.3.1.3	Conservation of the Purified MBD-Fc.....	- 52 -
4.3.1.4	Quantification and Quality Control of MBD-Fc .....	- 52 -
4.3.2	Discontinuous SDS-PAGE .....	- 52 -
4.3.3	Western Blot Analysis and Immunostaining.....	- 53 -
4.3.4	Coomassie Staining of SDS-Gels .....	- 54 -
<b>4.4</b>	<b>Proliferation Assay (Thymidine Incorporation).....</b>	<b>- 55 -</b>
<b>4.5</b>	<b>Flow Cytometry.....</b>	<b>- 55 -</b>
<b>5</b>	<b>RESULTS .....</b>	<b>- 56 -</b>
<b>5.1</b>	<b>Creating a Tool to Analyse the Effects of CpG Methylation within Gene Promoters... - 56 -</b>	
5.1.1	Effects of CpG Methylation in Vector Backbones on Reporter Activities.....	- 56 -
5.1.2	Construction and Application of the Novel CpG-free Luciferase Reporter pCpGL .....	- 58 -
<b>5.2</b>	<b>Active DNA Demethylation during the Differentiation of Monocytes .....</b>	<b>- 62 -</b>
5.2.1	The Cell Model .....	- 62 -
5.2.2	Molecular Characterization of an Actively Demethylated Promoter during Monocyte Differentiation .....	- 63 -

5.2.2.1	Correlation of mRNA Expression and DNA Demethylation Events .....	- 64 -
5.2.2.2	Attempts to Interfere with the Active DNA Demethylation Process.....	- 65 -
5.2.3	Global mRNA Expression Analysis .....	- 68 -
5.2.3.1	Expression Profiles of Highly Regulated Genes Associated with Transcription .....	- 70 -
5.2.3.2	Identification of DNA Repair Associated Genes Significantly Regulated during Dendritic Cell Development .....	- 72 -
5.2.4	Genome-Wide Methylation Analysis of Dendritic Cells versus Monocytes and Macrophages .....	- 74 -
5.2.4.1	Global Screening for DMRs Using MC1p Combined to DNA Microarrays.....	- 74 -
5.2.4.2	Comparison of Microarray Data with MALDI-TOF MS (EpiTYPER) Data.....	- 76 -
5.2.4.3	Characterization of DNA Demethylation Events .....	- 78 -
5.2.5	Correlation between Active DNA Demethylation and mRNA Expression .....	- 82 -
5.2.6	Histone Modifications Surrounding DMRs .....	- 83 -
<b>5.3</b>	<b>Cell Type-Specific DNA Demethylation.....</b>	<b>- 87 -</b>
5.3.1	Identification of Cell Type-Specific Transcription Factors .....	- 87 -
5.3.2	Promoter Methylation Profiles of Cell Type-Specific Transcription Factors .....	- 89 -
<b>6</b>	<b>DISCUSSION &amp; PERSPECTIVES .....</b>	<b>- 93 -</b>
6.1	Transient Transfection as a Tool to Assess the Effect of DNA Methylation on Gene Expression .....	- 93 -
6.2	Dynamic Methylation Patterns of CpG-poor DNA Stretches as Important Regulators for Differentiation .....	- 94 -
6.3	Perspectives .....	- 104 -
<b>7</b>	<b>SUMMARY .....</b>	<b>- 105 -</b>
<b>8</b>	<b>REFERENCES .....</b>	<b>- 108 -</b>
<b>9</b>	<b>ABBREVIATIONS .....</b>	<b>- 120 -</b>
	<b>PUBLICATIONS .....</b>	<b>- 122 -</b>
	<b>EIDESSTÄTTLICHE ERKLÄRUNG .....</b>	<b>- 123 -</b>
	<b>ACKNOWLEDGEMENT .....</b>	<b>- 124 -</b>

# List of Figures

Figure 1-1 DNA packaging	- 2 -
Figure 1-2 Histone modifications	- 2 -
Figure 1-3 Reading the histone code	- 6 -
Figure 1-4 Methylation of CpG dinucleotides	- 7 -
Figure 1-5 Schematic presentation of transcriptional silencing by DNA methylation	- 8 -
Figure 1-6 DNA repair mechanisms during active DNA demethylation	- 10 -
Figure 1-7 Hierarchy of hematopoietic cells	- 12 -
Figure 4-1 Schematic outline of the EpiTYPER process	- 45 -
Figure 5-1 Effect of methylated backbone CpGs on promoter activity in transient transfection assays	- 57 -
Figure 5-2 Control experiment using the novel CpG-free reporter vector	- 58 -
Figure 5-3 Effect of promoter methylation in transient reporter assays using pCpGL	- 59 -
Figure 5-4 Comparative analysis of differential promoter methylation	- 60 -
Figure 5-5 Methylation control	- 61 -
Figure 5-6 Schematic presentation of the used cell model	- 62 -
Figure 5-7 Proliferation assay	- 63 -
Figure 5-8 Schematic presentation of changes at the <i>CCL13</i> promoter during differentiation	- 63 -
Figure 5-9 Characterization of the <i>CCL13</i> promoter region	- 64 -
Figure 5-10 Influence of adherence	- 67 -
Figure 5-11 Hierarchical clustering of all genes showing significant changes in expression during dendritic cell development	- 69 -
Figure 5-12 Hierarchical clustering of genes associated with transcriptional regulation	- 71 -
Figure 5-13 Hierarchical clustering of genes associated with DNA repair	- 72 -
Figure 5-14 mRNA expression profile of <i>GADD45</i> genes	- 73 -
Figure 5-15 Schematic outline of MCIp for comparative genome-wide methylation analysis	- 75 -
Figure 5-16 Representative scatter plots of CpG and mCpG pool hybridizations	- 76 -
Figure 5-17 Comparison of hybridization and EpiTYPER data	- 77 -
Figure 5-18 Kinetics of DNA demethylation events	- 78 -
Figure 5-19 Reproducibility of DNA demethylation events	- 79 -
Figure 5-20 mRNA expression profiles of genes related to DMRs	- 82 -
Figure 5-21 Correlation of histone modifications with CpG demethylation at promoter regions	- 84 -
Figure 5-22 Correlation of histone modifications with CpG demethylation at intragenic regions	- 85 -
Figure 5-23 Correlation of histone modifications with CpG demethylation at intergenic regions	- 86 -



<b>Figure 5-24 Transcription factor gene expression in human blood cell types</b>	<b>- 88 -</b>
<b>Figure 5-25 Examples of methylation profiles for lineage enriched transcription factor genes</b>	<b>- 90 -</b>
<b>Figure 6-1 Hypothetical model of successive events accompanying active DNA demethylation during differentiation of dendritic cells</b>	<b>- 103 -</b>

# List of Tables

<b>Table 1-1 Examples for histone modifying enzymes (writers and erasers) along with several sites they modify</b>	<b>- 5 -</b>
<b>Table 1-2 Examples for active DNA demethylation events in mammalian cell systems</b>	<b>- 11 -</b>
<b>Table 4-1 Culturing and passaging conditions</b>	<b>- 28 -</b>
<b>Table 4-2 Elutriation parameter and cell types</b>	<b>- 33 -</b>
<b>Table 4-3 Agarose concentration for different separation ranges</b>	<b>- 38 -</b>
<b>Table 4-4 Reaction parameter for analytical PCR</b>	<b>- 40 -</b>
<b>Table 4-5 Reaction parameter for real time PCR</b>	<b>- 41 -</b>
<b>Table 4-6 Reaction parameter for outer nested PCR</b>	<b>- 42 -</b>
<b>Table 4-7 Reaction parameter for inner nested PCR</b>	<b>- 42 -</b>
<b>Table 4-8 SDS-PAGE stock solutions</b>	<b>- 52 -</b>
<b>Table 4-9 SDS-PAGE gel mixture</b>	<b>- 52 -</b>
<b>Table 5-1 Number of background CpGs in conventionally used luciferase reporter vectors</b>	<b>- 57 -</b>
<b>Table 5-2 Number of CpGs in the pCpGL derivatives</b>	<b>- 59 -</b>
<b>Table 5-3 Substances used to interfere with DNA demethylation</b>	<b>- 66 -</b>
<b>Table 5-4 Description of detected DMRs; ordered as in Figure 5-20</b>	<b>- 80 -</b>
<b>Table 5-5 Methylation analysis of cell type-specific transcription factors</b>	<b>- 91 -</b>

# 1 Introduction

## 1.1 Epigenetics

The term “epigenetics” (literally: outside traditional genetics) was originally coined by Conrad Waddington who defined epigenetics as “the branch of biology, which studies the casual interactions between genes and their products, which bring the phenotype into being” (Waddington, 1942). In other words, this term stands for the mechanisms turning genotypes into phenotypes during development. About 50 years later, epigenetics was typically defined as the study of heritable changes in genome function that are not due to alterations in the DNA sequence (Probst et al., 2009; Riggs et al., 1996). This definition persists until today. The epigenetic code thus represents a second level of gene regulation on top of the genetic code. DNA methylation, histone modifications and noncoding RNAs are the most prominent actors of epigenetic phenomena. The classical view that certain epigenetic marks indicate either an “on” or an “off” state turned out to be too simple and functional integration of different marks emerged as critical factor for gene regulation (Berger, 2007; Weissmann and Lyko, 2003).

### 1.1.1 Molecular Building Blocks of Epigenetics

#### 1.1.1.1 Histone Modifications

Epigenetic activation or silencing is not mediated by one event alone, but is a series of complex processes that cause remodelling of the chromatin structure.

In eukaryotes, genomic DNA is packaged into chromatin. The nucleosome represents the fundamental unit of chromatin and is composed of an octamer of the four core histones (H2A, H2B, H3 and H4) around which 147 bp of DNA are wrapped (Kornberg, 1974; Kornberg and Lorch, 1999) (Figure 1-1). Linker histone H1 plays a significant role in the higher-order packaging of chromatin and is located outside the histone octamer at the 50 bp linker DNA. The positioning of nucleosomes is a reversible ATP-dependent process which contributes to the variable, dynamic, compact and yet stable chromatin architecture.

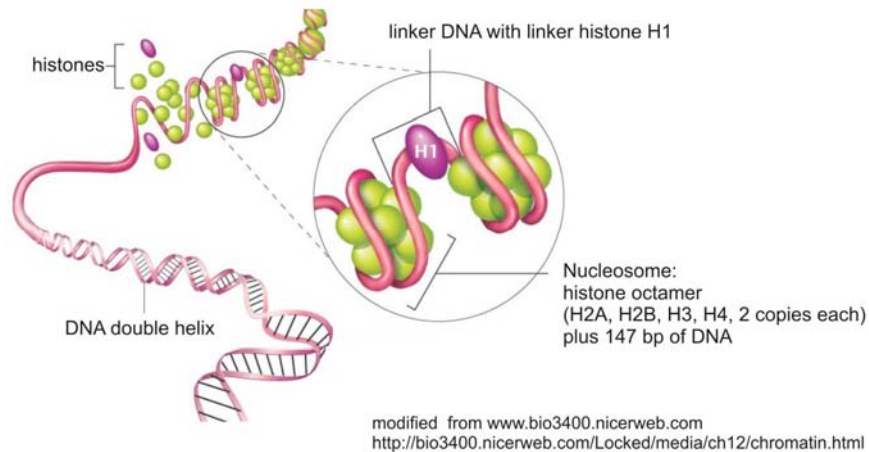


### Figure 1-1 DNA packaging

In eukaryotes, DNA is packed into a chromatin structure consisting of repeating nucleosome units. Nucleosomes comprise 147 base pairs (bp) of DNA that are wrapped around a histone octamer formed by two copies of each H2A, H2B, H3 and H4.

Histones are alkaline nuclear proteins whose N-terminal tails are subject to a large number of post-translational modifications (Bernstein et al., 2007; Kouzarides, 2007). There are at least eight different types of histone modifications including acetylation, methylation and phosphorylation which represent the best studied ones. Figure 1-2 shows some of the more than sixty histone residues that are known to be modified.

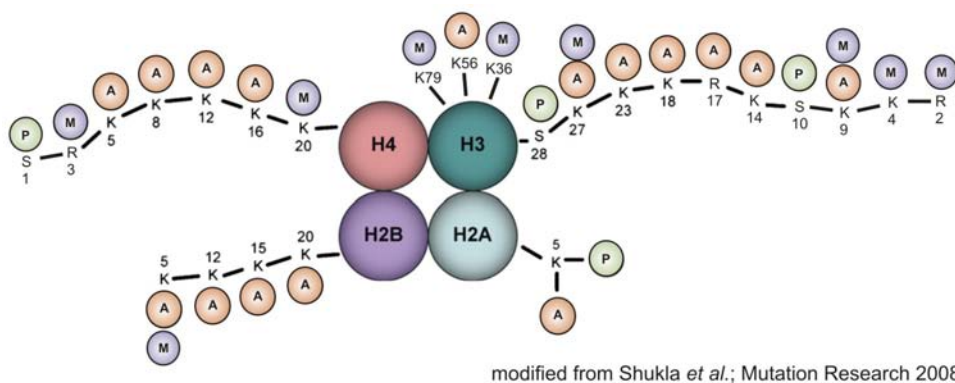


### Figure 1-2 Histone modifications

Schematic presentation of the best characterized histone modifications including acetylation (A), methylation (M) and phosphorylation (P) on lysine (K), arginine (R) and serine (S) residues. Post-translational modifications of histones occur primarily on N-terminal tails of the core histones H2A, H2B, H3 and H4.

Furthermore, lysine and arginine methylation may occur in different states that are interdependent: mono- (me1), di- or trimethylation (me3) at lysine residues and mono- or dimethylation on arginine residues. Such variable methylation states further contribute to the complexity of histone modifications and their biological consequences (Kouzarides, 2007).

About ten years ago, it has been hypothesized that specific histone tail modifications and/or their combinations constitute the histone-code, that determines the transcriptional state of the gene (de, X et al., 2005). According to this hypothesis, “multiple histone modifications, acting in a combinatorial or sequential fashion on one or multiple tails, specify unique downstream functions” (Strahl and Allis, 2000). This hypothesis has been supported and refined by the experimental identification of enzymes that induce, recognize or erase histone modifications. Further affirmation arises from data, revealing that one histone mark may either have repressive or activating consequences, depending on the context of surrounding modifications. Methylation of histone 3 lysine 9 (H3K9me) can initiate transcriptional silencing. However, in the context of methylated H3K4 and H4K20, it contributes to the maintenance of active marks (de, X et al., 2005). Consequently, the histone-code does not provide a simple “on or off” decision. The biological outcome is dependent on the dynamic cooperation of various epigenetic marks as well as on their translation and is therefore adaptable to diverse biological requirements. Furthermore, modifications on the same (*cis* effect) or different (*trans* effect) histone tails may be interdependent. The activating role of H3K4 is mediated via preventing the binding of the remodelling and deacetylating complex NuRD (nucleosome remodelling histone deacetylase complex) as well as through blocking H3K9 methylation, representing an example for *cis* effects. Among others, *trans* effects were observed between H2B and H3, as ubiquitination of H2BK123 is required for efficient H3K4 methylation (de, X et al., 2005).

Development of the chromatin immunoprecipitation technique (ChIP) using modification-specific antibodies and its adaptation to DNA microarrays (chip) permitted insights into the genome-wide distribution of histone modifications. Generally, histone acetylation is associated with transcriptional activation, whereas histone methylation may be linked to either activation or repression, depending on the position and state of the methyl mark. Promoter regions of active genes are characterized by histone acetylation and histone H3 lysine 4 (H3K4) methylation (Bernstein et al., 2005; Kim et al., 2005). Methylation of H3K27, however, seems to correlate with transcriptional repression (Boyer et al., 2006; Lee et al., 2006; Roh et al., 2006). High resolution profiling using ChIP-Seq (ChIP-Sequencing; direct sequencing of ChIP DNA) revealed typical histone methylation patterns for promoters, enhancers, insulators and transcribed regions (Barski et al., 2007). Actively transcribed

regions, e.g., are characterized by high levels of H3K36me3 (trimethylation of histone H3 lysine 36), H3K27me1 (monomethylation of H3 lysine 27), H3K9me1, H4K20me1 and H2BK5me1. Additionally, H3K4 methylation shows increased signals surrounding the transcription start sites (TSS) of known genes and positively correlates with gene expression. H3K4me3 presence is highest near the TSS at -300 and +100 bp whereas the major peaks for H3K4me1 and H3K4me2 were detected more than 500 bp away from the TSS (Barski et al., 2007).

The comprehensive ChIP-Seq technique provides more sensitive and detailed information about the global incidence of histone modifications and their association to regulatory elements than ChIP-on-chip assays (ChIP combined to microarray analysis). This might be one reason for minor discrepancies about the functional role of several modifications in literature. Based on ChIP-on-chip analyses, Heintzman *et al.* postulated that active promoter regions may be distinguished from active enhancers by high levels of H3K4me3, whereas enhancers are marked by high levels of H3K4me1 (Heintzman et al., 2007). However, using the ChIP-Seq technique, Barski *et al.*, found that all three methylation states of H3K4 are highly enriched at both active promoters and active enhancers. They in turn characterize active promoter regions by high levels of H3K27me1, H3K36me3, H3K9me1, H4K20me1 and H2BK5me1 downstream of TSSs (Barski et al., 2007). Up to now, relatively little is known about the extent to which such combinatorial patterns of histone modifications exist in the human genome. First progress was made by Wang *et al.* who identified a common modification module consisting of 17 histone modifications at 25% of human promoters (Wang et al., 2008). Genes exhibiting this modification module tended to have higher expression levels. However, histone modifications themselves do not uniquely determine expression levels, they rather function cooperatively in order to prepare chromatin for transcriptional activation (Wang et al., 2008). The conclusions drawn of those high-throughput analyses are in concordance with other studies suggesting a cross-talk between different histone modifications (Berger, 2007; Fischle et al., 2003; Schreiber and Bernstein, 2002).

### **Setting, Reading and Erasing Histone Modifications**

Numerous enzymes that catalyze the addition and removal of histone modifications have been identified (examples are shown in Table 1-1). Among all histone modifying enzymes, methyltransferases and lysine demethylases belong to the most specific ones. This might be one reason why methylation is the best characterized modification to date (Kouzarides, 2007). Although several histone acetyltransferases (HAT) seem to have a preference for

individual residues, target specificity of both acetyltransferases and histone deacetylases (HDAC) has not been extensively explored. However, just recently, SIRT6 was shown to be crucial for H3K9 deacetylation (Kawahara et al., 2009). During this work, analyses were limited to lysine acetylations and methylations. Therefore, further descriptions are focused on factors affecting those modifications.

**Table 1-1 Examples for histone modifying enzymes (writers and erasers) along with several sites they modify**

Histone modifying enzyme	Resulting modification	Enzymes erasing the methyl mark
<b>Histone Acetyltransferases (HAT)</b>	<b>Acetylation</b>	<b>Histone deacetylases (HDAC)</b>
PCAF/GCN5	H3K9	SIRT6
CBP/P300, PCAF/GCN5	H3K14	Not specified
HB01, TIP60, CBP/P300	H4K8	Not specified
HAT1, HB01, TIP60	H4K12	Not specified
<b>Methyltransferases (HMT)</b>	<b>Methylation</b>	<b>Histone demethylases</b>
MLL1-5, SET1A, SET1B	H3K4	LSD1
G9a, SUV39H1, SUV39H2 ESET	H3K9	JHDM2a, JHDM2b, JMJD2B, JMJD2D
EZH2	H3K27	JMJD3
SET2, NSD1	H3K36	JHDM1a, JHDM1b
DOT1	H3K79	Not specified
PR-SET7/8, SUV4 20H1/H2	H4K20	Not specified

In order to serve as a mark with the potential to distinguish between different regions of the genome, a modification has to be directed to specific loci. There are several possibilities of targeting histone modifying enzymes to their sites of action. First, sequence specific transcription factors including nuclear hormone receptors were shown to recruit histone modifying enzymes to promoter regions (Imhof, 2006; Rice et al., 2007; Robert et al., 2004). For example, the yeast Hst1 histone deacetylase is recruited by the transcriptional repressor Sum1 (Robert et al., 2004). Likewise, glucocorticoid receptors are able to recruit the ATP dependent BRG1 chromatin remodelling complex to the MMTV (mammary tumor virus) promoter (Hebbar and Archer, 2003). Second, histone deacetylases may be recruited by methyl-binding proteins (MBD) to sites of DNA methylation (Ballestar and Wolffe, 2001); see also section 1.1.1.2). Another targeting possibility involves interactions with non-coding RNAs from the corresponding gene locus (Imhof, 2006; Rinn et al., 2007). For example, recruitment of a histone methyltransferase complex responsible for H3K27 methylation at the

inactive X chromosome of females depends on the non-coding *Xist* (X inactive specific transcript) RNA (Plath et al., 2003).

The question arising now is, how are the combinations of histone marks recognized and transformed into a biological function. Histone modifications may influence the higher-order chromatin structure by affecting the contacts between adjacent nucleosomes or between histones and DNA. Among all known histone modifications, acetylation holds the highest potential to unfold chromatin, as it neutralizes the positive charge of lysine residues and thereby weakens the interactions with the negatively charged DNA. Furthermore, the interpretation of the histone code is carried out by chromatin-binding domains that are able to recognize distinct histone modifications on specific residues (Figure 1-3A). Chromodomains (chromatin organization modifier domain) bind to methylated histone residues whereas bromodomains (first reported in *Drosophila* brahma proteins, from which its name derived in analogy to the chromodomain) recognize histone acetylation (Kouzarides, 2007). Figure 1-3B illustrates examples for histone-code reading proteins which fulfil effector functions like (i) ATP-dependent remodelling of the chromatin fiber (BPTF, CHD1, HP1), (ii) induction of further histone modifications (ING2, HP1, PC2, EAF3, JMJD2A, GCN5, TAF1), (iii) allowing transcriptional elongation (CHD1, proposed for BRD2 (LeRoy et al., 2008)) or (iv) recruitment of the DNA repair machinery (53BP1) (Daniel et al., 2005; Kouzarides, 2007; Lee and Shilatifard, 2007; Lomber et al., 2006; Sims, III et al., 2007; Taverna et al., 2007).

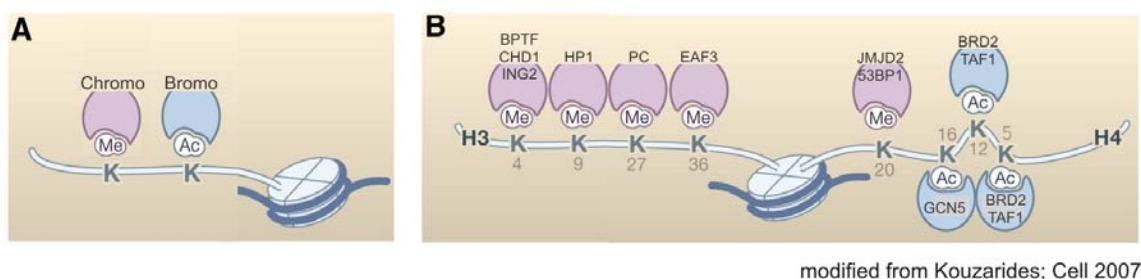


**Figure 1-3 Reading the histone code**

**(A)** Domains used for recognition of methylated (me) or acetylated (ac) lysines (K) at histone tails. **(B)** Examples for proteins that recognize specific histone modifications.

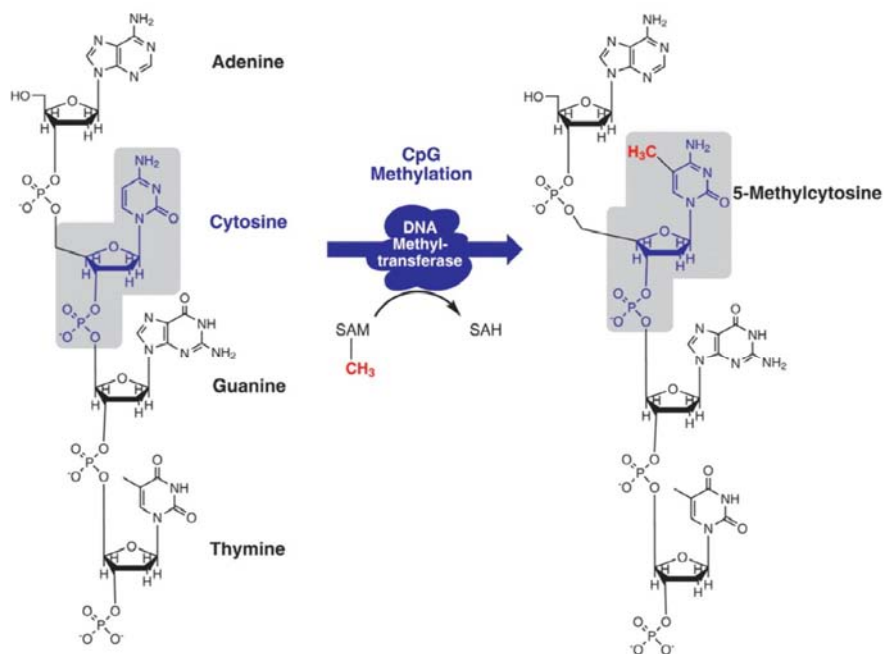
Notably, chromatin modifications are not only involved in transcriptional regulation but also play important roles during DNA replication, repair and condensation (Kouzarides, 2007). Additionally, evidence for a linkage between histone modifications and DNA methylation emerged during the past decade as histone deacetylation and primarily H3K9 methylation



seem to be a necessary prerequisite for CpG methylation in fungi, plants and mammals (Fuks, 2005). This relationship is further emphasised through direct interactions of DNMTs as well as MBDs with histone modifying complexes (see also section 1.1.1.2) (D'Alessio et al., 2007; Klose and Bird, 2006).

### 1.1.1.2 DNA Methylation

DNA methylation is the longest known epigenetic modification. In mammals, this modification predominantly occurs on cytosine residues that are followed by a guanine and is therefore also termed as methylation of CpG dinucleotides (Figure 1-4). Methylated cytosines, however, bear the risk of deamination resulting in cytosine to thymine transitions. Probably, due to this tendency of methylated cytosines to deaminate, the overall frequency of CpGs within the genome is less than statistically expected (Herman and Baylin, 2003). Despite their relative underrepresentation, CpG dinucleotides can be accumulated in small stretches of DNA called CpG islands (CGI). CGIs are often associated with gene promoter regions and are usually unmethylated. In contrast, about 80% of the CpG dinucleotides outside CpG islands are methylated (Bird, 2002; Herman and Baylin, 2003).



taken from Maxwell et al; labmedicine 2009

**Figure 1-4 Methylation of CpG dinucleotides**

DNA methyltransferases (DNMTs) transfer methyl-groups from the methyl-group donor S-Adenosylmethionine (SAM) to the carbon 5 position of cytosine residues. In mammals, DNA methylation occurs mainly on cytosines followed by a guanine residue.

Controlled DNA methylation is crucial for gene regulation during embryonic development (Okano et al., 1999), X-chromosomal inactivation (Goto and Monk, 1998), parental imprinting as well as for cellular differentiation (Mohn and Schubeler, 2009). Furthermore, silencing of repetitive and retroviral sequences is achieved by DNA methylation (Robertson and Wolffe, 2000; Walsh et al., 1998). Altered levels of cytosine methylation may lead to neoplastic development and eventually to cancer (Costello and Plass, 2001; Esteller et al., 2002; Esteller, 2007; Plass and Soloway, 2002).

The setting of methyl marks is carried out by DNA methyltransferases (DNMT), which transfer methyl groups from methyl group donors to the carbon 5 position of cytosines (Figure 1-4). In 1988, Bestor *et al.* identified the first eukaryotic DNA methyltransferase, named DNMT1 (Bestor et al., 1988). DNMT1 seemed to have a preference for hemimethylated DNA and was therefore assigned to function in maintenance methylation during DNA replication by catalyzing the methylation of the nascent, unmethylated strand (Bestor, 2000; Yoder et al., 1997). Two other enzymes, DNMT3a and DNMT3b, are thought to be responsible for *de novo* methylation (*i.e.* methylation of completely unmethylated DNA) that plays a crucial role during early development (Okano et al., 1998; Okano et al., 1999). However, a strict functional division does not exist, as both enzymes seem to participate in both *de novo* and maintenance methylation (Bestor, 2000; Bird, 2002; Szyf, 2009).

CpG methylation often leads to gene silencing (Figure 1-5). Transcriptional repression may either be achieved directly, by preventing the binding of transcription factors or the basal transcription machinery to the methylated DNA sequence or indirectly, by the recruitment of methyl-binding proteins (MBD) which in turn induce a silent chromatin state (Bestor, 2000; Bird, 2002; Bird and Wolffe, 1999; Clouaire and Stancheva, 2008; Kass et al., 1997).



modified from Lopez et al.; Br J Cancer. 2009

**Figure 1-5 Schematic presentation of transcriptional silencing by DNA methylation**

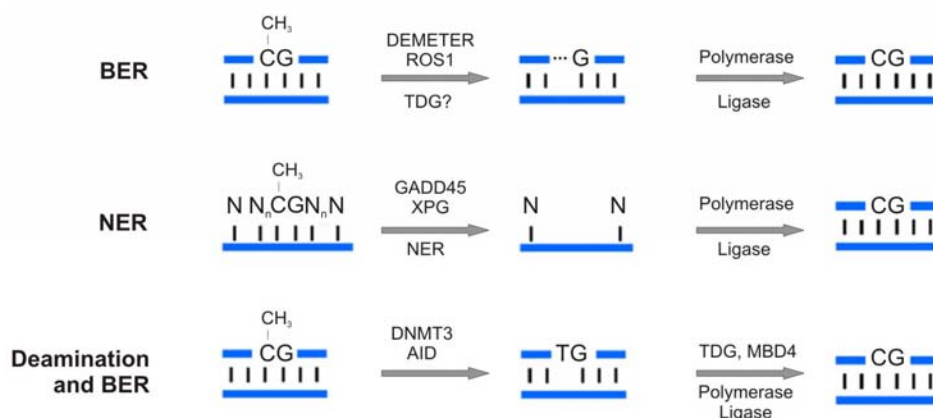
White lollipops represent unmethylated CpG dinucleotides and black ones stand for methylated CpGs. Arrows represent the transcription start site. Methyl-binding proteins (MBD) bind to methylated cytosines and recruit histone deacetylases (HDAC) that contribute to turning open chromatin (euchromatin) into a compact and inaccessible structure (heterochromatin). Histone acetyltransferases are indicated by HAT and promote an accessible chromatin structure.

MeCP2, for example, serves as a bridge that links DNA methylation with chromatin remodelling by recruiting histone deacetylases through the corepressor mSin3A (Jones et al., 1998; Nan et al., 1998) and histone methyltransferases like SUV39H1 (Fuks et al., 2003; Lunyak et al., 2002).

Compared to the DNMT-dependent methylation processes, the mechanisms responsible for the removal of methylated cytosines are less well understood. The failure of maintenance DNMTs to methylate a newly synthesized daughter strand during cell-cycle represents a non-enzymatic, passive way of erasing the 5-methylcytosine (5-MeC) mark that requires at least two cycles of replication for complete DNA demethylation. The existence of replication-independent DNA demethylation processes implies the presence of demethylating enzymes that actively remove either the methyl group, the methylated cytosine or whole nucleotides (Gehring et al., 2009). Since the last 15 years, DNA repair enzymes have been discussed as important factors during active demethylation. In flowering plants, the active demethylation process is well characterized. DME (DEMETER) and ROS1 (REPRESSOROFSILENCING1) are 5-methylcytosine glycosylases/lyases (Agius et al., 2006; Morales-Ruiz et al., 2006) catalyzing the first step of an active demethylation process that is linked to base excision repair (BER) in plants (Figure 1-6). The base excision repair process removes incorrect (mismatched) bases resulting from deamination (T:G or U:G) as well as methylated bases such as 3-methyladenine (Niehrs, 2009). DNA glycosylases and apurinic/apyrimidinic endonucleases hydrolyse the N-glycosidic bond, resulting in an abasic site that is filled and sealed by DNA polymerases and ligases, respectively (Fromme and Verdine, 2004). The use of DNA repair mechanisms for demethylating purposes in animal cells was first suggested in the early 90s when Jost and colleagues reported evidence for an enzymatic system replacing 5-methylcytosine by cytosine. Nuclear extracts from chicken embryos promoted demethylation of selectively mCpGs in hemimethylated DNA through formation of specific nicks 5' from 5-methyldeoxycytidine (Jost, 1993). Later on, the responsible enzyme was identified as a thymine DNA glycosylase (TDG) (Jost et al., 1995). Recently, it was shown that loss of methylation at an estrogen responsive element coincides with the recruitment of DNMT3a/b, TDG and other BER enzymes confirming the implication of base excision repair (Metivier et al., 2008). Additionally, the authors assigned deaminating activities to both DNA methyltransferases under special conditions. However, this deaminating role resulting in DNA demethylation remains controversial (Gehring et al., 2009; Ooi and Bestor, 2008).

Assuming that DNA repair mechanisms represent the basis of active DNA demethylation, one question arises: which signal prompts the DNA repair machinery to operate at a certain locus at a defined developmental time point? GADD45a (growth arrest and DNA damage

inducible alpha) emerged as linking element between DNA repair machineries and active 5-MeC demethylation. This protein seems to support the active demethylation process by (i) localizing to specific sites of demethylation through TAF12 (TBP-associated factor) interaction and recruitment of the nucleotide excision repair (NER) machinery through XPG (Barreto et al., 2007; Schmitz et al., 2009) or (ii) by facilitating the AID (activation induced deaminase) mediated 5-meC deamination and subsequent BER via MBD4 (Rai et al., 2008) (summarized in Figure 1-6). The nucleotide excision repair machinery recognizes DNA lesions, affecting multiple bases like those caused by UV irradiation. The NER pathway is a multistep process comprising the recognition of DNA damage, followed by incisions at sites flanking the lesion and removal of the about 29 bp oligonucleotide containing the lesion (Hakem, 2008). DNA polymerases then fill in the resulting gap using the undamaged strand as template (Niehrs, 2009).



modified from Niehrs, Differentiation 2009

**Figure 1-6 DNA repair mechanisms during active DNA demethylation**

DNA double strands are indicated in blue. Methylated CpG dinucleotides may be demethylated by (i) substitution of the methylated cytosine through base excision repair (BER), (ii) nucleotide excision repair (NER) or (iii) by deamination of methylated cytosines followed by base excision or mismatch repair. In the NER example, N represents any of the 4 DNA bases and N<sub>n</sub> indicates up to 20 bp that may be excised.

In the course of time, other factors than repair components have been described to function as “demethylases” such as RNA molecules (Weiss et al., 1996). However, the demethylating role of such a ribozyme-like enzyme was re-evaluated later (Swisher et al., 1998). Similarly, the demethylase activity of methyl-binding domain 2 (MBD2) reported by Bhattacharya *et al.* (Bhattacharya et al., 1999) could not be reproduced (Kress et al., 2006; Ng et al., 1999).

In summary, the mechanisms of active DNA demethylation still remain unclear, even though active events were detected in different cell systems (Table 1-2) and some promising factors have already been identified. Surprisingly, relatively little is described about the correlation

between histone modifications and nucleosome remodelling during active DNA demethylation. Especially regarding the question how repair machineries are recruited to sites of 5-meC demethylation, it would be interesting to analyse if that information roots in the histone code.

**Table 1-2 Examples for active DNA demethylation events in mammalian cell systems (reviewed in Niehrs, Differentiation 2009)**

Demethylated gene	Cell / tissue	Evidence for an active process
<b>Immune cells</b>		
<i>Interleukin 2</i>	T lymphocytes	Fast kinetics
<i>Th2 cytokine locus control region</i>	CD4 T helper cells	Non-dividing cells
<b>Embryonal cells</b>		
<i>Oct4</i>	Xenopus oocytes	Non-dividing cells
Genome	Mouse primordial germ cells	Fast kinetics
<b>Neural cells</b>		
<i>Glucocorticoid receptor</i>	Hippocampal neurons	Post-mitotic cells
<i>BDNF</i>	Primary mouse neurons	Transfected DNA, post-mitotic cells
<b>Cancer cells</b>		
<i>Oct4</i>	HEK293T cell line	Transfected DNA
<i>pS2</i>	MDAMB231, MCF7 cell lines	Fast kinetics, TDG dependence

### 1.1.1.3 Non-Coding RNA

Recently, RNA molecules, particularly non-coding RNAs such as miRNA and siRNA, emerged as important factors in the field of epigenetic signalling. Non-coding RNAs are known to cooperate with histone modifications and DNA methylation machineries in order to achieve long-term silencing that is heritable through cell divisions. The most famous and best understood example for their role in gene silencing is dosage compensation mediated by the *Xist* (X inactive specific transcript) RNA in mammals and the *roX* (RNA on X) RNA in *Drosophila* (Bernstein and Allis, 2005). Recently, the functional interaction of non-coding RNA and other epigenetic mechanisms could have been demonstrated in yeast and invertebrates. However, in mammals relatively little is known about this crosstalk (Li and Zhao, 2008). Although, the knowledge about the influence of non-coding RNA on transcriptional changes is far away from being complete, those molecules are considered to be important epigenetic regulators.

## 1.2 Epigenetics in Hematopoiesis

### 1.2.1 Hematopoiesis

Hematopoiesis describes the generation of all blood cells. Initially, during fetal development, hematopoiesis occurs in blood islands of the yolk sac and the paraaortic mesenchym and later on in liver and spleen (Abbas et al., 2007). Postnatally, development of blood cells takes place in the bone marrow (BM) where hematopoietic stem cells (HSC) as well as a complex mix of dividing and maturing cells of different lineages can be found.

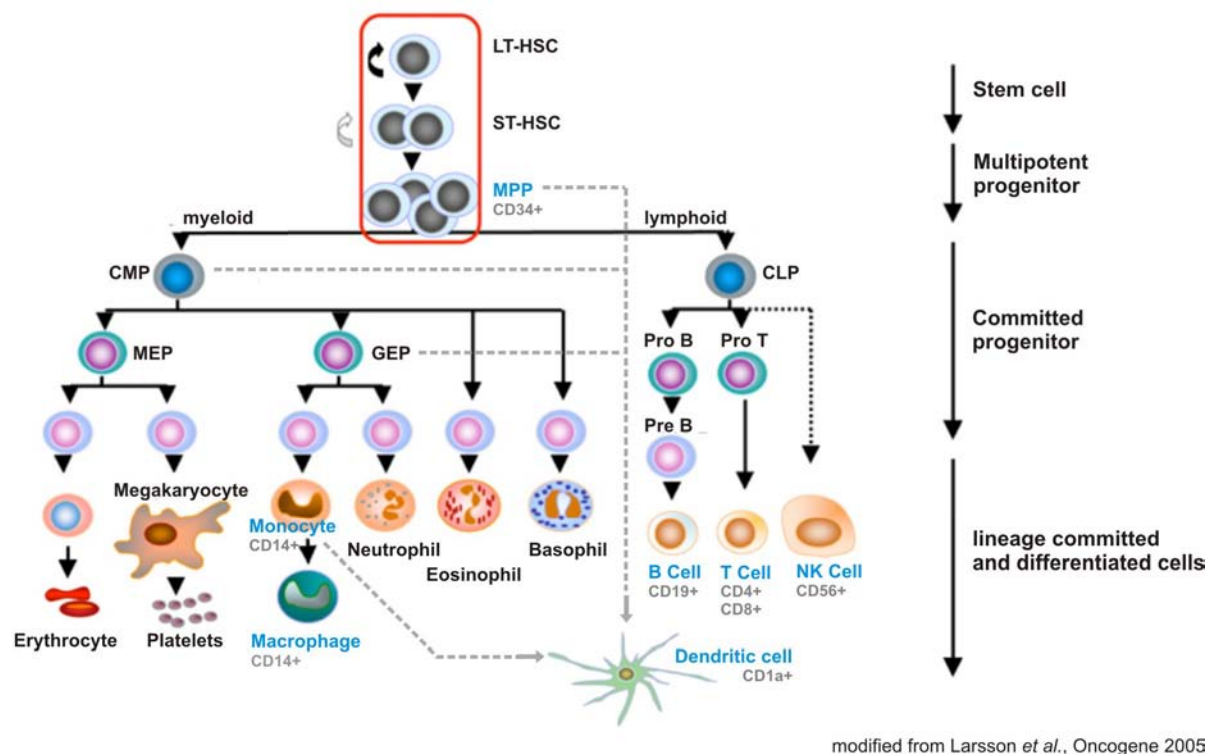


**Figure 1-7 Hierarchy of hematopoietic cells**

LT-HSC: long term self-renewing hematopoietic stem cell; ST-HSC: short term hematopoietic stem cell; MPP: multipotent progenitor; CMP: common myeloid progenitor; CLP: common lymphoid progenitor; MEP: megakaryocyte/erythroid progenitor; GMP: granulocyte-macrophage progenitor. CD: Cluster of differentiation. Cell-types relevant for this work are indicated in blue; their cell-type or lineage specific surface antigens (CD antigens) are illustrated in grey. The *in vivo* origin of dendritic cells still remains unclear (see section 1.2.2.2), illustrated by the grey broken lines towards the dendritic cell.

As illustrated in Figure 1-7, there is a continuum of progenitors at different stages between the HSC and completely differentiated cells. Dependent on various stimuli, those progenitors divide and progress towards certain lineages (Larsson and Karlsson, 2005).

Hematopoietic stem cells (HSC) may either develop towards the myeloid or the lymphoid lineage. Common myeloid progenitors give then rise to granulocytes, macrophages as well

as erythrocytes and megakaryocytes, whereas common lymphoid progenitors finally differentiate into B cells, T cells or natural killer cells (Figure 1-7) (Orkin, 2000). In this work, epigenetic analyses were limited to lymphocytes and mononuclear phagocytes. Therefore, further description is focused on those lineages.

For precise proliferation and differentiation processes, controlled expression of lineage- and cell type-specific transcription factors (TF) is essential. PU.1, for example, is a key regulator for the myeloid development (McKercher et al., 1996; Scott et al., 1994), whereas GATA1 is required for the erythroid and megakaryocytic lineage (Rice et al., 2007; Zhu and Emerson, 2002). Lymphoid development and especially further T cell differentiation are dependent on Ikaros (Georgopoulos et al., 1997; Quirion et al., 2009) while Pax5 assumes a key regulator function during B cell differentiation (Adams et al., 1992; Urbanek et al., 1994).

## **1.2.2 The Mononuclear Phagocyte System**

The mononuclear phagocyte system (MPS) comprises non-granulocytic, myeloid cells that play crucial roles during innate and adaptive immune responses as well as in tissue remodelling and homeostasis (van Furth and Cohn, 1968; Varol et al., 2009). Circulating CD14 positive monocytes account for 5 to 10% of peripheral leukocytes in humans and represent the key members of the MPS. Depending on the cytokine environment, monocytes have the capacity to differentiate into various immune cells with distinct functions including macrophages, dendritic cells and osteoclasts (Seta and Kuwana, 2007).

### **1.2.2.1 Macrophages in the Immune Response**

Macrophages represent the most ancient cell type in the hematopoietic system and comprise numerous subpopulations with various functions. Up to now, this heterogeneity including the resulting diverse functions during immune response and tissue remodelling as well as the interplay with other inflammatory cells is not completely understood (Ricardo et al., 2008). Following infection, circulating monocytes are recruited to affected sites, enter the injured tissue and differentiate into macrophages whose phenotype and function is determined by the present stimuli (Abbas et al., 2007). Phagocytosis and destruction of a variety of pathogens are mediated by receptor molecules, expressed on the macrophage's cell surface. Apart from eliminating microbes, macrophages govern many other functions in defence against infections. Production of cytokines like TNF (tumor necrosis factor) or IL-1 (interleukin 1) leads to activation of endothelial cells and neutrophils whereas IL-12 secretion results in stimulation of natural killer (NK) cells and T cells, reinforcing the immune response.

On the other hand, activated macrophages also produce growth factors for fibroblasts and endothelial cells, contributing to tissue remodelling after injury or infection (Abbas et al., 2007).

### **1.2.2.2 Dendritic Cells in the Immune Response**

Dendritic cells (DC) were initially described in the 1970s (Steinman and Cohn, 1973) and since then numerous subpopulations differing in surface markers, localization and immunological function have been described. Although the generation of different subtypes is a consequence of diverse infectious and inflammatory stimuli, all DC subpopulations share the ability to capture, process and present antigens to T cells (Conti and Gessani, 2008). DCs are predominantly located in lymphoid organs and at sites of possible pathogen entry like mucosal surfaces and epidermis (Abbas et al., 2007). Intrinsically, DCs reside in a resting, immature state and their main function is to capture antigens. Following encounter with microbes, DC undergo maturation while they migrate to the draining lymph nodes. Mature dendritic cells finally settle in T cell zones of the lymph node where they efficiently present the captured antigens and stimulate naïve T cells (Abbas et al., 2007).

Until today, it is unclear where and when commitment to DC development occurs *in vivo*. Additionally, the precursor-to-progeny relationship between monocytes and DCs has been discussed since the identification of DCs (Liu et al., 2009). It is even unclear, if different DC subtypes really originate from the same hematopoietic precursor. Initially, Sallusto and Lanzavecchia identified monocytes as potential precursors of immature dendritic cells *in vitro* by supplementing cultures of human peripheral blood monocytes with the granulocyte-macrophage colony stimulating factor (GM-CSF) and interleukin 4 (IL-4) (Sallusto and Lanzavecchia, 1994). The resulting immature DCs may then be matured by addition of toll-like receptor ligands such as LPS or by addition of TNF (De Smedt et al., 1996). Although various protocols describe how to trigger monocyte differentiation towards dendritic cells (reviewed in (Conti and Gessani, 2008)), the “Sallusto cytokine combination” is the best characterized and most utilized one. Another *in vitro* model that is based on the transendothelial migration of monocytes without the addition of cytokines, supported the idea that monocytes may also differentiate towards DCs under physiological conditions (Randolph et al., 1998). Randolph *et al* postulated that DCs arise from monocytes crossing the endothelium, whereas macrophages develop from monocytes remaining in the subendothelial matrix.

Finally, it has to be mentioned that the *in vivo* existence of dendritic cells as a separate cell type is controversially discussed (Hume, 2008). According to Hume, dendritic cells just represent a heterogeneous subpopulation of mononuclear phagocytes as neither pathways



of development, markers, nor functions in antigen presentation exist, which definitely distinguish them from macrophages.

### **1.2.3 The Lymphoid Lineage**

While macrophages and dendritic cells participate in innate immunity (also called natural or native immunity) that provides initial defence against microbes, lymphocytes mediate adaptive immunity. Adaptive immunity or specific immunity is characterized by its antigen-specificity for distinct macromolecules and by a memory which enables the lymphocytes to react much faster and more vigorously to a repeated encounter with the same pathogen (Abbas et al., 2007). Lymphocytes are divided in distinct subtypes due to different functions and gene products. B lymphocytes (or B cells) mature in the bone marrow and are responsible for antibody production upon infection. B cells express high levels of the cell surface marker CD19 that is used to distinguish them from other leukocytes. T lymphocytes (T cells) refer to thymus-derived lymphocytes as their precursors migrate from the bone marrow to the thymus where they differentiate into T cells. CD4 expressing T helper cells (CD4+ T cells) contribute to B cell differentiation and macrophage activation whereas CD8 expressing cytotoxic T lymphocytes (CD8+ T cells) are responsible for killing tumor cells or cells infected with microbes (Abbas et al., 2007). The CD56 positive natural killer (NK) cells are responsible for destruction of virus-infected and damaged cells. Although they fulfil similar effector functions as cytotoxic T cells, NK cells rather contribute to innate immune defence than to adaptive immunity.

### **1.2.4 Role of Epigenetic Modifications for Lineage Commitment**

Throughout hematopoiesis, multipotent and proliferating progenitor cells differentiate into specialized effector cells thereby losing their proliferation potential. How these cell fate decisions are made and which regulatory processes trigger differentiation towards one lineage or the other is not completely understood. One important factor for differentiation processes is the proper balance and timing of transcription factor (TF) expression (Akashi, 2005; Bonifer et al., 2006). However, transcription factors are dependent on the present chromatin architecture at the corresponding binding sites because DNA accessibility is determined by histone modifications and CpG methylation. The chromatin structure of multiple lineage specific genes is believed to keep hematopoietic precursors in a kind of “primed” state (Bonifer et al., 2006; Bottardi et al., 2007; Reiner, 2005). In hematopoietic progenitor cells, several lineage-specific genes reside within transcriptionally potent

(accessible) chromatin and are therefore prepared for a potentiated expression when the proper signals and factors are present (Bottardi et al., 2007). The human  $\beta$ -globin locus of hematopoietic progenitors, for example, is characterized by H3 hyperacetylation and H3K4 dimethylation. However, high-level globin expression is only achieved in erythroid cells where the proper signal and transcription factor environment is given (Bottardi et al., 2007). The promiscuous (epi)genetic program of hematopoietic precursors, resulting from coexpression of various lineage-specific genes (albeit to a low level), allows differentiation into distinct cell types at the multipotent stage (Akashi, 2005).

The importance of proper epigenetic regulation and orchestration in different cell types is emphasised by the fact that differential methylation patterns of lineage determinants may contribute to severe malignancies like shown for the GATA genes in lung cancer (Guo et al., 2004) or for PU.1 hypomethylation in B cell lymphomas (Ivascu et al., 2007). The reasons for abnormal methylation patterns are currently not understood but aberrant expression of the methylating enzymes, DNA-methyltransferases (DNMT), seems to play a crucial role during those processes (Rice et al., 2007). More and more publications link abnormal methylation patterns to cancer development, but up to date comparatively little is known about the regulating role of DNA methylation during differentiation of healthy somatic cells. It is known that DNA methylation is crucial for the expression of cytokines like IL-4 during T cell activation and also for event memorization resulting in a faster and more vigorous immune response in case of a second encounter with a pathogen (Murayama et al., 2006; Reiner, 2005). Furthermore, several methylation patterns have been linked to transcriptional activation of lineage specific transcription factors (Ivascu et al., 2007), but there is no systematic analysis, helping to clarify the global role of DNA methylation and its interplay with other chromatin modifications during lineage commitment and cell fate decision in the hematopoietic system.

## 2 Research Objectives

Defined methylation patterns are crucial for the normal progression of vital biological processes including embryogenesis and development. Alterations in methylation profiles and the associated dysregulation of affected genes are implicated in various diseases like neoplastic transformation. However, surprisingly little is known about the function of DNA methylation in normal somatic cells. A major aim of this thesis was to investigate methylation changes during differentiation processes of post-proliferative monocytes. This system is particularly well suited to study active, proliferation-independent DNA demethylation events, a process which is currently not well documented in mammals and controversially discussed. Based on an earlier identified example for active demethylation in differentiating monocytes, other examples should be identified to enable the further characterization of the active demethylation process. To find regions subjected to demethylation, novel methodological approaches had to be developed, since existing techniques were not well suited to study this phenomenon. Finally, the active demethylation process should be characterized at several regions and for several donors, e.g. in terms of timing, its relation to mRNA expression and other epigenetic marks, to shed light on possible mechanisms.

## 3 Material and Equipment

### 3.1 Equipment

8-Channel PipettorImpact2 Equalizer 384	Thermo Fisher Scientific, Hudson, US
Autoclave	Technomara, Fernwald, Germany
Bioanalyzer 2100	Agilent Technologies, Böblingen, Germany
BioPhotometer	Eppendorf, Hamburg, Germany
Centrifuges	Heraeus, Hanau; Eppendorf, Hamburg, Germany
Densitometer	Molecular Dynamics, Krefeld, Germany
Electrophoresis equipment	Biometra, Göttingen; BioRad, Munich, Germany
FACS Calibur	BD, Heidelberg, Germany
Heat sealer (Fermant 400)	Josten & Kettenbaum, Pensberg, Germany
Heat sealer	Eppendorf, Hamburg, Germany
Heatblock	Stuart Scientific, Staffordshire, UK
Incubators	Heraeus, Hanau, Germany
J6M-E centrifuge	Beckmann, Munich, Germany
Laminar air flow cabinet	Heraeus, Hanau, Germany
Luminometer (Sirius)	Berthold Detect. Systems, Pforzheim, Germany
MassARRAY Compact System	Sequenom, Hamburg, Germany
MassARRAY MATRIX Liquid Handler	Sequenom, Hamburg, Germany
MassARRAY Phusio chip module	Sequenom, Hamburg, Germany
Megafuge 3,0 R	Heraeus, Osterode, Germany
Microarray hybridization chambers SureHyb	Agilent Technologies, Böblingen, Germany
Microarray scanner; 5 micron resolution	Agilent Technologies, Böblingen, Germany
Microarray slide holder	Agilent Technologies, Böblingen, Germany
Microscopes	Zeiss, Jena, Germany
Multifuge 3S-R	Heraeus, Osterode, Germany
Multipipettor Multipette plus	Eppendorf, Hamburg, Germany
NanoDrop	PeqLab, Erlangen, Germany
PCR-Thermocycler PTC-200	MJ-Research/Biometra, Oldendorf, Germany
PCR-Thermocycler Veriti 384 well	Applied Biosystems, Foster City, USA
pH-Meter	Knick, Berlin, Germany
Picofuge	Heraeus, Osterode, Germany
Power supplies	Biometra, Göttingen; Germany
Realplex Mastercycler epGradient S	Eppendorf, Hamburg, Germany
Sigma 2 – Sartorius	Sartorius, Göttingen, Germany
Sonifier 250	Branson, Danbury, USA
Sorvall RC 6 plus	Thermo Fisher Scientific, Hudson, USA

Speed Vac	Christ, Osterode, Germany
Thermomixer	Eppendorf, Hamburg, Germany
Typhoon™	Amersham Biosciences, Germany
Ultracentrifuge Optima L-70	Beckman, Munich, Germany
Waterbath	Julabo, Seelstadt, Germany
Water purification system	Millipore, Eschborn, Germany

## 3.2 Consumables

384-well PCR plates	Thermo Fisher Scientific, Hudson, USA
8-channel pipettor tips Impact 384	Thermo Fisher Scientific, Hudson, USA
Adhesive PCR sealing film	Thermo Fisher Scientific, Hudson, USA
Cell culture flasks and pipettes	Costar, Cambridge, USA
CLEAN resin	Sequenom, Hamburg, Germany
Cryo tubes	Nunc, Wiesbaden, Germany
Filter tubes: Millipore Ultrafree-MC	Millipore, Eschborn, Germany
Heat sealing film	Eppendorf, Hamburg, Germany
Luminometer vials	Falcon, Heidelberg, Germany
MATRIX Liquid Handler D.A.R.Ts tips	Thermo Fisher Scientific, Hudson, USA
Micro test tubes (0.5, 1.5, 2 ml)	Eppendorf, Hamburg, Germany
Microarray gasket slides	Agilent Technologies, Santa Clara, USA
Multiwell cell culture plates and tubes	Falcon, Heidelberg, Germany
nProteinA Sepharose 4 FastFlow	GE Healthcare, Munich, Germany
PCR plate Twin.tec 96 well	Eppendorf, Hamburg, Germany
rProteinA Sepharose 4 FastFlow	GE Healthcare, Munich, Germany
Sepharose CI-4 beads	Sigma-Aldrich, Munich, Germany
SpectroCHIP bead array	Sequenom, Hamburg, Germany
Syringes and needles	Becton Dickinson, Heidelberg, Germany
Sterile combitips for Eppendorf multipipette	Eppendorf, Hamburg, Germany
Sterile micropore filters	Millipore, Eschborn, Germany
Sterile plastic pipettes	Costar, Cambridge, USA
Teflon foils	Heraeus, Hanau, Germany

### 3.3 Chemicals

All reagents used were purchased from Sigma-Aldrich (Taufkirchen, Germany) or Merck (Darmstadt, Germany) unless otherwise noted. Oligonucleotides for Real-Time PCR were synthesized and high-pressure liquid chromatography purified by Metabion (Planegg-Martinsried, Germany). Oligonucleotides adapted to methylation analysis with the MassARRAY system (see section 4.2.5.15) were purchased from Sigma-Aldrich (Taufkirchen, Germany).

### 3.4 Enzymes and Kits

aCGH Hybridization Kit	Agilent Technologies, Waldbronn, Germany
Alkaline phosphatase	Roche, Mannheim, Germany
Aprotinin	Roche, Mannheim, Germany
BioPrime Purification Module	Invitrogen, Karlsruhe, Germany
BioPrime Total Genomic Labelling System	Invitrogen, Karlsruhe, Germany
Blood & Cell Culture DNA Midi Kit	Qiagen, Hilden, Germany
Blood and Tissue Culture Kit	Qiagen, Hilden, Germany
DNA Ladder 1 kb plus	Invitrogen, Karlsruhe, Germany
DNA molecular weight standard	Invitrogen, Karlsruhe, Germany
dNTPs	NEB, Frankfurt, Germany
Dual-Luciferase Reporter Assay System	Promega, Madison, USA
EpiTect Bisulfite Kit	Qiagen, Hilden, Germany
EZ DNA methylation kit	Zymo Research, Orange, USA
FatsStart TaqDNA polymerase	Roche, Mannheim, Germany
Gene expression hybridization Kit	Agilent, Waldbronn, Germany
HhaI Methylase	NEB, Frankfurt, Germany
HpaII Methylase	NEB, Frankfurt, Germany
Human Cot-1 DNA	Invitrogen, Karlsruhe, Germany
Klenow Enzyme	NEB, Frankfurt, Germany
Klenow exo- (3'-5' exo minus)	NEB, Frankfurt, Germany
Lipofectamin transfection reagent	Invitrogen, Karlsruhe, Germany
Linear Amp. Kit plus, one colour	Agilent Technologies, Waldbronn, Germany
NucleoSpin Plasmid Quick Pure	Macherey-Nagel, Düren, Germany
NucleoSpin® Extract II	Macherey-Nagel, Düren, Germany
Pepstatin	Roche, Mannheim, Germany
Plasmid Midi Kit	Qiagen, Hilden, Germany

Proteinase K	Roche, Mannheim
QIAquick PCR Purification Kit	Qiagen, Hilden, Germany
QuantiFast SYBR green	Qiagen, Hilden, Germany
Repli-G Midi Kit	Qiagen, Hilden, Germany
Restriction endonucleases	NEB, Frankfurt; Roche, Mannheim; Germany
Reverse Transkriptase SuperSkript II	Promega, Madison, USA
RNA 6000 Nano Kit	Agilent Technologies, Waldbronn, Germany
RNA Spike-in Kit	Agilent Technologies, Waldbronn, Germany
RNeasy Midi and Mini Kit	Qiagen, Hilden, Germany
S-Adenosyl-Methionin (SAM)	NEB, Frankfurt, Germany
Shrimp Alkaline Phosphatase (SAP)	Sequenom, Hamburg, Germany
SssI CpG methylases	NEB, Frankfurt, Germany
T-Cleavage MassCleave Reagent kit	Sequenom, Hamburg, Germany
TaqDna Polymerase	Roche, Mannheim, Germany
T4 DNA Ligase	Promega, Madison, USA
T4 DNA Ligase buffer	NEB, Frankfurt, Germany

## 3.5 Oligonucleotides

### 3.5.1 cDNA Primer

<b>C9ORF78</b>	Forward: 5' CAGATGAAGACAGGTGGTATGGTGGGA 3' Reverse: 5' CCTCATCCCTTCGGTTGGTTTCTG 3'
<b>CCL13</b>	Forward: 5' GAAGATCTCCTTGCGAGAGGCT 3' Reverse: 5' GGGTCAGCACAGATCTCCTTG3'
<b>GADD45A</b>	Forward: 5' TCCTGCTCTTGGAGACCGAC 3' Reverse: 5' GACTTAAGGCAGGATCCTTCCATTGAG 3'
<b>GADD45B</b>	Forward: 5' AGTCGGCCAAGTTGATGAATGTG 3' Reverse: 5' GATGAGCGTGAAGTGGATTTGCAG 3'
<b>GADD45G</b>	Forward: 5' CAGGACACAGTTCCGGAAAGCA 3' Reverse: 5' ACACAGAAGGTCACATTGTCCG 3'
<b>HPRT</b>	Forward: 5' AAGTTTGTGTAGGATATGCCC 3' Reverse: 5' GAACATTGATAATTTTACTGGCG 3'
<b>JDP2</b>	Forward: 5' GAAGAACAAAGTCGCAGCAGCC 3' Reverse: 5' CTCCTCAATCTGGGTCTTCAGCTC 3'
<b>MLXIPL</b>	Forward: 5' CATGTTTGATGACTACGTCCGAACC 3' Reverse: 5' GACACCATCCCGTTGAAGGAC 3'
<b>STAT5A</b>	Forward: 5' CAGCCAGGACCACAATGCCA 3' Reverse: 5' CAGCACTTTGTCAGGCACGG 3'

<b>STAT5B</b>	Forward: 5' AACAACTGCTGCGTCATGGA 3' Reverse: 5' TTCTGTCACCGACTCTGCCC 3'
<b>TCEA3</b>	Forward: 5' GCTTATAGCCAAGATGACGGCAG 3' Reverse: 5' GGGTCATGGCATTCTCAACTC 3'
<b>USP20</b>	Forward: 5' CCTTTGCCCTCACCTTGA CT C 3' Reverse: 5' CAGACAGGCCCATAGTTTGGT 3'
<b>VDR</b>	Forward: 5' CTCATGGCCATCTGCATCGT 3' Reverse: 5' CTGGATGGCCTCAATCAGCG 3'

### 3.5.2 ChIP/MCIP Primer

<b>C9ORF78/USP20</b>	Forward: 5' AGTACGCGTGTTTGGATTTGGG 3' Reverse: 5' TGCTCTGAACACTCAGCTCCAC 3'
<b>CCL13</b>	Forward: 5' CTAGAAAAGTCTTTGGTGCC CAG 3' Reverse: 5' CTTGGA ACTCTCAGAGGACCTTG 3'
<b>CCL23</b>	Forward: 5' GTGTTTACCAGCAGAGATCACAG 3' Reverse: 5' CACCTTCAGATGCTCAAATAGCC 3'
<b>CD207</b>	Forward: 5' TGCCCTCTCATTGGTCCCAG 3' Reverse: 5' TACCTACCTCAGCCTGCATTCCA 3'
<b>CLEC10A</b>	Forward: 5' TCTCCCTGCTTCCTCTGACATCC 3' Reverse: 5' AATCACACCCTCCAGACCTCCC 3'
<b>DNase1L3</b>	Forward: 5' GGGCTCACCTTCACAATGACATCC 3' Reverse: 5' TCTGCTCCTTCAACGTCAGGTC 3'
<b>P2RY6</b>	Forward: 5' CTGCTGACACCGACACAGAG 3' Reverse: 5' GAGCTGGCAAGAGATGAGAGTCC 3'
<b>STAT5</b>	Forward: 5' GCACAGACTCTGCATCCTCTTCTC 3' Reverse: 5' AGTCCTGCTTCCTCTGCCCA 3'
<b>Upstream</b>	Forward: 5' CAGACAAGCCTTATCGGTATCACCT 3' Reverse: 5' AATCGCTATCTCATTACGATGTTGGG 3'

### 3.5.3 Primer for *in vivo* Footprinting

<b>Mcp1s</b>	biotin-ACAGCTCCTTTATGGCTTCC
<b>Mcp2s</b>	CATGGTGAATGGCTGGGGCG
<b>Mcp1as</b>	biotin-ATGTTGAAGGTTAAGAGTTGG
<b>Mcp3as</b>	TGTTTCTTTGCCTCTCTGCTCCTCTGG
<b>LP25 linker primer</b>	Cy5-GCGGTGACCCGGGAGATCTGAATTC



### 3.5.4 Primer for Cloning Experiments

CPM\_S 5' TGACAGATCTGGAGTGGGCCGGAGCGAC 3'  
 CPMpi\_AS 5' ATGACCATGGCCATGTTCTAGAGATGAATAAAAATAAGAAGAACC 3'

### 3.5.5 Bisulfite Amplicon Generation (Nested PCR)

M4-CpGas\_outer Forward: 5' ACCAACTTTCTCTTCTAACTTTCC 3'  
 Reverse: 5' AGATTTTTATGTTGAAGGTTAAGAG 3'

M4-CpGas\_inner Forward: 5' TTCTCTTCTAACTTTCCCTCTC 3'  
 Reverse: 5' GGTTAAGAGTTGGAGATTTTATAATG 3'

### 3.5.6 Bisulfite Amplicon Generation (MassARRAY)

Epi00100_SPI1.1_10F Epi00100_SPI1.1_T7R	aggaagagagGATTGGGTTAGGGTTTTAGATAGGA cagtaatacgactcactataggagaaggctCCAAACCCCTTAAACTTAACCATAC
Epi00103_STAT5A.1_10F Epi00103_STAT5A.1_T7R	aggaagagagAGTTGTTTGGTTTTGTGTGTTTTT cagtaatacgactcactataggagaaggctAAAAAATCCTACTTCTCTACCCA
Epi00104_STAT5A.2_10F Epi00104_STAT5A.2_T7R	aggaagagagAAAGTGATTTTTTTGAAGAGTGGTG cagtaatacgactcactataggagaaggctTCCAAAAAACAAATCAAAACCTAA
Epi00105_SLC27A3.1_10F Epi00105_SLC27A3.1_T7R	aggaagagagGAAGGGATTTGGTTTTGGTTATTAT cagtaatacgactcactataggagaaggctAAAAAACATCTCTATCCCTCCCTA
Epi00106_SLC27A3.2_10F Epi00106_SLC27A3.2_T7R	aggaagagagGGAGAGTTTTTTGGTTATGTTGTTG cagtaatacgactcactataggagaaggctAACCCCTAACCCATTTAATTCTACA
Epi00107_SLC27A3.3_10F Epi00107_SLC27A3.3_T7R	aggaagagagGGAGAGTATTTGTTGGTTGGTTTTA cagtaatacgactcactataggagaaggctAACCCCTAACCCATTTAATTCTACA
Epi00108_STAT5A.1_10F Epi00108_STAT5A.1_T7R	aggaagagagTTTATAGGGAGGTATTAGGGTTTGG cagtaatacgactcactataggagaaggctTCCCTTCTTCAAAAAAATTCCTAT
Epi00109_CCL13.1_10F Epi00109_CCL13.1_T7R	aggaagagagTTTGTTGGTTTGAATAGTTAGAAGGA cagtaatacgactcactataggagaaggctCAACAAACACAAAAACACTACAAAAA
Epi00110_CCL13.2_10F Epi00110_CCL13.2_T7R	aggaagagagTTTATGGTTTTTTATGGTGAATGGT cagtaatacgactcactataggagaaggctAAAATAACTTACCTAACCTAAACAAATCCC
Epi00111_P2RY6.1_10F Epi00111_P2RY6.1_T7R	aggaagagagTTTGTTATGTTTGGAGTTTGTAGA cagtaatacgactcactataggagaaggctAAAAAATACCCCTTACCAACCATT
Epi00112_P2RY6.2_10F Epi00112_P2RY6.2_T7R	aggaagagagGAGTGTAATGGTTGGTAAGGGTAT cagtaatacgactcactataggagaaggctAAATCCCAAATATCTTCAAAAAACC
Epi00116_CD207.2_10F Epi00116_CD207.2_T7R	aggaagagagATTTTTGGATTTTTATGTTTGGGAT cagtaatacgactcactataggagaaggctAACCCAAAATTCATACCTTTACTC
Epi00117_CBR3.1_10F Epi00117_CBR3.1_T7R	aggaagagagAGTTGATTGGTGAGTATGGGTTTTA cagtaatacgactcactataggagaaggctAAAATTAACCACCCCAATAAAAAA
Epi00123_DNASE1L3.1_10F Epi00123_DNASE1L3.1_T7R	aggaagagagTTTTTTAGGAAAGGGTTTATTTTT cagtaatacgactcactataggagaaggctAAAATCCAACACTCCAACACTACT

Epi00124_DNASE1L3.2_10F Epi00124_DNASE1L3.2_T7R	aggaagagagGGAGGAGAAGTAGTAGTGGGGTTAG cagtaatacgactcactataggagaaggctCACCCCAAATACCCTCTAAAATAAA
Epi00125_DNASE1L3.3_10F Epi00125_DNASE1L3.3_T7R	aggaagagagTGGTTTATTTTAGAGGGTATTTGGG cagtaatacgactcactataggagaaggctTCTCTAACAACACACTCCTAATATTTATAC
Epi00128_ANGEL1.1_10F Epi00128_ANGEL1.1_T7R	aggaagagagTTGATTTGATTATTGATGTTTTGAA cagtaatacgactcactataggagaaggctATCAATTTTCTTCTACCCAACCTCTTC
Epi00129_ANGEL1.2_10F Epi00129_ANGEL1.2_T7R	aggaagagagGAAGAGTTGGGTAGAAGAAAATTGAT cagtaatacgactcactataggagaaggctAACTCAAAAACCACTTTCATTTTCAT
Epi00131_CHI3L1.1_10F Epi00131_CHI3L1.1_T7R	aggaagagagGTAGAGTAGGGTAGGGTGTGGTTTT cagtaatacgactcactataggagaaggctTTCCACCTAACCAAAAACCTAAAAT
Epi00132_CHI3L1.2_10F Epi00132_CHI3L1.2_T7R	aggaagagagGTTTTTAGGTTGGGTAAGGGTTAGA cagtaatacgactcactataggagaaggctCATCAAACCTTAAATTCAAAAACCTC
Epi00133_CHI3L1.3_10F Epi00133_CHI3L1.3_T7R	aggaagagagAGAGGGAAAGATAGGGAAATTTTTA cagtaatacgactcactataggagaaggctCTTAAAAAACCTTAAACCCATTC
Epi00136_CCL13.2.1_10F Epi00136_CCL13.2.1_T7R	aggaagagagTTGTGATTTTGTGTTAATATTGAGTGT cagtaatacgactcactataggagaaggctCTTACAAACCAAAACAAAAATAAAC
Epi00143_MIA.2_10F Epi00143_MIA.2_T7R	aggaagagagGGTGGTTTTATGTTTAAAGTTGGTTG cagtaatacgactcactataggagaaggctCCTCAAATCTTCCCTTCATAAAAAAT
Epi00147_C9ORF78.2_10F Epi00147_C9ORF78.2_T7R	aggaagagagAGAGGTTTTGTGAGGAAGTTTTTT cagtaatacgactcactataggagaaggctACTACCCACACACTTCTATATCTCCTC
Epi00148_C1ORF78.3_10F Epi00148_C1ORF78.3_T7R	aggaagagagGGAATTTTGTATTTTTTTAGGGTGG cagtaatacgactcactataggagaaggctAAAACCACCATCCTCTAACTCTC
Epi00150_ZNF642.1_10F Epi00150_ZNF642.1_T7R	aggaagagagTTTTGGTTTTATTTGGGTTTAAAGT cagtaatacgactcactataggagaaggctAAAACCTATAAAAAATATCCCACCCC
Epi00153_ADPGK.1_10F Epi00153_ADPGK.1_T7R	aggaagagagAGGTTATGTTTAAAGGTTAGAGTTAGAGT cagtaatacgactcactataggagaaggctCTCATAAATCCCTACCAAACAAAAA
Epi00154_ADPGK.2_10F Epi00154_ADPGK.2_T7R	aggaagagagGTTTTTGTGGTAGGGATTTATGA cagtaatacgactcactataggagaaggctATTAaaaaacAAACTTCCCATTTC
Epi00156_C14ORF8.1_10F Epi00156_C14ORF8.1_T7R	aggaagagagATTGAAATAGTGGTTGGAAGTAAGA cagtaatacgactcactataggagaaggctCACTCCCAACTCCCTAACCTTAATA
Epi00159_RAP1GAP.2_10F Epi00159_RAP1GAP.2_T7R	aggaagagagTAGTTTTATAGGGTTGGGGATTAG cagtaatacgactcactataggagaaggctTCCTAAACAAAAAATCAAAAAACCC
Epi00162_MMP7.1_10F Epi00162_MMP7.1_T7R	aggaagagagGGAATTTTAAAGTAAGTGGGTTGTGA cagtaatacgactcactataggagaaggctACAATCACTAACAAAAAACACCAAA
Epi00165_CCL17.1_10F Epi00165_CCL17.1_T7R	aggaagagagTTGAGAATATATTGTAGGGGGTAAGG cagtaatacgactcactataggagaaggctCCCCAAATCTAAAACCTAAATTTCT
Epi00166_CCL17.2_10F Epi00166_CCL17.2_T7R	aggaagagagAGAAATTTAGTTTTAGATTTGGGGG cagtaatacgactcactataggagaaggctATTTTAAATTCAACTCTCCCATCAA
Epi00167_CCL17.3_10F Epi00167_CCL17.3_T7R	aggaagagagTTGAGGTTTAGAGAGAAGTGATTTTG cagtaatacgactcactataggagaaggctAACACCTCCCTCATCAACTACATAC
Epi00170_BACH2.1_10F Epi00170_BACH2.1_T7R	aggaagagagGTGTTAGTGTGTTGGTGGTGGTGGT cagtaatacgactcactataggagaaggctCAACACCTTCAACTTACTTTCAACC
Epi00171_BACH2.2_10F Epi00171_BACH2.2_T7R	aggaagagagTGGTTGAAAGTAAGTTGAAGGTGTT cagtaatacgactcactataggagaaggctTTTATCCTAAAAAACACCAAAACCAA

Epi00172_BACH2.3_10F Epi00172_BACH2.3_T7R	aggaagagagAATTTTTGGTTTGGTTAGGT cagtaatacgactcactataggagaaggctTCTCAAAATAAAAAACTCCAATCT
Epi00176_PLLP.1_10F Epi00176_PLLP.1_T7R	aggaagagagGAAAGTAAAGAAGATTTTGGGAGATT cagtaatacgactcactataggagaaggctAACCTCCCATCTTCTAAATAACCCC
Epi00178_KIAA0430.1_10F Epi00178_KIAA0430.1_T7R	aggaagagagTTAGTGAGAGTGGTTGAAGTTTTAGA cagtaatacgactcactataggagaaggctCCCTAATAAAACCCTCCAAAAATAA
Epi00179_KIAA0430.2_10F Epi00179_KIAA0430.2_T7R	aggaagagagTTGTGTATTTTATTTTGGAGGGTT cagtaatacgactcactataggagaaggctAAAAACAATATCCCCTCTTTCCC
Epi00181_TPP2.1_10F Epi00181_TPP2.1_T7R	aggaagagagGGGGTGGGTAGAGGTTAGAGTTAG cagtaatacgactcactataggagaaggctAAAAATCCCTAAAACCAAAAAAAAA
Epi00182_TPP2.2_10F Epi00182_TPP2.2_T7R	aggaagagagGGGGAAGTTTGGGTTTTTTTTT cagtaatacgactcactataggagaaggctTTACCTATCTAATATCTCCACCCCA
Epi00184_CLEC10A.1_10F Epi00184_CLEC10A.1_T7R	aggaagagagGAAGATAAGGTTGGAATGGGTTAT cagtaatacgactcactataggagaaggctACCTCTAATCCTTACAACACAACCA
Epi00185_CLEC10A.2_10F Epi00185_CLEC10A.2_T7R	aggaagagagTATTATTATTTGTGGGAGGTTTGGGA cagtaatacgactcactataggagaaggctAACAAAATAACCTCAAACCCAACT
Epi00188_MAPKAPK3.1_10F Epi00188_MAPKAPK3.1_T7R	aggaagagagGGGTGTAGAGGATAGTTTTAGAAATGA cagtaatacgactcactataggagaaggctCTCTTCTCCCCTAACTAACAAAACC
Epi00189_MAPKAPK3.2_10F Epi00189_MAPKAPK3.2_T7R	aggaagagagGGTTTTGTTAGTTAGGGGAGAAGAG cagtaatacgactcactataggagaaggctATAAACCTACAACCTCTCCAATC
Epi00191_TRIM15.1_10F Epi00191_TRIM15.1_T7R	aggaagagagGGTTATTATGGGTAGATGTGGTGAG cagtaatacgactcactataggagaaggctAATACCAACACAAAAAACCACTA
Epi00192_TRIM15.2_10F Epi00192_TRIM15.2_T7R	aggaagagagAAGGTGTGTTTATAGGGAATGGTTA cagtaatacgactcactataggagaaggctCCAACCACTATAATCTACAAATTCCA

### 3.6 Antibiotics

Ampicillin	Ratiopharm, Ulm, Germany
Hygromycin	Clontech, Mountain View, USA
Zeozin	Invitrogen, Karlsruhe, Germany

### 3.7 Plasmids

pCpG-mcs	Invivogen, San Diego, USA
pGL3-Basic	Promega, Mannheim, Germany
phRL-TK	Promega, Mannheim, Germany
pMOD-LucShS	Invivogen, San Diego, USA

### 3.8 E.coli Strains

PIR1(F-  $\Delta$ lac169 rpoS(Am) robA1 creC510  
hsdR514 endA recA1 uidA[ $\Delta$ mluI]:pir-116) Invitrogen, Karlsruhe, Germany

### 3.9 Antibodies

#### Chromatin Immunoprecipitation (ChIp)

Anti-acetyl-Histone H3	Millipore, Temecula, USA
Anti-acteyl-Histone H4	Millipore, Temecula, USA
Anti-dimethyl-Histone H3 (Lys4)	Millipore, Temecula, USA
Anti-trimethyl-Histone H3 (Lys4)	Millipore, Temecula, USA
Rabbit polyclonal to Histone H3 (monomethyl K4)	abcam, Cambridge, UK
Rabbit polyclonal to RNA pol II	abcam, Cambridge, UK
CTD repeat YSPTSPS (phosphor S5)	
STAT6	Santa Cruz Biotechnology Inc., Santa Cruz, USA

#### FACS Staining

Anti CD1a_PE	BD, Heidelberg, Germany
Anti CD14_FITC	BD, Heidelberg, Germany
Anti CD3_FITC	BD, Heidelberg, Germany
Anti CD20_FITC	Beckmann Coulter; Fullerton, USA
Anit IgG <sub>gesamt</sub> _FITC	Beckmann Coulter; Fullerton, USA

#### Western Blot

Goat anti IgG F(c), HRP conjugated	Rockland, Gilbertsville, USA
------------------------------------	------------------------------

## 3.10 Cell Lines

### Human Cell Lines

THP-1	Human acute monocytic leukemia (DSMZ ACC 16)
HepG2	Human hepatocellular carcinoma (DSMZ ACC 180)
U-937	Human histiocytic lymphoma (DSMZ no. ACC5)

### Murine Cell Lines

NIH3T3	Swiss mouse embryo fibroblast (DSMZ no. ACC 59)
RAW	Mouse monocyte-macrophage BALB/c (ATCC TIB-71)

### Insect Cell Lines

Drosophila Schneider2 (S2) cells	Derived from a primary culture of late stage <i>Drosophila melanogaster</i> embryos (20-24h) (ATCC CRL-1963)
----------------------------------	--

## 3.11 Databases and Software

Agilent feature extraction 9.5.1	Agilent Technologies, Waldbronn, Germany
BLAT	<a href="http://genome.brc.mcw.edu">http://genome.brc.mcw.edu</a>
EpiTYPER 1.0	Sequenom, Hamburg, Germany
Generunner version 3.05	
Genespring 10.0.2	Agilent Technologies, Waldbronn, Germany
Perlprimer version 1.1.14	
PubMed	<a href="http://www.ncbi.nlm.nih.gov/entrez">www.ncbi.nlm.nih.gov/entrez</a>
Spotfire decision site 7.0	
UCSC Genome. Browser	<a href="http://www.genome.ucsc.edu">www.genome.ucsc.edu</a>

## 4 Methods

### 4.1 General Cell Culture Methods

For washing and harvesting, mammalian cells were centrifuged using the general cell program: 8 min, 300×g, 4°C.

#### 4.1.1 Cell Line Culture

##### 4.1.1.1 Culture Conditions and Passaging

If not otherwise indicated, cells were cultured in RPMI 1640 (HyClone) or DMEM (Gibco) (Table 4-1) routinely supplemented with 10% inactivated FCS, L-glutamine (2 mM), sodium pyruvate (1 mM), antibiotics (50 U/ml penicillin and 50 µg/ml streptomycin), 2 ml vitamins, non essential amino acids and 50 µM β-mercaptoethanol. Media supplements were purchased from Gibco and Biochrome (L-glutamine) respectively.

FCS was heat inactivated for 30 min at 56°C before use. Exceeding incubation times and higher temperatures should be avoided because heat sensitive growth factors could be damaged. Each batch of FCS as well as each RPMI batch was tested before use.

Cells were cultured at 37°C, 5% CO<sub>2</sub> and with 95% relative humidity in an incubator.

**Table 4-1 Culturing and passaging conditions**

Cell Line	Culture medium	Passaging
U937	RPMI 1640	Cells in suspension
THP-1	RPMI 1640	Cells in suspension
HepG2	RPMI 1640	Splitting by trypsination
RAW264.7	RPMI 1640	Splitting by scraping
NIH3T3	DMEM	Splitting by trypsination

Cell cultures were split 1:4 to 1:8 in fresh medium every 2-4 days. Adherent cells were washed once with PBS and either scraped or disaggregated by incubation with 0.05% Trypsin/0.02% EDTA/PBS (3 ml per 75 cm<sup>2</sup> culture vessel area) at 37°C for 5 min until cells detached. Trypsin was then inactivated by adding 6 ml medium with 10% FCS.

#### **4.1.1.2 Culturing of Stably Transfected *Drosophila* S2 Cells and Production of MBD-Fc**

MBD-Fc stands for a fusion protein composed of the methyl-CpG binding domain (MBD) of human MBD2 (methyl-CpG binding domain protein 2) and the F<sub>c</sub>-tail of human IgG1. The MBD-Fc vector was stably transfected into *Drosophila* S2 cells using Effectene transfection reagent (Qiagen) and hygromycin selection. A detailed description of the design and the generation of the fusion protein is given in (Gebhard et al., 2006b; Gebhard et al., 2006a).

#### **Expansion in Cell Culture Bottles**

MBD-Fc S2 cells were seeded at a density of  $1-2 \times 10^6$  cells/ml in Insect-Xpress medium (Lonza) including 50 U/ml penicillin and 50 µg/ml streptomycin but without FCS at 21-23°C. 400 µg hygromycin were added for selection of plasmid containing cells. Cells were splitted once a week, without exceeding  $10 \times 10^6$  cells/ml.

#### **Protein Production**

Cells were transferred into 2000 ml roller bottles and cultured at a density of  $4 \times 10^6$  cells/ml in up to 400 ml Insect-Xpress medium supplemented with penicillin, streptomycin and hygromycin as described above. Cells should never exceed a density of  $10 \times 10^6$  cells/ml. For large-scale protein production, after 3-5 days the culture media was exchanged and  $5 \times 10^6$  cells/ml were seeded in 400 ml Insect-Xpress. Instead of hygromycin, 0.5 mM CuSO<sub>4</sub> were added to stimulate the metal-inducible promoter of the used vector. The MBD-Fc containing culture medium was harvested after 4 days like described in section 4.3.1. For recovery, cells were cultured again in Insect-Xpress medium containing standard antibiotics and selection antibiotic for 3-5 days. The cycle of production was repeated until protein quality and amount clearly decreased.

#### 4.1.1.3 Assessing Cell Number and Vitality

The number of viable and dead cells was determined by Trypan blue exclusion. Cell suspensions were diluted with Trypan blue solution and cells were then counted in a Neubauer haemocytometer. The concentration of viable cells was then calculated using the following equation:

$$\text{Number of viable cells/ml} = \frac{C}{N} \times D \times 10^4$$

With N: average of unstained cells per corner square (1 mm<sup>2</sup> containing 16 sub-squares)  
D: dilution factor

Required solutions and materials:

Trypan blue solution: 0.2% (w/v) Trypan blue in 0.9% NaCl solution  
Neubauer haemocytometer slide with coverslip

#### 4.1.1.4 Freezing and Thawing Cells

Cells were harvested and suspended at  $5\text{-}10 \times 10^6$  cells/ml in 800  $\mu\text{l}$  ice cold medium, including 10% FCS. After inverting the mix and transferring it into cryo-vials, 160  $\mu\text{l}$  DMSO (10% final) and 640  $\mu\text{l}$  FCS (40% final) were added. Tubes were rapidly inverted to mix cells properly. To allow gradual freezing at a rate of 1°C/min, the cryo-vials were placed into isopropanol-filled cryo-containers (Nalgene) and frozen at -80°C for 24 h. For long-term storage, the tubes were transferred in liquid nitrogen (-196°C) for.

#### 4.1.1.5 Mycoplasma Assay

Cell lines were routinely checked for mycoplasma contamination by the MycoAlert® Mycoplasma detection assay (Cambrex, Rockland, USA) according to the manufacturer's instructions.



## 4.1.2 Transient Transfection of Mammalian Cells

### 4.1.2.1 Lipofectamine Transfection

HepG2 as well as RAW264.7 were most efficiently transfected using the Lipofectamine™ 2000 reagent from Invitrogen (Karlsruhe, Germany) following the manufacturer's instructions with slight modifications. In brief, adherent cells were seeded ( $0.5 \times 10^6$  cells/ml; 2 ml) in 6-well plates using growth medium without antibiotics one day before transfection. For each transfection sample complexes were prepared as follows (referring to 6-well plates):

Solution A: 3 µg vector DNA were incubated with 100 ng Renilla vector (pHRL-TK, control reporter; usually 1/20 – 1/50 of the amount of the reporter of interest) and 100 µl Opti-MEM for 5 min at RT

Solution B: 7 µl lipofectamine were mixed with 100 µl Opti-MEM

Combined together, solutions A + B were incubated for 20 min at RT. Subsequently, the whole mixture was dropped slowly onto the cells followed by gently rocking the plate back and forth to mix the cells with the complexes. After approximately 24 hours, the cells were ready for measuring transgene expression via luciferase expression.

### 4.1.2.2 Transfection Using DEAE Dextran

To transfect THP-1 cells, one of the oldest transfection methods called “Transfection with DEAE Dextran” was used. The underlying principle is the binding of DNA to poly-cations resulting in DNA-Dextran-complexes that are dropped on cell suspensions. Those complexes were then taken up via endocytosis.

One day before transfection, cells were seeded at a density of  $0.5 \times 10^6$  cells/ml calculating with  $3 \times 10^6$  cells per transfection sample. 70 µl 1×STBS buffer were mixed with 10 ng Renilla control reporter (pHRL-TK ) and 200 ng plasmid DNA in an Eppendorf cup. Just prior to use, DEAE dextran was dissolved in STBS buffer and 70 µl were added to each prepared plasmid sample. Complexes were then gently dropped onto cells and incubated for 20 min at 37°C in an incubator. To stop the reaction, 1×STBS buffer was added before centrifugation. Cells were then washed twice with 1×STBS and finally transferred to cell culture dishes in 6 ml RPMI including 10% FCS. After 48 hours cells were ready for lysis and measuring luciferase activity.

Required buffers and solutions:

10×STBS buffer	25 ml 1 M	(25 mM)	Tris pH 7.4
	8 g	(137 mM)	NaCl
	6.372 g	(5 mM)	KCl
	0.160 g	(0.6 mM)	Na <sub>2</sub> HPO <sub>4</sub> 7H <sub>2</sub> O
	0.102 g	(0.7 mM)	CaCl <sub>2</sub>
	Add ddH <sub>2</sub> O to 1000 ml		
DEAE Dextran:	10 mg/ml in STBS		

### 4.1.2.3 Measuring Luciferase Activity

Luciferase activity was tested with the Dual-Luciferase Reporter Assay System (Promega) following the manufacturer's instructions. Briefly, 24-48 hours after transfection, cells were transferred to 14 ml polystyrene round-bottom tubes (Falcon), centrifuged at 300×g for 10 minutes and washed with PBS. After discarding the supernatant, cells were lysed by adding 100 µl – 150 µl diluted lysis buffer and incubation for at least 10 min at RT. The lysate was cleared and Firefly as well as Renilla luciferase activities were measured on a Sirius photometer. Firefly luciferase activity of individual transfections was normalised against Renilla luciferase activity.

## 4.1.3 Primary Cells

### 4.1.3.1 Isolation of Monocytes

Peripheral blood mononuclear cells (PB-MNCs) were separated by leukapheresis of healthy donors (Graw, Jr. et al., 1971), followed by density gradient centrifugation over Ficoll/Hypaque (Johnson, Jr. et al., 1977). Monocytes were then isolated from MNCs by counter current centrifugal elutriation (Sanderson et al., 1977).

Elutriation was performed in a J6M-E centrifuge equipped with a JE 5.0 elutriation rotor and a 50 ml flow chamber (Beckman, Munich, Germany). After sterilising the system with 6% H<sub>2</sub>O<sub>2</sub> for 20 min, the system was washed with PBS. Following calibration at 2500 rpm and 4°C with Hanks BSS, MNCs were loaded at a flow rate of 52 ml/min. Fractions were collected and the flow through rate was sequentially increased according to Table 4-2.

**Table 4-2 Elutriation parameter and cell types**

Fraction	Volume (ml)	Flow rate (ml/min)	Main cell type contained
Ia	1000	52	platelets
Ib	1000	57	B- and T- lymphocytes, NK cells
IIa	1000	64	
IIb	500	74	
IIc	400	82	
IId	400	92	
III	800	130	monocytes

Monocytes represent the largest cells within the MNCs and are therefore mainly obtained in the last fraction. Monocytes were >85% pure as determined by morphology and CD14 antigen expression. Low amounts of monocytes may be also detected in the IId fraction. Monocytes (fraction III) were centrifuged (8 min, 300×g, 4°C), resuspended in RPMI culture medium and counted. Monocyte yields were donor dependent, typically between 10-20% of total MNCs. Supernatants of monocyte cultures were routinely collected and analysed for the presence of interleukin-6 (IL-6), which was usually low, indicating that monocytes were not activated before or during elutriation.

#### 4.1.3.2 Cultivation of Monocytes

##### 4.1.3.2.1 Dendritic Cells

Immature monocyte-derived dendritic cells (DCs) were generated by culturing  $1 \times 10^6$ /ml elutriated monocytes in RPMI containing 10% FCS, 20 U/ml recombinant human IL-4 (Promokine, Heidelberg, Germany) and 280 U/ml GM-CSF (Berlex, Seattle, USA) as described earlier (Meierhoff et al., 1998). Note that culture concentrations of IL-4 and GM-CSF may vary when the company is changed.

##### 4.1.3.2.2 Macrophages

In order to generate macrophages *in vitro*,  $1 \times 10^6$ /ml monocytes were cultured in RPMI 1640 in presence of 2% human pooled AB-group serum on teflon foils. For harvesting, macrophages were cooled to 4°C for 30 min and subsequently detached by carefully “juddering” the teflon foils (Andreesen et al., 1983).

## 4.2 General Molecular Biology

### 4.2.1 Bacterial Culture

#### 4.2.1.1 Bacterial Growth Medium

*E.coli* strains were streaked out on solid LB-agar with appropriate antibiotics and grown overnight (O/N) at 37°C. Single colonies were then picked into liquid LB-medium containing the corresponding antibiotics (see section 3.6) and grown overnight at 37°C with shaking at 200 rpm.

LB-medium:    10 g            NaCl  
                   10 g            Bacto Tryptone (Difco)  
                   5 g                Yeast extract  
                   Add ddH<sub>2</sub>O to 1000 ml, autoclave

LB-agar plates: 15 g            Agar  
                   10 g            NaCl  
                   10 g            Bacto Tryptone (Difco)  
                   5 g                Yeast extract  
                   Add ddH<sub>2</sub>O to 1000 ml, autoclave, cool to 50°C and add the appropriate antibiotic  
                   Pour the agar solution into 10 cm Petri dishes, and store inverted at 4°C

#### 4.2.1.2 Transformation of Chemically Competent *E.coli*

Chemically competent *E.coli* (50 µl) were thawed on ice, 1-25 ng plasmid DNA in 2-5 µl volume was added and the suspension was mixed gently and incubated on ice for 30 min. Cells were heat-shocked in a water bath at 42°C for 30 s, immediately cooled on ice for 2 min and 250 µl SOC medium was added. To express the resistance, bacteria were incubated for 1 h at 37°C with shaking and 50-150 µl of the transformation were plated and incubated overnight at 37°C on LB-agar containing the antibiotic necessary for selection of transformed cells.

SOC medium    20 g    (2%)            BactoTrypton (Difco)  
                   5 g    (0.5%)        BactoYeastExtract (Difco)  
                   0.6 g   (10 mM)      NaCl  
                   0.2 g   (3 mM)        KCl  
                   Add ddH<sub>2</sub>O to 1000 ml, autoclave and add to the cooled solution:  
                   10 ml   (10 mM)      MgCl<sub>2</sub> (1 M), sterile filtered  
                   10 ml   (10 mM)      MgSO<sub>4</sub> (1 M), sterile filtered  
                   10 ml   (20 mM)      Glucose (2 M), sterile filtered

### 4.2.1.3 Glycerol Stock

For long-term storage, bacteria were stored at -80°C in 20% glycerol by adding 600 µl liquid culture to 200 µl of 80% glycerol.

### 4.2.2 Plasmid Isolation from *E.coli*

To check if the isolated single *E.coli* colonies contained the correct plasmid, a DNA mini-prep was carried out using NucleoSpin® Plasmid Quick Pure Kit from Macherey-Nagel following the supplied instructions. To isolate larger amounts of ultra pure DNA (100 µg) for transfection experiments, plasmids were isolated using the endotoxin-free QIAGEN Plasmid Midi Kit.

### 4.2.3 Molecular Cloning

DNA fragments to be cloned were prepared by PCR from genomic DNA or cDNA. For directional cloning, restriction sites were introduced by adding the appropriate recognition sequences to the primer sequences. Excised fragment and vector were gel-purified and combined in a 10 µl ligation reaction at a 3- to 5-fold molar excess of insert to vector, using 25-50 ng of vector. Ligation was carried out overnight at 16°C with 1 U T4 DNA ligase and 1 µl 10×T4 DNA ligase buffer. 2 µl of the reaction were used to transform chemically competent *E.coli* (see section 4.2.1.2). Successful insertion of the fragment into the vector was controlled by preparing plasmid DNA from liquid cultures (see sections 4.2.1.1 and 4.2.2.). To control correct insertion and sequence integrity, plasmid constructs were sequenced by Genart (Regensburg, Germany) using vector-specific primers.

#### 4.2.3.1 Construction of the pCpGL-basic Vector

The enhancer/promoter region of the CpG-free plasmid pCpG-mcs (Invivogen) was excised using *Pst I/Nhe I* (see also sections 4.2.5.5 to 4.2.5.9) and replaced by a short CpG-free linker, representing the multiple cloning site (MCS; with *Pst I*, *Spe I*, *BamHI*, *Bgl II*, *Hind III* and *Nco I* sites):

5'-CTG CAG GAC TAG TGG ATC CAG ATC TTA AGC TTA GTC CAT GGA CAA TTG CTA GC-3'

The CpG-free luciferase coding region was released from pMOD-LucShS (Invivogen) by restriction with *Mfe I* (blunted using Klenow polymerase) and *Nco I*. The fragment was then subcloned into the *Nhe I* (also blunted with Klenow polymerase) and *Nco I* digested, linker ligated CpG-free backbone. After controlling the insert by sequencing, the newly synthesized CpG-free reporter vector, called pCpGL-basic, was now ready for subcloning promoters of interest or for *in vitro* methylation, directly followed by transient transfection. A physical map of this vector is given in Figure 5-2.

The plasmid uses a modified *E.coli* R6K gamma origin of replication (R6Kori) and therefore has to be grown in cells expressing the *pir* gene that encodes the R6K specific initiator protein. All following cloning experiments using the pCpGL-backbone, were performed with *E.coli* PIR1 bacteria under zeocin selection (25 µg/ml).

#### 4.2.3.2 Cloning of Reporter Vectors

- pGL3-EF1:** Reporter construct with 286 CpGs in the vector backbone  
The human *EF1A*-promoter was released from pCpG-mcs (Invivogen) using *Spe I* and *Hind III* and inserted into *Nhe I/Hind III* sites of pGL3-basic.
- pCpGL-CMV:** CpG-free control promoter-enhancer construct  
The human *EF1A*-promoter/CMV-enhancer cassette was released from pCpG-mcs using *Pst I/Hind III* and inserted into equivalent sites of pCpGL-basic
- pCpGL-CPM:** CpG-island containing promoter construct (40 CpGs)  
The *CPM*-promoter was amplified from gDNA using the CPM\_S and CPMpi\_AS primers (see section 3.5.4) and subcloned into pCpGL-basic vector via *Nco I* and *Bgl II* sites.
- pCpGL-CHI3L1:** Low CpG-density promoter construct (8 CpGs)  
The *Nhe I/Bgl II* fragment of a previously described CHI3L1 reporter vector (HC-377; (Rehli et al., 2003)) was cloned into *Spe I/Bgl II* sites of pCpGL-basic.

#### 4.2.4 *In Vitro* Methylation of Plasmid DNA

Luciferase reporter constructs were methylated *in vitro* using *Sss I*, *Hha I* and *Hpa II* methylases according to the manufacturer's recommendation. Briefly, 10-20 µg plasmid DNA were incubated with 2.5 U/µg methylase in the presence of 160 µM S-Adenosylmethionine (SAM; methyl group donor) for four hours at 37°C. After 2 hours the reaction was supplied with another 160 µM SAM. Simultaneously, control reactions were treated as above but without addition of SAM and methylating enzymes. After the methylation reaction, plasmids were purified using the NucleoSpin® Plasmid Quick Pure Kit from Macherey-Nagel or by phenol-chloroform extraction followed by ethanol precipitation and finally quantified using a NanoDrop Spectrophotometer. Completeness of methylation was controlled by digesting both methylated and unmethylated DNA using the methylation sensitive restriction enzymes *Hha I* and *Hpa II* as well as the methylation insensitive *Msp I*.

#### 4.2.5 Preparation and Analysis of DNA

##### 4.2.5.1 Isolation and Quality Control of Genomic DNA

Genomic DNA (gDNA) was isolated using the Qiagen Blood & Cell Culture DNA Midi Kit or, for smaller cell numbers, the Blood and Tissue Culture Kit (Qiagen). gDNA concentration was then determined with the NanoDrop spectrophotometer and quality was assessed by agarose gel electrophoresis.

##### 4.2.5.2 Precipitation of DNA Using PEG (Polyethylene Glycol)

To precipitate DNA from small volumes, e.g. PCR reactions or endonuclease digestion, one volume of PEG-mix was added to the DNA-containing solution, vortexed and incubated for 15 min at RT. After centrifugation (15 min, 13000 rpm, RT), the supernatant was discarded and the precipitated DNA was washed by carefully adding 200 µl 100% EtOH to the tube wall opposite of the (often invisible) pellet. Following centrifugation (10 min, 13000 rpm, RT), the supernatant was carefully removed. The pellet was dried and resuspended in H<sub>2</sub>O in half to three-quarters of the initial volume.

PEG-mix	26.2 g	(26.2%)	PEG 8000
	20 ml	(0.67 M)	NaOAc (3 M) pH 5.2
	660 µl	(0.67 mM)	MgCl <sub>2</sub> (1 M)
	Add ddH <sub>2</sub> O to 250 ml		

#### 4.2.5.3 Purification of DNA with Phenol Chloroform Extraction

1 Volume (V) Phenol-Chloroform-Isoamylalcohol (25:24:1; pH 8) was mixed with the DNA containing solution. After centrifugation the DNA containing, aqueous phase was transferred into new Eppendorf cups, mixed with 1 V Chloroform-Isoamylalcohol (49:1) and centrifuged again. The aqueous phase was transferred again into a new cup and precipitated with 0.1 V 3 M NaAc (pH 5.2) and 2.5 V 100% EtOH for at least 1 hour at -20°C. Precipitated DNA was then washed with 80% EtOH and dissolved in 1×TE buffer.

Required buffers:

1×TE pH 8.0	1 ml	(1 M)	Tris (1 M; pH 8.0)
	0.2 ml	(1 mM)	Na <sub>2</sub> EDTA (0.5 M; pH 8.0)
	Add ddH <sub>2</sub> O to 100 ml		

#### 4.2.5.4 Agarose Gel Electrophoresis

The required amount of agarose as determined according to Table 4-3, was added to the corresponding amount of 1×TAE. The slurry was heated in a microwave oven until the agarose was completely dissolved. Ethidium bromide was added after cooling the solution to 50-60°C. The gel was cast, mounted in the electrophoresis tank and covered with 1×TAE. DNA-containing samples were diluted 4:1 with DNA loading dye (5×), mixed and loaded into the slots of the submerged gel. Depending on the size and the desired resolution, gels were run at 40-100 Volt for 30 min to 3 h

**Table 4-3 Agarose concentration for different separation ranges**

Efficient range of separation (kb)	% agarose in gel
0.1 – 2	2.0
0.2 – 3	1.5
0.4 – 6	1.2
0.5 – 7	0.9
0.8 - 10	0.7
genomic DNA	0.5



Required buffers:

TAE (50×)	252.3 g 20.5 g 18.5 g Add ddH <sub>2</sub> O to 1000 ml	(2 M) (250 mM) (50 mM)	Tris NaOAc/HOAc, pH 7.8 EDTA
EDTA (0.5 M)	18.6 g Add ddH <sub>2</sub> O to 100 ml	(0.5 M)	EDTA/NaOH, pH 8.0
DNA loading dye DNA-LD (5×)	500 µl 500 µl 1 ml 4 ml 10 mg Add ddH <sub>2</sub> O to 10 ml, store at 4°C	(50 mM) (1%) (50 mM) (40%) (1%)	Tris/HCl, pH 7.8 SDS (20%) EDTA (0.5 M), pH 8.0 Glycerol Bromphenol blue
1.0% Agarose	1 g Add 1× TAE to 100 ml and heat in a microwave until agarose is completely dissolved Cool to 50°C and add 2.5 µl Ethidium bromide (10 mg/ml) (Sigma)	(1%)	Agarose (Biozym)

#### 4.2.5.5 Restriction Endonuclease Digestion

To verify the presence and orientation of plasmid-inserts, or to clone insert DNA into a plasmid, DNA was digested with appropriate restriction enzymes. Enzymes and their buffers were purchased from Roche or New England Biolabs (Germany). The digestion of plasmid DNA or PCR products was carried out using 10 U enzyme/1 µg DNA in 20 µl at 37°C for 2 hours. Digestion of genomic DNA was performed overnight with 1.5 U/µg DNA in 30 µl reaction volume.

#### 4.2.5.6 Dephosphorylation of DNA with Alkaline Phosphatase

To prevent self ligation, digested vectors were treated with AP (calf intestinal alkaline phosphatase, Roche) at 37°C for 30 min before gel extraction.

#### 4.2.5.7 Fill in 5'-Overhangs with Klenow-DNA-Polymerase

To ligate two DNA fragments cut with two incompatible enzymes, blunt ends were generated by filling the 5'- or the 3'-overhangs. To fill in 5'-overhanging ends of DNA fragments, digested DNA was mixed with 1 µl of dNTPs (0.5 mM each), 4 U Klenow fragment and H<sub>2</sub>O to a total volume of 20 µl, and incubated for 15 min at 30°C. The inactivation of Klenow was done by heating for 10 min at 75°C. The DNA fragment with blunt ends was then either digested with a second enzyme or purified and used for ligation.

#### 4.2.5.8 Generation of Blunt Ends with T4 DNA Polymerase

To fill in 3'-overhanging ends of DNA, T4 polymerase was used. Digested DNA was incubated with T4 polymerase at 11°C for 20 min. T4 polymerase was then inactivated for 20 min at 70°C.

#### 4.2.5.9 Purification of DNA Fragments by Gel Extraction

DNA fragments were purified by running on an ethidium bromide-containing agarose gel. The band containing the fragment of interest was excised under UV illumination. Fragments were then purified by gel extraction using QIAEX II Gel Extraction Kit (Qiagen) or NucleoSpin® Extract II following the manufacturer's instructions.

#### 4.2.5.10 Polymerase Chain Reaction (PCR)

The polymerase chain reaction (PCR) allows *in vitro* synthesis of large amounts of DNA by primed, sequence-specific polymerization of nucleotide triphosphates, catalysed by DNA polymerase (Mullis et al., 1986). PCRs were generally performed in "thick" PCR tubes with a reaction volume of 20-100 µl in a MJ research PTC 200 thermocycler (Biozym). The "calculated temperature" feature was used to decrease temperature hold times. The nucleotide sequences of the utilised primers are given in section 3.5. The primer annealing temperatures varied between 57 and 65°C. General parameter settings for analytical PCR are summarized in Table 4-4.

<b>Reaction set up:</b>	0.04 – 0.67 U/µl	Taq DNA polymerase or Expand High Fidelity polymerase mix with the supplied reaction buffer
	0.2 – 1 µM	Sense-/antisense primer (10 – 100 µM)
	0.2 – 0.25 mM	dATP, dCTP, dGTP, dTTP

**Table 4-4 Reaction parameter for analytical PCR**

PCR step		Cycling parameter
Initial melting		95°C 2 min
20 - 35 cycles	Melting	95°C 15 s
	Annealing	65°C 15 s
	Extension	72°C 60 s
Final extension		72°C 5-7 min
Cool to		15°C

## Real Time PCR

Quantitative Real Time PCR (qPCR) was used for quantification of cDNA after reverse transcription (4.2.6.3) as well as for analysis after chromatin immunoprecipitation (4.2.8). PCR reactions were performed using the QuantiFast SYBR Green Kit from Qiagen in 96-well format adopted to the Eppendorf Realplex Mastercycler EpGradient S (Eppendorf, Hamburg, Germany). The relative amount of amplified DNA is measured through the emission of light by the SYBR green dye, when it is intercalated in double stranded DNA.

**Reaction setup:** 5  $\mu$ l SYBR Green mix (2 $\times$ ) (QuantiFast, Qiagen)  
 2  $\mu$ l ddH<sub>2</sub>O  
 0.5  $\mu$ l primer forward (10  $\mu$ M)  
 0.5  $\mu$ l primer reverse (10  $\mu$ M)  
 2  $\mu$ l DNA

**Table 4-5 Reaction parameter for real time PCR**

PCR step		Cycling parameter
Initial melting		95°C, 5 min
45 cycles	Melting	95°C, 8 s
	Combined annealing and extension	60°C, 20 s
Final cycle	Melting	95°C, 15 s
	Combined annealing and extension	60°C, 15 s
Melting curve		10 – 20 min
		95°C 15 sec

To calculate amplification efficiency, a dilution series (1:10; 1:50; 1:100, 1:1000) of a suitable sample was additionally measured for each primer pair. Realplex software calculated automatically DNA amounts based on the generated *slope* and *intercept*. Specific amplification was controlled by melting-curve analysis and data were imported and processed in Microsoft Excel 2003. All samples were measured in duplicates and normalised to the  $\beta$ -Actin or the HPRT housekeeper when analysing mRNA Expression. Duplicates of ChIP samples were normalised to the input or a control region.

#### 4.2.5.11 Bisulfite Sequencing

Modification of gDNA with sodium bisulfite, leading to conversion of unmethylated cytosine residues into uracil while not affecting 5-methylcytosine (Frommer et al., 1992), was performed using the Qiagen EpiTect Bisulfite Kit as recommended by the manufacturer. 10 µl of bisulfite treated DNA were used for the first nested PCR reaction.

<b>Outer PCR set up:</b>	5 µl	(1×)	Taq-PCR-buffer (10×)
	1 µl	(0.2 mM)	dNTP (10 mM each)
	2 µl	(0.4 µM)	sense primer (1s; 10 µM)
	2 µl	(0.4 µM)	anti-sense primer (1as; 10 µM)
	2.5 U	(0.5 µl)	TaqDNA Polymerase
	27.5 µl		ddH <sub>2</sub> O
	10 µl	(1 µg)	Bisulfite treated DNA

**Table 4-6 Reaction parameter for outer nested PCR**

PCR step		Cycling parameter
Initial melting		93° C, 5 s
31 cycles	Melting	93°C, 15 s
	Annealing	55°C, 15 s
	Elongation	72°C, 70 s
Final elongation		72 °C, 5 min
Cooling		4°C for ever

After finishing the first PCR, amplification products were directly used for the second, inner PCR step:

<b>Inner PCR set up</b>	5 µl	(1×)	FastStart Taq PCR-buffer (10×)
	1 µl	(0.2 mM)	NTP (10 mM each)
	2 µl	(0.4 µM)	sense primer (2s; 10 µM)
	2 µl	(0.4 µM)	anti-sense primer (2as; 10 µM)
	0.5 µl	(2.5 U)	FastStart TaqDNA Polymerase
	39 µl		ddH <sub>2</sub> O
	0.5 µl		outer PCR product

**Table 4-7 Reaction parameter for inner nested PCR**

PCR step		Cycling parameter
Initial melting		94° C, 3 min
31 cycles	Melting	94°C, 15 s
	Annealing	55°C, 15 s
	Elongation	72°C, 80 s
Final elongation		72 °C, 5 min
Cooling		4°C for ever

After the second amplification reaction, products were PEG-purified (see section 4.2.5.2) and analysed on an agarose gel to control the assay. Samples were then send to Entelechon for sequencing.

#### 4.2.5.12 DNA Sequencing and Sequence Analysis

DNA sequencing was done by Entelechon (Regensburg, Germany) with ABI sequencing technology based on the Sanger didesoxy method. Sequence files were analysed and aligned with Generunner or with the BLAT function of the UCSC genome browser (see section 3.11 for the web address).

#### 4.2.5.13 Methyl-CpG-Immunoprecipitation (MCIp)

Production of the recombinant MBD-Fc protein and MCIp of single DNA loci was carried out as previously described using *Mse I* digestion for fragmentation (Gebhard et al., 2006a; Gebhard et al., 2006b) (see also section 4.3.1). For global methylation analyses that were combined to microarray hybridization, MCIp was performed with slight modifications. Briefly, genomic DNA was sonicated to a mean fragment size of 350-400 bp using a Branson Sonifier 250 (Danbury, CT). 4 µg of each sample were rotated with 200 µl protein A-Sepharose 4 Fast Flow beads (GE Healthcare) coated with 70 µg purified MBD-Fc protein in 2 ml Ultrafree-MC centrifugal devices (Amicon/Millipore) for 3 h at 4°C in a buffer containing 250 mM NaCl (Buffer A). Beads were centrifuged to recover unbound DNA fragments (250 mM fraction) and subsequently washed with buffers containing increasing NaCl concentrations (300, 350, 400, 450, 500 mM; Buffers B - F). Densely CpG-methylated DNA was eluted with 1000 mM NaCl (Buffer G) and all fractions were desalted using the QIAquick PCR purification Kit (Qiagen). The separation of CpG methylation densities of individual MCIp fractions was controlled by qPCR using primers covering the imprinted *SNRPN* and a region without any CpGs (*Empty*), respectively. A schematic presentation of the method is given in Figure 5-15.

Required buffers and solutions:

TME (10×)	4 ml	(200 mM)	Tris-HCl (1 M) pH 8.0
	400 µl	(20 mM)	MgCl <sub>2</sub> (1 M)
	200 µl	(5 mM)	EDTA (500 mM)
	Add ddH <sub>2</sub> O to 20 ml		

Buffer A	4 ml	(1×)	TME (10×)
	2 ml	(250 mM)	NaCl (5 M)
	400 µl	(0.1%)	NP40 (10%)
	Add ddH <sub>2</sub> O to 40 ml		
Buffer B – H	1 ml	(1×)	TME (10×)
	600 µl – 2 ml	(300–1000 mM)	NaCl (5 M)
	100 µl	(0.1%)	NP40 (10%)
	Add ddH <sub>2</sub> O to 10 ml		

#### 4.2.5.14 DNA Microarray Handling and Analysis

Enriched methylated and enriched unmethylated fractions of cell types were labelled with Alexa Fluor 5-dCTP (dendritic cells) and Alexa Fluor 3-dCTP (macrophages) using the BioPrime Total Genomic Labelling System (Invitrogen) as indicated by the manufacturer. Hybridization on 244K Custom-Oligonucleotide-Microarrays (-4000 to +1000bp relative to the TSS with a few regions tiled over a large genomic interval; about 17000 annotated genes) and washing was performed as recommended by the manufacturer (Agilent). Images were scanned immediately using a DNA microarray scanner (Agilent) and processed using Feature Extraction Software 9.5.1 (Agilent) and a standard CGH protocol. Processed signal intensities were then normalised using GC-dependent regression and imported in Excel 2007 for further analysis. Probes with abnormal hybridization behaviour (extremely high or extremely low signal intensities in one of the channels) were excluded. To detect differentially methylated regions (DMRs), Log<sub>10</sub> ratios of individual probes from both comparative genome pool hybridizations were subtracted.

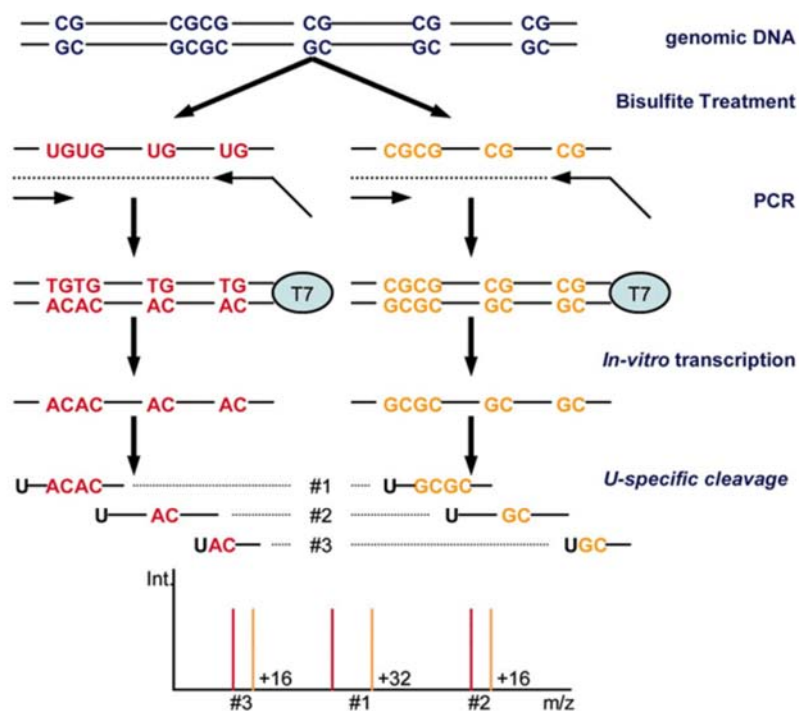
#### 4.2.5.15 Quantitative DNA Methylation Analysis Using the MassARRAY System

##### Principle

EpiTYPER (Sequenom, San Diego, USA) is a tool for detection and quantification of methylated DNA based on bisulfite conversion. If genomic DNA is treated with bisulfite, unmethylated cytosine residues are deaminated to uracil and transformed into thymine during PCR amplification, whereas methylated cytosine residues still appear as cytosines. Consequently, bisulfite treatment results in methylation dependent sequence variations of C to T after PCR amplification. Amplification products are then treated with shrimp alkaline phosphatase (SAP) to dephosphorylate unincorporated dNTPs from PCR. Subsequently, *in vitro* transcription is performed followed by RNase A specific cleavage to produce smaller fragments. Cleavage products are now prepared for analysis in the mass spectrometer. MALDI-TOF MS (matrix-assisted laser desorption/ionization time-of-flight mass spectrometry)

detects the 16 Da mass difference between guanine and adenine residues (resulting from C/T variations at the opposite strand) due to methylated and unmethylated DNA templates. MALDI-TOF MS data are then processed using the EpiTYPER software generating quantitative results for each cleavage product.

A detailed description of the method is given in (Ehrich et al., 2005) and in the EpiTYPER User Guide ([www.sequenom.com](http://www.sequenom.com)).



taken from Ehrich *et al.*, Proc Natl Acad Sci 2005

#### Figure 4-1 Schematic outline of the EpiTYPER process

Genomic DNA is treated with bisulfite and amplified using specific primers with one primer tagged with a T7 promoter sequence. PCR products are subsequently transcribed into RNA, followed by RNase cleavage after every uracil residue. Cleavage products are then analyzed by MALDI-TOF MS. In the example shown here, PCR products are transcribed from the reverse strand. In the unmethylated template (illustrated in red), cytosine residues are deaminated into uracil and therefore appear as adenosine residues after PCR. Cytosine residues of a methylated template (indicated in yellow) are not affected and remain cytosines. The conversion of guanine to adenine yields 16 Da mass shifts. Cleavage product 1 comprises 2 CpGs and the mass difference constitutes 32 Da if both CpGs are either methylated or unmethylated. Cleavage products 2 and 3 each contain only one CpG site that is differentially methylated and therefore yield a 16 Da mass shift.

#### Protocol

Bisulfite conversion of genomic DNA was carried out using the EZ DNA methylation Kit (Zymo) according to the manufacturer's instructions with slight modifications given in the EpiTYPER application guide from Sequenom. Oligonucleotides for PCR amplification were designed using MethPrimer ([www.urogene.org/methprimer/](http://www.urogene.org/methprimer/)). PCR, SAP treatment, *in vitro*

transcription, RNase cleavage and MALDI-TOF MS analysis were performed as described in the Sequenom protocols. Raw data were then processed using the EpiTYPER software (version 1.0).

## 4.2.6 Preparation and Analysis of RNA

### 4.2.6.1 Isolation of Total RNA

Total RNA was isolated using the Qiagen RNeasy Midi, Mini or Micro Kit according to the available number of cells. RNA concentration was then determined with the NanoDrop spectrophotometer and quality was assessed by agarose gel electrophoresis or using the Agilent Bioanalyzer according to the manufacturer's instructions.

### 4.2.6.2 Formaldehyde Agarose Gel

The agarose was dissolved in MOPS/H<sub>2</sub>O<sub>DEPC</sub> by heating in a microwave oven and cooled to 60°C. Formaldehyde was added while stirring the solution under a fume hood and the gel was cast, mounted in an electrophoresis tank and overlaid with 1× MOPS as electrophoresis buffer. RNA samples were heated to 37°C for 30 min to control RNase contamination and placed on ice afterwards. Samples were subsequently diluted with four volumes RNA loading buffer (1:4), denatured for 20 min at 65°C and briefly incubated on ice. Following centrifugation, the samples were loaded into the gel slots. Gels were run at 40-60 V.

#### Required buffers

MOPS (20×)	42 g (0.4 M)	MOPS/NaOH, pH 7.0
	4.1 g (100 mM)	NaOAc
	3.7 g (20 mM)	EDTA
	Add H <sub>2</sub> O <sub>DEPC</sub> to 500 ml, store in the dark	
RNA loading buffer	10 ml (50%)	Formamide, deionised
	3.5 ml (2.2 M)	Formaldehyde (37%)
	1 ml (1×)	MOPS (20×)
	0.8 ml (0.04%)	Bromophenol blue (1% in H <sub>2</sub> O)
	0.2 g (1%)	Ficoll 400, Pharmacia (dissolve in 2 ml H <sub>2</sub> O)
	Add H <sub>2</sub> O <sub>DEPC</sub> to 20 ml, store in 1 ml aliquots at -20°C	
	Add 5 µl/ml Ethidium bromide (10 mg/ml) before use	



#### 4.2.6.3 Reverse Transcription PCR (RT-PCR)

To quantify mRNA transcripts of genes, total RNA was reverse transcribed using the MMLV reverse transcriptase (Promega, Germany) combined with random decamers (Ambion, Germany) in a total reaction volume of 20  $\mu$ l.

Reaction setup:           1  $\mu$ g    Total RNA  
                              1  $\mu$ l    Random decamers (Ambion)  
                              1  $\mu$ l    dNTPs (10 pmol/ml)  
                              Add H<sub>2</sub>O<sub>USB</sub>

                              Incubate for 5 min at 65°C, cool on ice and centrifuge

                              4  $\mu$ l    M-MLV Buffer (5 $\times$ )  
                              Mix and incubate for 2 min at 42°C

                              1  $\mu$ l    M-MLV Reverse transcriptase (Promega)  
                              Incubate for 50 min at 42°C followed by 15 min at 70°C

The resulting cDNA was then diluted 1:5 and quantified with specific primers by real time PCR (see section 4.2.5.10). The combination of RT-PCR and real time PCR is called RT-qPCR.

#### 4.2.6.4 Whole Genome Expression Analysis

Labelling of high quality RNA, hybridization and scanning were performed using the Agilent Gene Expression system according to the manufacturer's instructions. In brief, 200 ng to 1000 ng high-quality RNA were amplified and Cyanine 3-CTP labelled with the one colour Low RNA Input Linear Amplification Kit from Agilent. Labelling efficiency was controlled using the NanoDrop spectrophotometer and 1.65  $\mu$ g labelled cRNA were fragmented and hybridized on the Whole Human Genome Expressionarray (4 $\times$ 44K, Agilent). After 17 hours of hybridization at 65°C, the microarrays were washed and subsequently scanned with an Agilent scanner. Data were then extracted with Feature Extraction 9.5.1 software (GE1 v5\_95\_Feb07 protocol, Agilent) and finally analysed using GeneSpring GX 10.0.2 software (Agilent). To validate microarray data, several genes were selected and verified by RT-PCR followed by qPCR (see sections 4.2.5.10 and 4.2.6.3).

#### Data Analysis Using GeneSpring Software

Text files resulting from Feature Extraction were imported to GeneSpring software in order to compare gene expression profiles between various differentiation time points or cell types.

First, probes showing large variations either between donors or among each other (if more than one probe for one gene is available) were excluded. Data were then normalised in two steps:

“per chip” normalisation: all expression data on an array were normalised to the 75<sup>th</sup> percentile of all values on that array

“per gene” normalisation: the data for a given gene were normalised to the median expression level of that gene across all samples

Generally, only more than 5 fold signal changes were defined as gene induction or repression. Finally, using One-way ANOVA (analysis of variance) with a p-value cut-off of 0.05, the gene list was reduced to significantly regulated genes. Hierarchical cluster analysis was used to identify genes with similar expression profiles and to reveal common functions of significantly regulated genes.

#### **4.2.7 *In Vivo* Genomic Footprinting with DMS**

Genomic footprinting experiments allow the investigation of DNA-protein interactions at a specific locus including the study of alterations in the underlying chromatin structure. Principally, this technique consists of two steps. First, the creation of DNA lesions by DMS (dimethyl sulfate) and second, the visualization of those lesions using ligation mediated PCR (LM-PCR) (Tagoh et al., 2006). DMS treatment leads to the formation of N-7-methylguanine (~ 70%) and, to a lesser extent, to the formation of N-3-methyladenine (~30%). The addition of piperidine then results in single strand breaks after every methylated guanine which can be detected by linker ligation, region specific PCR and finally by a labelling reaction with a Cy5 end-labelled-linker primer (Tagoh et al., 2006). As sequences occupied with DNA binding proteins are protected from methylation and cleavage, those sites will not display a PCR product. By comparing the PCR products resulting from DMS treatment of living cells to the products from naked DNA modified *in vitro* - where no protection is provided - it is possible to draw conclusions about transcription factor binding events *in vivo*.

*In vivo* DMS footprinting was performed as published previously (Tagoh et al., 2006) using 1.5 µg of purified genomic DNA from DMS-treated cells. *In vitro* DMS treatment of naked DNA was carried out as described by Maxam and Gilbert (Maxam and Gilbert, 1980). LM-PCR was then performed by using a LP21-25 linker and sequence specific primers for the *CCL13* promoter region (oligonucleotide sequences are given in 3.5.3). Differences in

DMS accessibility between gDNA isolated from DMS-treated cells and naked DNA that was *in vitro* modified, were visualized on a 6% denaturing polyacrylamide gel after the labelling reaction with the Cy5 labelled LP25 primer. Gels were then scanned on a 9200 Typhoon scanner. A detailed protocol of the complete procedure including the required solutions and PCR parameters is given by Tagoh et al. (Tagoh et al., 2006).

#### 4.2.8 Chromatin Immunoprecipitation (ChIP)

Chromatin immunoprecipitation is used to determine whether particular proteins are associated with a specific genomic region in living cells or tissues. The method is based on the principle that formaldehyde reacts with primary amines located on amino acids and the bases on DNA molecules, resulting in a covalent cross-link between proteins and DNA. Preparation of cross-linked chromatin and immunoprecipitation were performed as described previously (Metivier et al., 2003) with some modifications. Briefly, cells were treated with 1% formaldehyde solution for 7 min at room temperature and quenched by 0.125 M glycine. After washing with PBS including 1 mM PMSF,  $2 \times 10^6$  cells were resuspended in 50  $\mu$ l lysis buffer 1A (L1A: 10 mM, HEPES/KOH, pH 7.9, 85 mM KCl, 1 mM EDTA, pH 8.0) and lysed by adding 50  $\mu$ l lysis buffer 1B (L1A + 1% Nonidet P-40) for 10 min on ice. Note that lysis buffers were supplemented with phosphatase inhibitors (50 mM  $\beta$ -glycerophosphate and 1 mM  $\text{Na}_2\text{O}_4$ ) when phosphorylated proteins had to be precipitated. Cross-linked chromatin was sheared to an average DNA fragment size around 400 – 600 bp using a Branson Sonifier 250 (Danbury, CT). After centrifugation, 4  $\mu$ l of the lysate were used as input. After preclearing with 50  $\mu$ l Sepharose CL-4B beads (blocked with 0.2% BSA and 5  $\mu$ g sheared salmon sperm for 1 h at 4°C) for 2 h, chromatin samples were immunoprecipitated overnight with 2.5  $\mu$ g of the appropriate antibody. Before precipitation, ProteinA Sepharose beads (GE Healthcare) were treated with 2  $\mu$ g sheared salmon sperm DNA for 1 h at 4°C. Immunocomplexes were then recovered by incubation for 2 h with the blocked beads at 4°C. After reverse cross-linking, DNA was purified using the QIAquick PCR purification kit (Qiagen) according to the manufacturer's instructions except that the samples were incubated with PB buffer for 30 min and that they were eluted with 100  $\mu$ l EB. Enrichment of specific DNA fragments in the immunoprecipitated material was determined by quantitative PCR on the Realplex Mastercycler as described above.

Required buffers and solutions:

Glycine	9.85g (2.625 M)	Glycine
	To 50 ml with ddH <sub>2</sub> O	

Cell Buffer Mix	20 $\mu$ l (10 mM) 57 $\mu$ l (85 mM) 4 $\mu$ l (1 mM) To 1.98 ml with ddH <sub>2</sub> O	HEPES / KOH (1 M), pH 7.9 KCL (3 M) EDTA (0.5 M, pH 8.0)
	Add just prior to use:	
	20 $\mu$ l (1 mM) 2 $\mu$ l (1 $\mu$ g/ml) 2 $\mu$ l (2 $\mu$ g/ml)	PMSF (100 mM in Iso-prop, nostalgia) Pepstatin (1 $\mu$ g/ $\mu$ l) Aprotinin (2 $\mu$ g/ $\mu$ l)
Nuclear Lysis Buffer (L2)	100 $\mu$ l (50 mM) 100 $\mu$ l (1%) 33.3 $\mu$ l (0.5%) 40 $\mu$ l (10 mM) To 1.98 ml with ddH <sub>2</sub> O	Tris/HCl (1 M), pH 7.4 @ 20°C SDS (20%) Empigen BB (30%) EDTA (0.5 M), pH 8.0
	Add just prior to use:	
	20 $\mu$ l (1 mM) 2 $\mu$ l (1 $\mu$ g/ml) 2 $\mu$ l (2 $\mu$ g/ml)	PMSF (100 mM in Iso-prop, nostalgia) Pepstatin (1 $\mu$ g/ $\mu$ l) Aprotinin (2 $\mu$ g/ $\mu$ l)
Dilution Buffer (DB)	50 $\mu$ l (20 mM) 50 $\mu$ l (100 mM) 10 $\mu$ l (2 mM) 125 $\mu$ l (0.5%) To 2.47 ml with ddH <sub>2</sub> O	Tris/HCl (1 M), pH 7.4 @20°C NaCl (5 M) EDTA (0.5 M, pH 8.0) Triton X-100 (10%)
	Add just prior to use:	
	25 $\mu$ l (1 mM) 2.5 $\mu$ l (1 $\mu$ g/ml) 2.5 $\mu$ l (2 $\mu$ g/ml)	PMSF (100 mM in Iso-prop, nostalgia) Pepstatin (1 $\mu$ g/ $\mu$ l) Aprotinin (2 $\mu$ g/ $\mu$ l)
Wash Buffer I (WB I)	200 $\mu$ l (20 mM) 300 $\mu$ l (150 mM) 50 $\mu$ l (0.1%) 1 ml (1%) 40 $\mu$ l (2 mM) To 10 ml with ddH <sub>2</sub> O	Tris/HCl (1 M), pH 7.4 @ 20°C NaCl (5 M) SDS (20%) Triton X-100 (10%) EDTA (0.5 M, pH 8.0)
Wash Buffer II (WB II)	200 $\mu$ l (20 mM) 1 ml (500 mM) 1 ml (1%) 40 $\mu$ l (2 mM) To 10 ml with ddH <sub>2</sub> O	Tris/HCl (1 M), pH 7.4 @ 20°C NaCl (5 M) Triton X-100 (10%) EDTA (0.5 M, pH 8.0)
Wash Buffer III (WB III)	100 $\mu$ l (10 mM) 250 $\mu$ l (250 mM) 1 ml (1%) 1 ml (1%) 20 $\mu$ l (1 mM) To 10 ml with ddH <sub>2</sub> O	Tris/HCl (1 M), pH 7.4 @ 20°C LiCl (10 M) hard to dissolve, try 2.5 M NP-40 (10%) Deoxycholate (10%) EDTA (0.5 M, pH 8.0)
Elution Buffer (EB)	450 $\mu$ l (0.1 M) 225 $\mu$ l (1%) To 4.5 ml with ddH <sub>2</sub> O	NaHCO <sub>3</sub> (1M) SDS (10%)

## 4.3 General Protein Biochemical Methods

### 4.3.1 Purification of the Recombinant Protein MBD-Fc

#### 4.3.1.1 Dialysis

The MBD-Fc containing culture supernatant (see section 4.1.1.2) was harvested by centrifugation of the cells at 320×g for 10 min at 4°C. To get rid of remaining (dead) cells and debris, the supernatant was centrifuged at 2000×g for 20 min at 4°C before the final centrifugation step of 15000×g for 1 hour at 4°C to separate smaller debris. The supernatant was dialyzed against 1×TBS (pH 7,4) for 3-4 days exchanging the buffer twice a day.

Required buffers:

10×TBS pH 7.4	151.4 g	(500 mM)	Tris
	219.2 g	(1.5 M)	NaCl
	9.3 g	(10 mM)	EDTA
	125 mg	(0.05%)	NaN <sub>3</sub>
	Add ddH <sub>2</sub> O to 2500 ml		

#### 4.3.1.2 Affinity Chromatography

After dialysis, the protein-containing supernatant was purified and enriched using a ProteinA sepharose column (Amersham):

The column was filled with 3 ml rProteinA sepharose beads (Amersham) in 1×TBS. After washing the column with 1×TBS, the dialyzed protein supernatant was loaded, followed by another washing step with 1×TBS. The MBD-Fc protein was recovered in 1.5 ml fractions using elution buffer. To neutralize the low pH of the elution buffer, each collecting Eppendorf cup was prepared with 50 µl neutralization buffer. The protein-containing fractions (verified by a photometer) were combined and dialyzed again as described above.

Regeneration was performed by washing the column with 3 M KCl and finally with 1×TBS. The column was now prepared for another purification cycle or for storage at 4°C.

Required buffers and solutions:

Elution buffer pH 3.0	2.9 g	(0.1 M)	Citric acid
	Add ddH <sub>2</sub> O to 100 ml		
Neutralization buffer pH 8.8	18 g	(1.5 M)	Tris
	Add ddH <sub>2</sub> O to 100 ml		
Recovering solution	22.4 g	(3.0 M)	KCl
	Add ddH <sub>2</sub> O to 100 ml		

#### 4.3.1.3 Conservation of the Purified MBD-Fc

To stabilize and preserve the protein, 0.2% gelatine and 0.05% NaN<sub>3</sub> were added. The MBD-Fc fusion protein was now ready for further experiments or for long-term storage at 4°C.

#### 4.3.1.4 Quantification and Quality Control of MBD-Fc

Quality of each protein batch was assessed by SDS-PAGE (see section 4.3.2) followed by Coomassie staining (or Western Blot analysis like described in 4.3.3) as well as by control-MC1p (see section 4.2.5.13).

Protein concentration was determined relative to a BSA standard curve using a densitometer after SDS-PAGE.

### 4.3.2 Discontinuous SDS-PAGE

Protein samples were separated by using a discontinuous gel system, which is composed of stacking and separating gel layers that differ in salt and acrylamide (AA) concentration.

**Table 4-8 SDS-PAGE stock solutions**

Stock solution	Separating gel stock solution	Stacking gel stock solution
Final AA concentration	13.5%	5%
Stacking gel buffer	-	25 ml
Separating gel buffer	25 ml	
SDS (10%)	1 ml	1 ml
Rotiphorese Gel 30 (30%)	45 ml	16.65 ml
H <sub>2</sub> O	Adjust to 100 ml	

**Table 4-9 SDS-PAGE gel mixture**

Stock solution	Separating gel	Stacking gel
Separating gel stock solution	10 ml	-
Stacking gel stock solution	-	5 ml
TEMED	10 µl	5 µl
Ammoniumpersulfate 10% (freshly prepared)	50 µl	40 µl

The separating gel was prepared the day before electrophoresis and overlaid with water-saturated isobutanol until it was polymerized. Isobutanol was exchanged by separating gel buffer diluted 1:3 with water and the gel was stored overnight at 4°C. The following day, the stacking gel was poured on top of the separating gel, and the comb was inserted immediately. After polymerization, the gel was mounted in the electrophoresis tank, which was filled with 1×Laemmli buffer. Protein samples were loaded and the gel was run with 25 mA/110 volts until the sample buffer bands reached the surface of the stacking gel. Next, the voltage was increased to 200 V and the gel was run for 2-4 h. Proteins were then resolved through the separating gel according to their size.

Required buffers and solutions:

Separating gel buffer	90.83 g (1.5 M) Add ddH <sub>2</sub> O to 500 ml	Tris/HCl, pH 8.8
Stacking gel buffer	30 g (0.5 M) Add ddH <sub>2</sub> O to 500 ml	Tris/HCl, pH 8.8
SDS (10%)	10 g (10%) Add ddH <sub>2</sub> O to 100 ml	SDS
Ammonium persulfate (APS)	100 mg (10%) Add ddH <sub>2</sub> O to 1 ml	Ammonium persulfate
Laemmli buffer (5×)	15 g (40 mM) 21 g (0.95 M) 15 g (0.5%) Add ddH <sub>2</sub> O to 3000 ml	Tris Glycine SDS

### 4.3.3 Western Blot Analysis and Immunostaining

After separation by SDS-PAGE, proteins were blotted electrophoretically onto PVDF membrane (Immobilon-P, Millipore) using a three-buffer semi-dry system and visualized by immunostaining using specific antibodies and the ECL detection kit.

The membrane was cut to gel size, moistened first with methanol followed with buffer B and placed on top of three Whatman3MM filter paper soaked with buffer A (bottom, on the anode), followed by three Whatman3MM filter paper soaked with buffer B. The SDS-PAGE gel was then removed from the glass plates, immersed in buffer B and placed on top of the membrane. Another three Whatman 3MM filter papers soaked with buffer C were placed on top of the gel followed by the cathode. Air bubbles in-between the layers had to be avoided. Protein transfer was conducted for 30 – 45 min at 0.8 mA/cm<sup>2</sup> gel surface area.

Required buffers:

Buffer A	36.3 g 200 ml Add ddH <sub>2</sub> O to 1000 ml	(0.3 M) (20%)	Tris, pH 10.4 Methanol
Buffer B	3.03 g 200 ml Add ddH <sub>2</sub> O to 1000 ml	(25 mM) (20%)	Tris, pH 10.4 Methanol
Buffer C	5.2 g 200 ml Add ddH <sub>2</sub> O to 1000 ml	(4 mM) (20%)	ε-amino-n-caproic acid, pH 7.6 Methanol

Blotted membranes were blocked with 5% milk in PBST for 1 h at RT, washed once for 5 min with PBST or TBST before incubation at RT for 1 h with the primary antibody. After washing three times 10 min with the appropriate washing buffer, the membrane was incubated for 1 h at RT with a horseradish-peroxidase (HRP)-coupled secondary antibody, detecting the isotype of the first antibody. Three washing steps of 3×10 min preceded the visualization of bound antibody using the ECL kit. Blots were exposed to an autoradiography film (Hyperfilm™ ECL, Amersham) for 5 seconds to 30 min depending on the signal intensity.

Required buffers and materials:

TBS (2×)	9.16 g 35.1 g Add ddH <sub>2</sub> O to 2000 ml	(20 mM) (150 mM)	Tris /HCl, pH 7.4 NaCl
TBST (1×)	500 ml 1 ml Add ddH <sub>2</sub> O to 1000 ml	(1×) (0.1%)	TBS (2×) Tween 20

#### 4.3.4 Coomassie Staining of SDS-Gels

SDS-gels were tossed in ddH<sub>2</sub>O (three times, 5 min each) and subsequently incubated in the Coomassie solution for about 20 – 60 min. After washing overnight in ddH<sub>2</sub>O, proteins appear as blue bands on a transparent background.

Required solution:

Coomassie Bio Safe    Bio Rad, Munich, Germany



## 4.4 Proliferation Assay (Thymidine Incorporation)

Proliferation capacity of cells was measured using incorporation of radioactively labelled thymidine. Cells were seeded in 96-well microtiter plates ( $30 - 100 \times 10^5$  cells per well) and pulsed with  $0.5 \mu\text{Ci}$  [methyl- $^3\text{H}$ ]-thymidine/well (Hartmann Analytics, Braunschweig, Germany) for 20 hours. Cells were harvested onto UniFilter plates using a Wallac harvester and incorporated  $^3\text{H}$ -thymidine was determined with a Wallac Betaplate counter (all from PerkinElmer, Gaithersburg, MD).

## 4.5 Flow Cytometry

To characterize phenotypes of different cell types, the cell surface expression pattern of several membrane proteins was analysed by flow cytometry.  $1 - 5 \times 10^6$  cells per staining reaction were washed twice with  $1000 \mu\text{l}$  cold FACS buffer and immunostained for 30 min at  $4^\circ\text{C}$  with appropriate mouse antibodies recognizing human antigens (see section 3.9). After another two washing steps, cells were fixed with  $500 \mu\text{l}$  1% paraformaldehyde/PBS and flow cytometric analysis was performed on a BD FACS Calibur.

Required solutions:

FACS buffer	5 ml	(600 $\mu\text{g/ml}$ )	Immunoglobulins (60 $\text{mg/ml}$ )
	5 ml	(0.1%)	Sodium azide (10%)
	Add PBS to 500 ml		
Paraformaldehyde	1 g	(1%)	Paraformaldehyde
	Add PBS to 500 ml, stir O/N at RT		

## 5 Results

### 5.1 Creating a Tool to Analyse the Effects of CpG Methylation within Gene Promoters

Methylation-dependent repression is well established, especially for hypermethylated CpG-island promoters that are characterized by a high density of CpG dinucleotides (Costello and Plass, 2001; Esteller et al., 2002; Herman and Baylin, 2003). The effect of DNA methylation on CpG-poor promoters is less well characterized, probably due to the lack of convenient assay systems, like transient transfection, to test promoter activities *in vitro*. Previous studies used two approaches to analyse the effect of promoter methylation in transient transfection assays. The first method includes *in vitro* methylation of whole reporter vectors before transfection (DiNardo et al., 2001; Guo et al., 2002). Consequently, not only CpGs within the promoter of interest but also CpGs in the vector's backbone are methylated. The second approach involves digestion, purification, *in vitro* methylation and ligation of DNA fragments into unmethylated reporter vectors before transfection to avoid the methylation of backbone CpGs (Lu and Richardson, 2004; Yu et al., 2005). In order to bypass negative side effects of backbone methylation as well as the time-consuming and labor intensive alternative method, a novel CpG-free luciferase vector was designed.

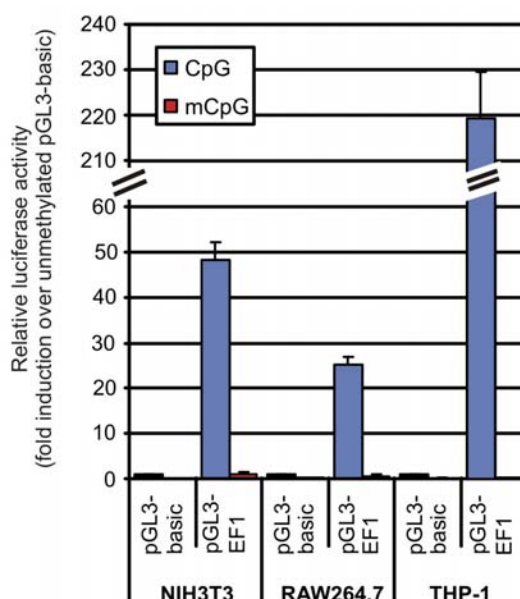
#### 5.1.1 Effects of CpG Methylation in Vector Backbones on Reporter Activities

Transient transfections provide a relatively simple and robust assay for analysing promoter activity. Usually, transfection assays are carried out using unmethylated reporter constructs. Since CpG residues can be methylated *in vitro* with methylases like *Sss I*, *Hha I* or *Hpa II*, this approach can be adopted for studying effects of promoter methylation on reporter activity. Conventionally used reporter vectors like luciferase vectors of the pGL series from Promega contain varying numbers of CpG dinucleotides in their backbone (Table 5-1).

**Table 5-1 Number of background CpGs in conventionally used luciferase reporter vectors**

Vector	Length	# of CpGs in the vector backbone
pGL2-basic	5598 base pairs	285
pGL3-basic	4818 base pairs	286
pGL4-basic	4242 base pairs	284

Those CpGs are also targeted by methylating enzymes, possibly affecting reporter activity. In order to assess effects of methylated CpGs in reporter backbones, a robust, CpG-free *EF1A*-promoter was cloned into the Promega pGL3-basic vector (see section 4.2.3.2). Using human and mouse cell-lines, the activity of unmethylated versus *Sss I* methylated plasmids was tested in transient transfections. *In vitro* methylation with *Sss I* results in methylation of every occurring CpG residue, irrespective of the surrounding sequence motifs. As shown in Figure 5-1, methylation of CpG dinucleotides in the pGL3-backbone strongly repressed the activity of the CpG-free *EF1A*-promoter in all cell lines tested.

**Figure 5-1 Effect of methylated backbone CpGs on promoter activity in transient transfection assays**

The indicated mouse (NIH3T3, RAW264.7) and human (THP-1) cell lines were transiently transfected with either *Sss I*-methylated (red bars) or unmethylated (blue bars) pGL3-plasmids. Luciferase activities were normalised for transfection efficiency by cotransfection with an unmethylated *Renilla* construct (phRL-TK; Promega). Results for individual cell lines are shown relative to the activity of the unmethylated, empty pGL3-basic reporter vector. Results represent the mean  $\pm$ SD obtained from three independent experiments.

Consequently, using the pGL3-backbone to analyse methylation-dependent changes of promoter activities by *in vitro* methylation and transient transfection leads to effects not necessarily due to methylation of promoter CpGs themselves.

## 5.1.2 Construction and Application of the Novel CpG-free Luciferase Reporter pCpGL

To avoid interfering effects of backbone methylation without using the time-consuming ligation of an *in vitro* methylated promoter fragment into the unmethylated reporter plasmid, a completely CpG-free luciferase reporter plasmid was designed (see section 4.2.3.1; Figure 5-2A).

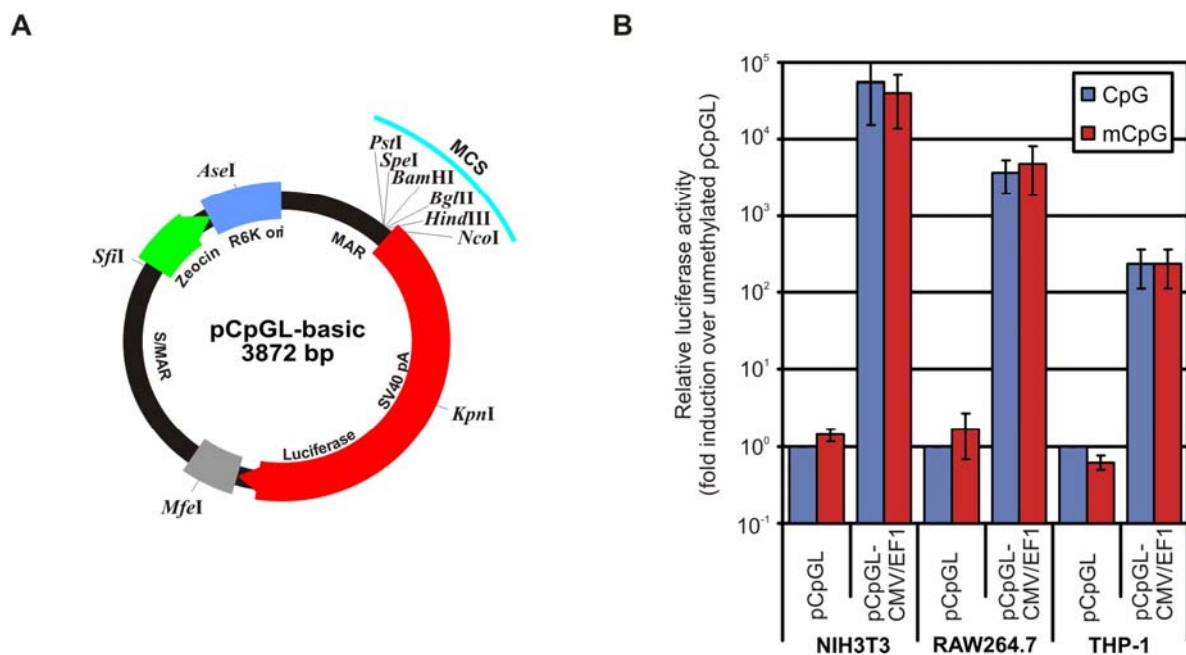


**Figure 5-2 Control experiment using the novel CpG-free reporter vector**

(A) Map of the novel CpG-free reporter vector pCpGL-basic. The luciferase reporter vector is completely free of CpG dinucleotides. The plasmid is propagated in *PIR1* bacteria, expressing the *pir* gene under zeocin (25 µg/ml) selection. All restriction sites of the multiple cloning site (MCS) are unique. (B) The indicated mouse (NIH3T3, RAW264.7) and human (THP-1) cell lines were transiently transfected with *Sss I* methylated (red bars) or unmethylated (blue bars) CpG-free pCpGL-CMV/EF1. Luciferase activity was normalised for transfection efficiency by cotransfection with the unmethylated *Renilla* construct. Results were calculated relative to the activity of unmethylated pCpGL-basic. Data are shown as the mean value obtained from two (NIH3T3, RAW) or three (THP-1) independent experiments including their statistical spread.

In order to test the usefulness and reliability of the novel CpG-free vector, three pCpGL derivatives containing varying numbers of CpG dinucleotides were generated (see section 4.2.3.2; Table 5-2). The first evidence for the utility of the novel reporter construct was the transient transfection of *Sss I* methylated and unmethylated CpG-free pCpGL-CMV/EF1 into the same cell lines used for the pGL3-tests. In all cell-lines tested, there was no significant difference in luciferase activity between methylated and unmethylated constructs suggesting

that the *Sss I* treatment does not affect reporter activities *per se* (Figure 5-2B). For each cell-line, three experiments were performed in duplicates and all showed the same correlation between methylated and unmethylated plasmids. Because transfection efficiency itself was variable in particular cases without changing the described correlation, only two experiments were averaged for the mouse cell-lines.

**Table 5-2 Number of CpGs in the pCpGL derivatives**

Vector	# of CpGs in the insert
pCpGL-CMV/EF1	0
pCpGL-CPM	40
pCpGL-CHI3L1	8

To further characterize the usefulness of the novel reporter vector, the CpG-containing constructs pCpGL-CPM (40 CpGs) and pCpGL-CHI3L1 (8 CpGs) were transfected into THP-1 cells that are known to endogenously express *CPM* as well as *CHI3L1*. As shown in Figure 5-3, activity of both promoters was markedly repressed after *Sss I* methylation, indicating that both CpG containing reporter vectors were efficiently silenced by DNA methylation.

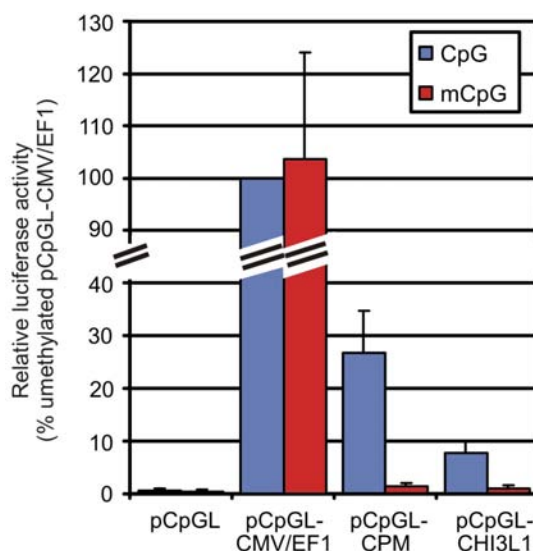


**Figure 5-3 Effect of promoter methylation in transient reporter assays using pCpGL**

THP-1 cells were transiently transfected with *Sss I* methylated (red bars) or unmethylated (blue bars) pCpGL vectors with pCpGL-CPM containing 40 CpGs and pCpGL-CHI3L1 containing 8 CpGs. Luciferase activity was normalised for transfection efficiency by cotransfection with the unmethylated Renilla plasmid. Results are shown relative to the activity of the CpG-free pCpGL-CMV/EF1 control vector. Data are shown as mean value  $\pm$ SD obtained from three independent experiments.

In order to test the sensitivity of the designed tool, effects of partial promoter methylation were analysed using site-specific DNA methylases. Whereas *Sss I* methylates every occurring CpG dinucleotide, *Hha II* methylase only methylates the first cytosine residue within –GCGC– and *Hpa II* methylase only those CpG dinucleotides occurring in –CCGG–. pCpGL-CPM, pCpGL-CHI3L1 as well as the CpG-free control pCpGL-CMV/EF1 were either methylated using one of the described methylases or left unmethylated. Resulting methylation patterns of the plasmids are given in Figure 5-4A. Transient transfection into THP-1 cells and luciferase measurement revealed variable reporter activities of differential methylated plasmids (Figure 5-4B). Furthermore, this effect seemed to be dependent on the position of the methylated cytosine residues. Regarding the CPM-promoter, for example, *in vitro* methylation using *Hha I* methylase caused stronger repression than methylation with *Hpa II* methylase. Methylation of one single CpG dinucleotide (using *Hpa II* methylase) was sufficient to cause a significant reduction of CHI3L1-promoter activity. As expected, *in vitro* methylation of the pCpG-CHI3L1 vector with *Hha I* methylase did not affect promoter activity, because this construct is free of *Hha I* sites.

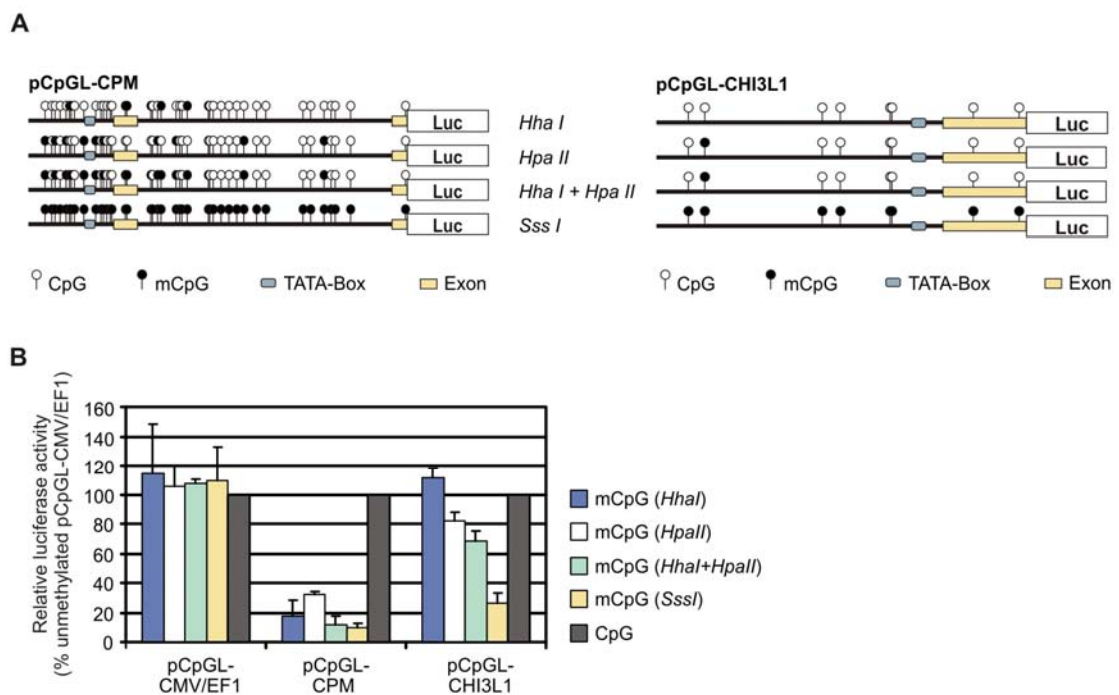


**Figure 5-4 Comparative analysis of differential promoter methylation**

**(A)** Schematical representation of the CPM- and CHI3L1-promoter vectors. Positions of methylated (black circles) and unmethylated (white circles) CpG dinucleotides as well as TATA-boxes and exons are indicated for all methylase treatments. **(B)** Transient transfection of THP-1 cells with differential methylated plasmids. Reporter constructs were methylated as indicated and luciferase activities were normalised for transfection efficiency by cotransfection with the unmethylated *Renilla* plasmid. Results were compared to the activity of corresponding unmethylated plasmids. Values are the mean  $\pm$  SD obtained from three independent experiments.

To control the completeness of methylation, both methylated and unmethylated plasmids were digested using the methylation sensitive restriction enzymes *Hha I* (cutting unmethylated –GCGC-) and *Hpa II* (cutting unmethylated –CCGG-) as well as the methylation insensitive *Msp I* recognizing the same sequence as *Hpa II*. As expected, CpG-free pCpGL-basic and pCpGL-CMV always showed the same band pattern after digestion irrespective of the used enzymes for methylation and digestion. *Hpa II* methylase methylated as well as *Sss I* methylated plasmids were not cut using *Hpa II* indicating complete methylation of the corresponding sites (Figure 5-5). Similarly, *Hha I* methylase methylated sites were protected from *Hha I* digestion. Plasmids, methylated with a combination of *Hha I* methylase and *Hpa II* methylase (1:1) were not cut using either *Hha I* and *Hpa II*. In fact, digestion with methylation insensitive *Msp I* should result in several digestion products depending on the sequence of the inserts. In some cases, the *Msp I*-digest was incomplete, probably a consequence of the exceeded expiry date. Nevertheless, complete methylation in every reaction could be demonstrated by digestion with *Hha I* and *Hpa II*, respectively.

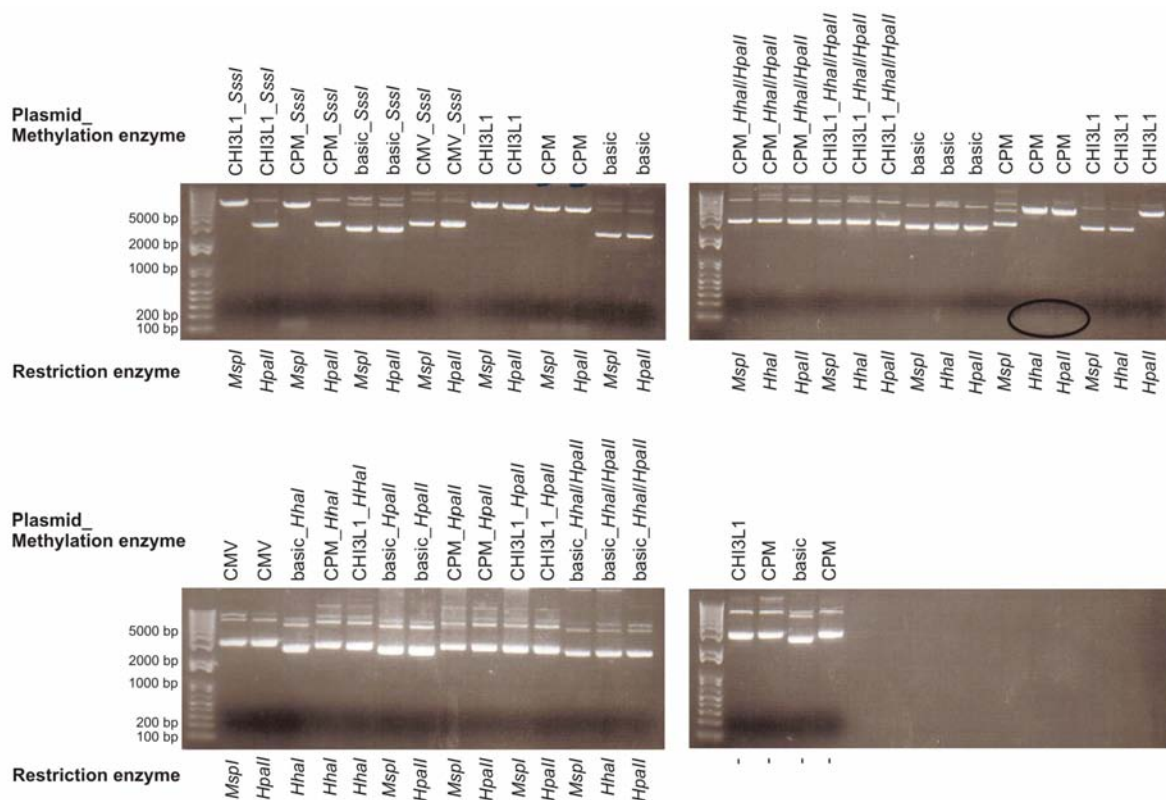


**Figure 5-5 Methylation control**

The methylation status of plasmids was controlled by digesting methylated and unmethylated plasmids with methylation sensitive (*Hha I* and *Hpa II*) as well as methylation insensitive restriction enzymes (*Msp I*).

## 5.2 Active DNA Demethylation during the Differentiation of Monocytes

### 5.2.1 The Cell Model

Peripheral blood monocytes are characterized by a unique phenotypic plasticity and are able to differentiate into a number of morphologically and functionally diverse cell types *in vivo*: the wide range of heterogeneous tissue macrophages (MAC), myeloid dendritic cells (DC) and multinucleated osteoclasts (Seta and Kuwana, 2007). The distinct differentiation pathways can be recapitulated *in vitro*. Culturing purified human monocytes for several days in the presence of human serum results in the generation of macrophages (Figure 5-6) (Andreesen et al., 1983), whereas they develop into myeloid dendritic cells in presence of the granulocyte-macrophage colony-stimulating factor (GM-CSF) and interleukin 4 (IL-4) (Sallusto and Lanzavecchia, 1994).

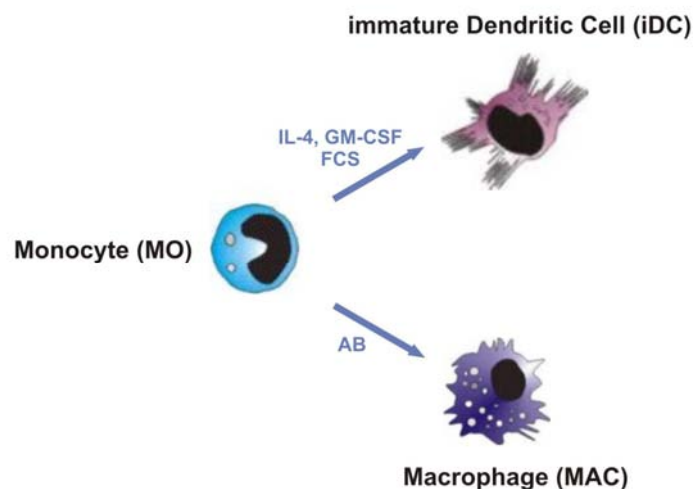


**Figure 5-6 Schematic presentation of the used cell model**

After leukapheresis and subsequent elutriation, monocytes (MO) were cultured either in presence of IL-4, GM-CSF and FCS to generate immature dendritic cells (iDC) or with human AB-sera to obtain macrophages (MAC).

Although it is largely accepted that monocytes do not proliferate under conventional culture conditions, the proliferation rate of monocytes was analysed during the first four days of differentiation by measuring the incorporation of radioactively labelled thymine.



As expected, no significant nucleotide incorporation was detected during the analysed time period (Figure 5-7). The differentiation of monocytes thus provides an ideal model to study epigenetic processes in post-mitotic cells.

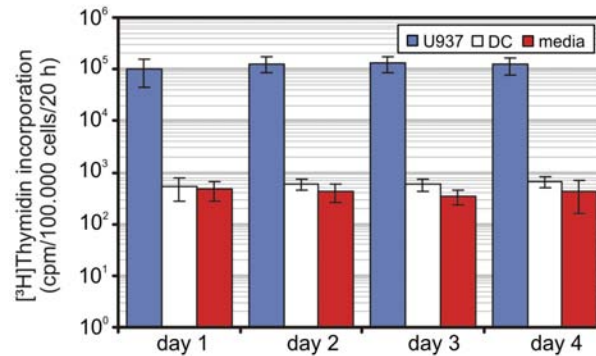


**Figure 5-7 Proliferation assay**

Dendritic Cells (DC) and U937 cells were cultured with [3H] thymidine for 20 h at different differentiation time points (d1, d2, d3, d4). Values represent mean  $\pm$ SD of three independent experiments. The U937 leukaemia cell line served as positive control showing high thymidine incorporation rates.

## 5.2.2 Molecular Characterization of an Actively Demethylated Promoter during Monocyte Differentiation

The DC specific chemokine CCL13 (chemokine (C-C motif) ligand 13; also known as MCP-4) serves as prime example for active DNA demethylation. In earlier studies, it was shown that the *CCL13* gene was strongly induced only in dendritic cells, whereas it was silent in monocytes and remained silent during the differentiation into macrophages (Heinz S., 2002). Furthermore, DC specific demethylation of two or three particular promoter CpGs adjacent to the transcription start site (one located at -80 bp and two in tandem at -20 bp) was observed (Figure 5-8).

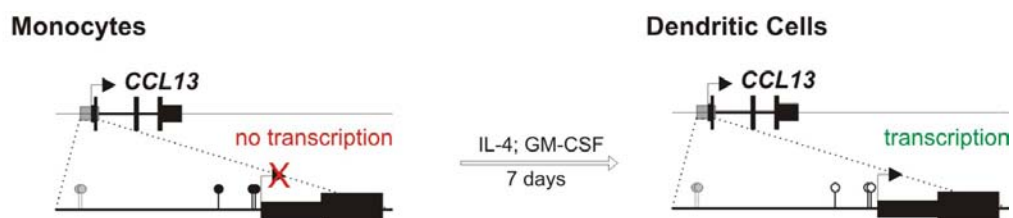


**Figure 5-8 Schematic presentation of changes at the CCL13 promoter during differentiation**

During differentiation of monocytes towards dendritic cells, two specific CpGs become demethylated. “Lollipops” represent CpG dinucleotides, with filled circles standing for methylated CpGs and white circles indicating unmethylated CpGs. CpGs (lollipops) in grey were not analysed. Arrows represent transcription start sites.

### 5.2.2.1 Correlation of mRNA Expression and DNA Demethylation Events

To get insights into the timing of DNA demethylation and mRNA expression, dendritic cells were harvested at different time points over a seven day time period. RNA as well as DNA were isolated, or, alternatively, chromatin was prepared. Using reverse transcription followed by qPCR (RT-qPCR), a detailed time course of *CCL13* mRNA expression was analysed revealing the continuously strong induction of *CCL13* during DC development (Figure 5-9A).

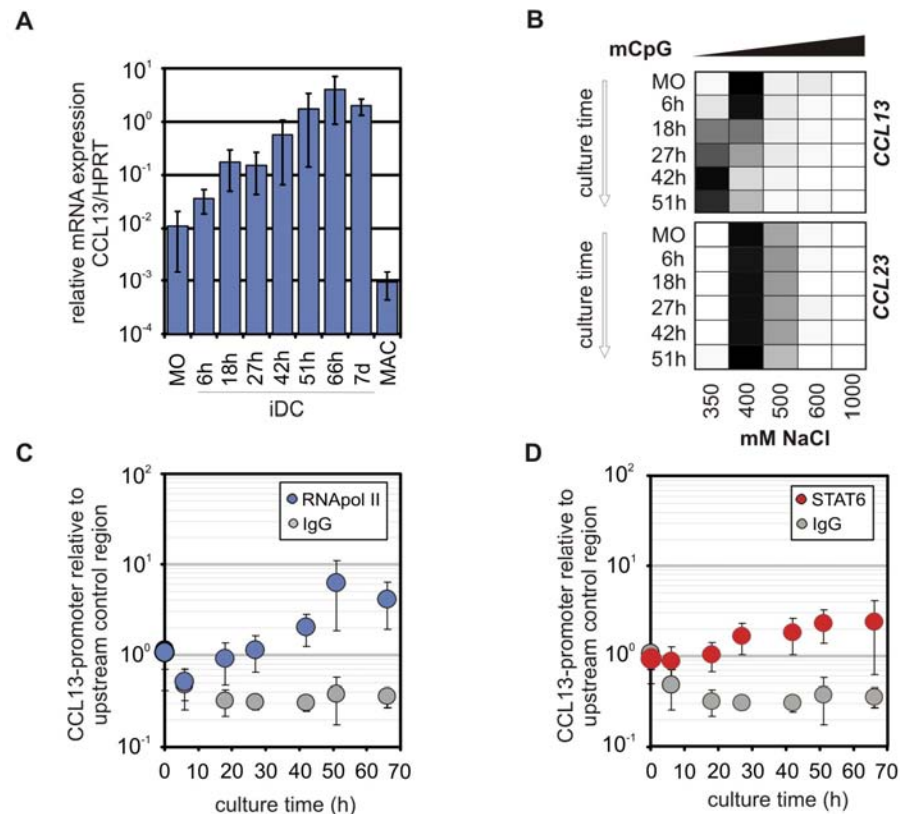


**Figure 5-9 Characterization of the *CCL13* promoter region**

**(A)** Expression profile of *CCL13* during differentiation of monocytes (MO) into immature dendritic cells (iDC) until day 7 (7d). Results were normalised for *HPRT* expression. Values are means  $\pm$  SD obtained from three independent experiments. **(B)** Time course of demethylation during the differentiation of DCs using MCIp and qPCR. Enrichment of DNA for *CCL13* and the *CCL23* control region is illustrated in grey gradations relative to the signal intensity with black representing the strongest enrichment. Highly methylated DNA fragments were eluted with higher salt concentrations than weakly methylated or unmethylated DNA fragments. Values of three independent donors were averaged. Chromatin immunoprecipitation for RNApol II **(C)** and the transcription factor STAT6 **(D)**. Grey spots indicate the IgG background level. Signals, specific for the *CCL13*-promoter region were normalised to the signals of an unaffected upstream control region. Values are the mean  $\pm$  SD of at least four independent experiments.

The active demethylation event in DCs was further characterized by methyl-CpG immunoprecipitation (MCIp). This technique is based on differential elution behaviours of methylated and non-methylated DNA fragments from the MBD-Fc fusion protein and therefore allowed the fractionation of genomic DNA fragments according to their methylation density (Gebhard et al., 2006b; Schilling and Rehli, 2007) (see also Figure 5-15A). The

enrichment of methylated and unmethylated DNA respectively was then quantified by real-time PCR using specific primers for the *CCL13* promoter. As demonstrated in Figure 5-9B, methylated DNA of monocytes and 6 hour DCs precipitated using 400 mM NaCl. After 18 hours in culture, more and more DNA eluted with lower salt concentrations indicating the initiation of demethylation. Finally, after 42 hours the demethylation process was finished, because the signal completely switched to the 350 mM fraction. Regarding the *CCL23* control region, genomic DNA from every analysed time point eluted with the same NaCl concentration (mainly 400 mM), indicating that there is no change in the methylation pattern. In order to detect factors bound to the *CCL13* promoter during the relevant time period and to determine the timing of occurring events, chromatin immunoprecipitations were performed. Corresponding to the expression data, increasing RNA-Pol II recruitment was detected with ongoing differentiation (Figure 5-9C). Furthermore, binding of the IL-4 induced transcription factor STAT6 increased slightly until culture day 3, although timing and signal intensities varied between different donors (Figure 5-9D).

*CCL13* mRNA seemed to be slightly up-regulated before demethylation of promoter CpGs was finished. Strongest signals, however, were obtained and maintained after all methyl groups were removed, suggesting that DNA demethylation is necessary for stable and continuous gene expression. One possibility to prove a direct correlation between transcription level and DNA demethylation would be the performance of transfection assays with methylated and unmethylated promoter constructs as described in chapter 5.1.2.. However, to my knowledge, there is no cell line available expressing the *CCL13* gene intrinsically. THP-1, U937, HepG2, RAW264.7 as well as NIH3T3 (all lacking *CCL13* expression) failed to transcribe unmethylated *CCL13* promoter reporter constructs after successful transfection. Therefore, a strict requirement of *CCL13* promoter demethylation for lasting mRNA expression could not be proven so far.

### **5.2.2.2 Attempts to Interfere with the Active DNA Demethylation Process**

In order to block DNA demethylation, monocytes were treated with inhibitory substances (Table 5-3) using various concentrations for up to three days. The selection of chemicals was directed on inhibiting mechanisms that are possibly involved in active DNA demethylation (Kress et al., 2006; Metivier et al., 2008; Perillo et al., 2008). During DC development, DNA as well as RNA were prepared at different time points followed by bisulfite sequencing to analyse the methylation status as well as by RT-qPCR to assess *CCL13* expression profiles, respectively.

**Table 5-3 Substances used to interfere with DNA demethylation**

Substance	Description	Observed effects
<b>5-me-dCTP</b> (5 $\mu$ M)	Possible substrate for a demethylating enzyme	none
<b>Aphidicolin</b> (2 or 5 $\mu$ g)	Inhibitor specific for polymerase alpha and beta; may influence repair mechanisms	none
<b>Ara-C</b> (1 – 200 $\mu$ M)	( $\beta$ -D-Arabinofuranosyl)cytosine. Inhibitor of DNA polymerases; may stabilize single strand breaks	DNA, RNA degradation; dose and time dependent apoptosis
<b>NAC</b> (10 mM)	<u>N</u> -Acetyl- <u>C</u> ysteine. Scavenger of reactive oxygen species. Blocks repair processes induced by radicals	none
<b>PJ34</b> (0.5 - 10 $\mu$ M)	Inhibitor of PARP-1 DNA repair polymerase; might stabilize DNA strand breaks	none
<b>RG108</b> (5 $\mu$ M)	Inhibitor of DNMTs	none
<b>TSA</b> (1 - 10 $\mu$ M)	<u>T</u> richo <u>s</u> tatin <u>A</u> . Inhibitor of histone deacetylases	toxic

None of the analysed substances showed a significant influence, neither on promoter demethylation nor on transcription of *CCL13*. Especially the missing effect of the DNMT inhibitor RG108 was surprising, as DNMT3a/b was shown to contribute to CpG demethylation and as this activity could be blocked by RG108 (Metivier et al., 2008). Although two independent preparations of RG108 (Calbiochem, Darmstadt, Germany; IGBMC, Hinrich Gronemeyer, Strasbourg, France) were tested, no effects of this inhibitor were observed.

Beside pharmacological manipulation, the effect of cell adherence during dendritic cell development was considered to influence DNA demethylation. Monocytes become adherent just after culturing and slowly detach from the culture flask, usually within approximately 24 hours, depending on the donor. To clarify, if the adherence stimulus provides an important step for DC specific DNA demethylation, DCs were cultured in rotating 200 ml Falcon tubes in the incubator for three days. The lack of adherence did not inhibit DC development itself as verified by FACS staining with the DC specific marker CD1a (Figure 5-10A). To study the effect of adherence on CpG methylation, the methylation status of the *CCL13* promoter was assessed by bisulfite sequencing. If genomic DNA is treated with sodium bisulfite, unmethylated cytosines are deaminated into uracil and transformed into thymidine residues during PCR, whereas methylated cytosines still appear as cytosines after amplification (Frommer et al., 1992).

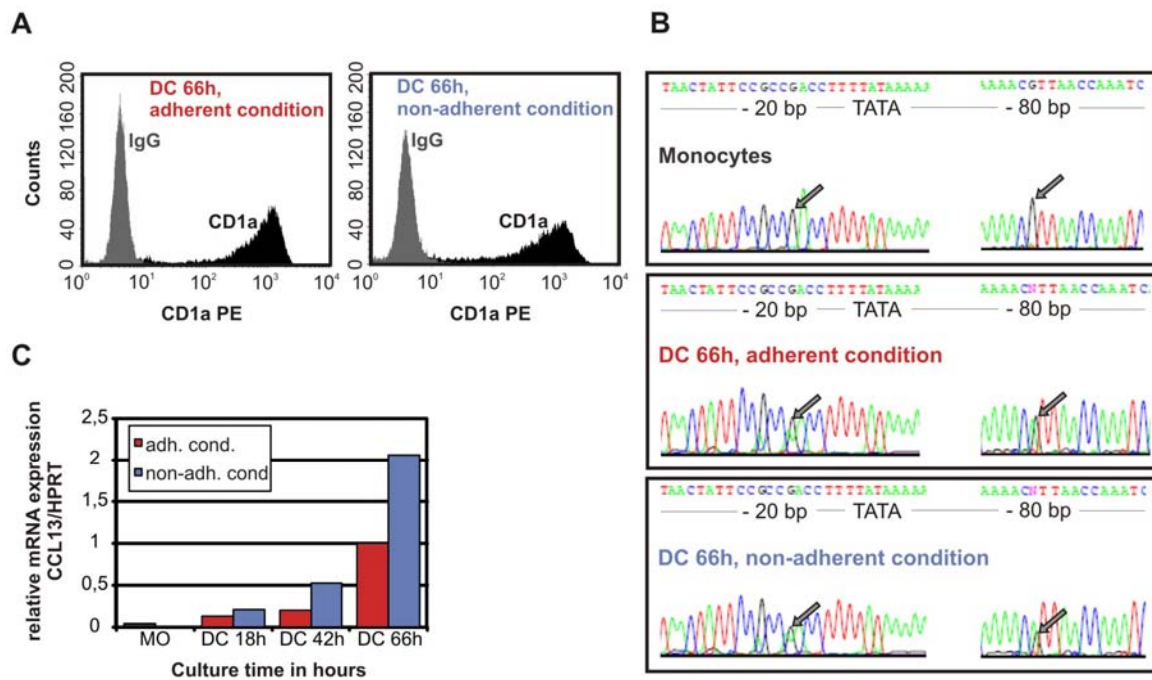


**Figure 5-10 Influence of adherence**

Monocytes were either cultured regularly in culture flasks or under rotating conditions in 200 ml Falcon tubes for 66 hours. **(A)** FACS analysis. DCs were stained with CD1a (PE) and IgG<sub>ges</sub> as isotype control after 66 hours in culture. **(B)** *CCL13* expression of monocytes (MO) and both DC “variants” at the indicated time points. Samples were analysed in duplicates and values were normalised to the *HPRT* housekeeping gene. **(C)** Sequencing pattern of the *CCL13* promoter after bisulfite conversion. Primers specific for the anti-sense strand were used for amplification. Amplicons were then sequenced by Entelechon. Grey arrows point to guanine residues partly exchanged by adenine residues (cytosine by thymine on the sense strand).

Bisulfite-treated DNA was amplified using primers specific for the anti-sense strand of the *CCL13*-promoter region. Therefore, methylation differences appeared as guanine-adenine transitions. Although the software termed the base at the -20 bp position still as a guanine, the sequencing curves showed a drastic reduction of the guanine peaks and elevated adenine peaks, indicating ongoing but not fully completed demethylation events (Figure 5-10B). In concordance with the previous data, demethylation of the -80 bp cytosine as well as of one of the -20 bp cytosines was observed during DC development in both flask and rotating falcon. Bisulfite conversion of DNA isolated after 18 and 42 h did not show any differences between conventional and rotating culture conditions as well (data not shown). The lack of adherence rather seemed to induce a stronger demethylation effect instead of inhibiting demethylation. Likewise, RNA expression levels of *CCL13* seemed to be higher under non-adherent conditions (Figure 5-10C). Because cell adherence did not seem to play a crucial role for signalling DNA demethylation in the preliminary experiment, this idea was not pursued further in order to focus on other approaches.

### 5.2.3 Global mRNA Expression Analysis

Genome-wide expression analysis were performed to identify groups of genes that may influence the active demethylation process as well as to study the correlation between CpG demethylation and expression status of candidate genes (see section 5.2.5). For this purpose, RNA was isolated at various time points during monocyte to dendritic cell differentiation and prepared for microarray hybridization using the Agilent labelling system. Raw data resulting from Agilent Feature Extraction software 9.5.1 were processed as described in 4.2.6.4. and values of independent donors were averaged for each time point. Figure 5-11A demonstrates expression kinetics of all significantly regulated genes relative to the expression values of monocytes. More than 7000 genes with an at least 5-fold change during the culture period were significantly regulated. According to the hierarchical clustering of time points (tree on top of the heat map in Figure 5-11), expression levels after 18 h/27 h as well as after 42 h/51 h/66 h were quite similar, whereas highest differences of transcription levels were observed between monocytes and DCs cultured for 6 hours.

Based on the complete gene list, two main clusters were defined: genes that were either consistently induced (up cluster) or consistently repressed (down cluster) during differentiation of monocytes towards dendritic cells (Figure 5-11A). The genes in between did not clearly fit in one of the other clusters as their expression profiles showed inconsistent, wave-like up- and down-regulation.

Assuming that coregulated genes share similarities in their regulatory mechanisms, their promoter regions may contain common motifs that are binding sites for transcription factors. The identification of transcription factor classes regulating the bulk of genes, possibly could indicate pathways that support the active DNA demethylation process. Thus, a *de novo* motif discovery algorithm (Brenner C et al; in preparation) was used to search for sequences that are significantly associated with each main cluster. The used algorithm only determines enriched motifs within gene promoters and does not account for other regulatory elements such as enhancers. Three binding motifs were highly enriched in the cluster of repressed genes (Figure 5-12B). The most significant one corresponds to the consensus binding site of the nuclear factor  $\kappa$ B (NF- $\kappa$ B), a critical regulator of many cellular processes including cell survival as well as immune response and anti-inflammatory actions. Furthermore, a motif corresponding to the interferon-stimulated response element (ISRE) was highly enriched within the cluster of down-regulated genes. ISREs represent the binding sites for IRF (interferon regulatory factor) transcription factors that are activated upon interferon (IFN) stimulation resulting in expression of genes important for viral defence. The third one

corresponds to the binding site of the repressor ZNF202 (zinc finger protein 202) that predominantly binds to elements which are found in genes involved in lipid metabolism and energy homeostasis (Wagner et al., 2000). Analysis of the cluster comprising up-regulated genes did not reveal any significant enriched motifs within their promoter regions.

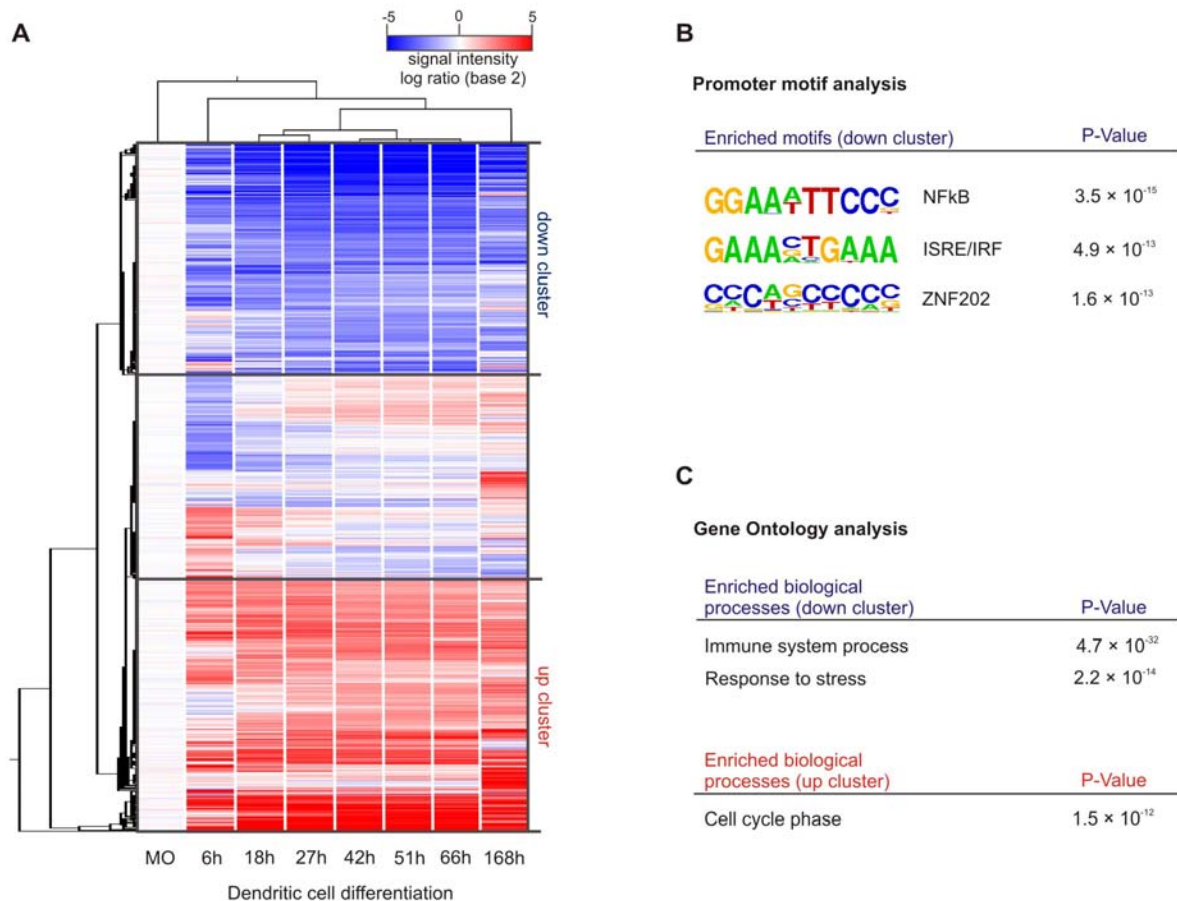


**Figure 5-11 Hierarchical clustering of all genes showing significant changes in expression during dendritic cell development**

(A) The expression levels of genes showing at least 5-fold up- or down-regulation are indicated by colour. Blue, white and red represent low, medium and high expression, respectively. The tree on top demonstrates similarities between the indicated time points and the tree on the left represents genes with similar expression patterns. After “per chip” and “per gene normalization” (see section 4.2.6.4), data of two (168 h time point), three (6 h to 66 h time points) or six (monocytes, indicated as MO) independent donors were averaged and evaluated relative to monocytes. Complete microarray data sets will be submitted with the corresponding publication, which is in preparation. (B) Enrichment of the indicated sequence motifs within the cluster of down-regulated genes with p-values from Fisher’s exact test. The motif discovery algorithm revealed no motif enrichment within promoters of up-regulated genes. (C) Gene Ontology (GO) categories that overlapped with either the up- or the down cluster. P-values were obtained from Fisher’s exact test.

In order to assess their biological interpretation, both gene cluster were searched for Gene Ontology (GO) categories that contained a large number of genes from each main cluster using the GO analysis tool. As listed in Figure 5-11C, there was a significant overlap

between the cluster of repressed genes and two related gene categories contributing to immune or stress responses. This is in concordance with the motif analysis that detected down-regulation of IFN and NFkB responsive genes. The cluster comprising highly up-regulated genes exhibited a slight enrichment of genes that are involved in cell cycle processes. Initially, enrichment of those genes was surprising, as dendritic cells do not proliferate (Figure 5-7). However, members of this gene category comprise genes that are not only implicated in mitosis or other cell cycle processes but are also important for DNA damage repair. Replication and damage checkpoints, for example, delay progression into mitosis and simultaneously promote transcription of repair proteins (de Bruin and Wittenberg, 2009). Additionally, DNA polymerases such as POLD1 (polymerase delta 1) or nucleases like exonuclease 1 (EXO1) are also involved in DNA repair processes (Hubscher et al., 2002; Parsons et al., 2007; Wei et al., 2003).

### **5.2.3.1 Expression Profiles of Highly Regulated Genes Associated with Transcription**

Genome-wide screenings for regulated genes and their classification may help to restrict the entity of genes to a smaller list of possible candidates for the active demethylation process and to assess the relevance of gene categories within our used model system. The combination of already published data and those screenings provides a tool to select putative candidate genes for further experiments.

Transcription factors and co-factors are believed to target histone modifying enzymes as well as the yet unknown demethylating machinery (Imhof, 2006; Niehrs, 2009; Rice et al., 2007; Schmitz et al., 2009). To study, which factors are regulated during DC differentiation, the expression of genes associated with transcription was analysed. Figure 5-12 depicts transcription factors that are highly regulated, varying in timing and intensity of expression. Interestingly, the bulk of genes changed their expression levels drastically within the first 6 hours in culture whereas only a small number of transcription factors was regulated at a later time point. The number of markedly regulated transcription factors emphasizes their importance for cellular processes including differentiation and might be a hint for their implication in targeting or regulating active DNA demethylation.



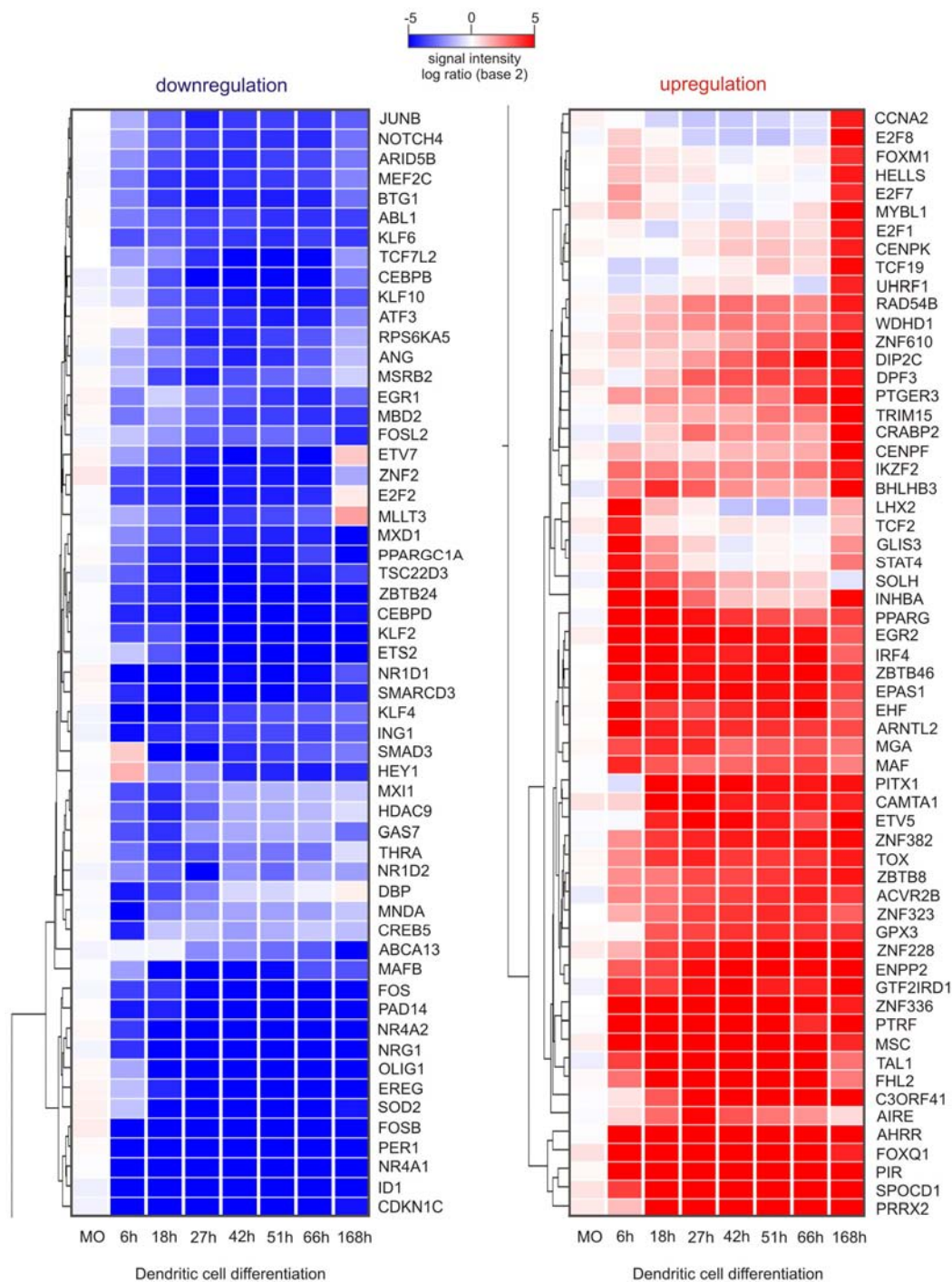


**Figure 5-12 Hierarchical clustering of genes associated with transcriptional regulation**

The expression levels of genes showing at least 16 fold up- (heatmap on the right) or down-regulation (heatmap on the left) are indicated by colour. Blue, white and red represent low, medium and high expression, respectively. Trees on the left side of both heatmaps represent the degree of similarity of regulated genes. After “per chip” and “per gene normalization” (see section 4.2.6.4), data of two (168 h time point), three (6 h to 66 h time points) or six (monocytes, indicated as MO) independent donors were averaged and analysed relative to monocytes.

### 5.2.3.2 Identification of DNA Repair Associated Genes Significantly Regulated during Dendritic Cell Development

The DNA repair machinery, or at least individual components of the DNA repair machinery, are thought to be involved in the active DNA demethylation process (Niehrs, 2009) (see also 1.1.1.2). The gene list of all significantly regulated genes was thus filtered for proteins that participate in DNA repair processes (Figure 5-13).

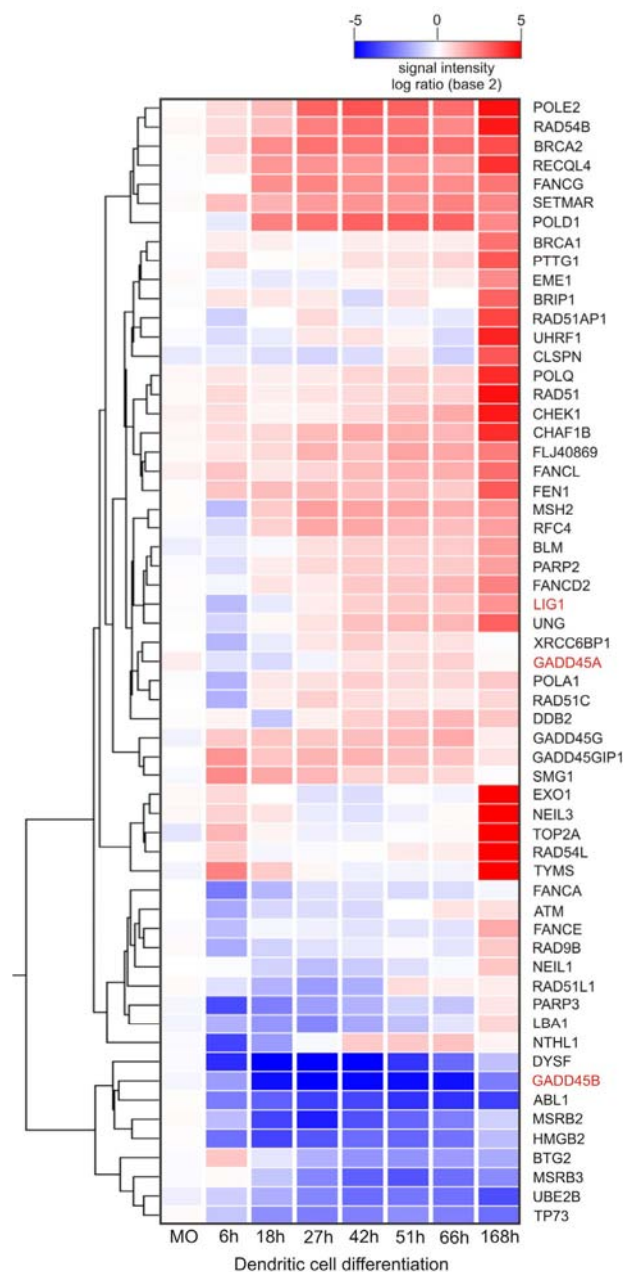


**Figure 5-13 Hierarchical clustering of genes associated with DNA repair**

The expression levels of genes showing at least 5 fold up- or down regulation are indicated by colour. Blue, white and red represent low, medium and high expression, respectively. Clustering on the left represents genes with similar expression patterns. After "per chip" and "per gene normalization" (see section 4.2.6.4), data of two (168 h time point), three (6 h to 66 h time points) or six (monocytes, indicated as MO) independent donors were averaged and evaluated relative to monocytes. Genes whose products were associated with active DNA demethylation in literature are indicated in red.

Timing and intensity of gene induction as well as repression were variable, ranging from early (6 h until 18 h) regulatory events to rather late effects (between 66 h and 168 h). In contrast to the transcription factors, the bulk of significantly up-regulated repair associated genes seemed to be highly induced not until a relatively late differentiation time point.

Within the last two years, *GADD45* (growth arrest and DNA damage-inducible) genes emerged as linking elements between DNA repair machineries and active DNA demethylation (Barreto et al., 2007; Ma et al., 2009b; Rai et al., 2008; Schmitz et al., 2009). The *GADD45* gene family includes *GADD45a*, *GADD45b* and *GADD45g*, whose products play a crucial role in cellular stress responses. In order to assess the role of *GADD45* proteins for active demethylation events during dendritic cell differentiation, *GADD45* expression profiles of the whole genome analysis were verified using RT-qPCR (Figure 5-14). Data of both approaches were highly consistent and revealed continuous up-regulation of *GADD45a* until the 66 h time point, following the decrease just after culturing the cells. *GADD45b* transcription was strongly repressed suggesting that *GADD45b* is not involved in CpG demethylation of dendritic cells. mRNA levels of *GADD45g* were not altered significantly during the analysed time window. Interestingly, macrophages and dendritic cells, both harvested after 168 hours in culture, showed comparable expression levels of every measured *GADD45* gene.

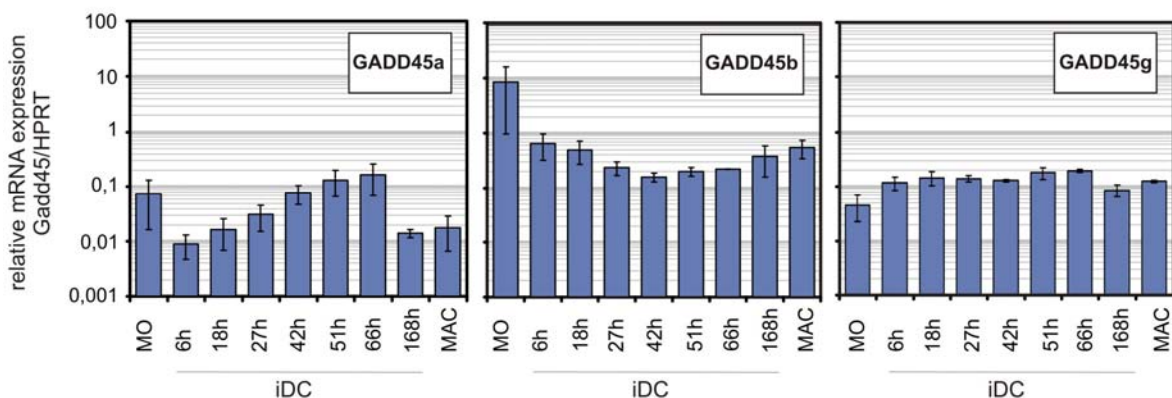


**Figure 5-14 mRNA expression profile of *GADD45* genes**

Real-time PCR for *GADD45* expression at the indicated differentiation time points of immature dendritic cells (iDC) compared to monocytes (MO) and macrophages after 168h in culture (MAC). Results were normalised for *HPRT* expression. Values are means  $\pm$  SD obtained from three independent experiments.

## 5.2.4 Genome-Wide Methylation Analysis of Dendritic Cells versus Monocytes and Macrophages

Assuming that the identification and characterization of additional examples of demethylated regions would help to understand the nature of active demethylation and, perhaps, common recruitment machineries, the MCIp (methyl CpG-Immunoprecipitation) approach was refined for a global screening of differentially methylated regions (DMRs) on microarrays. Validation of microarray data was then carried out using the MassARRAY System from Sequenom.

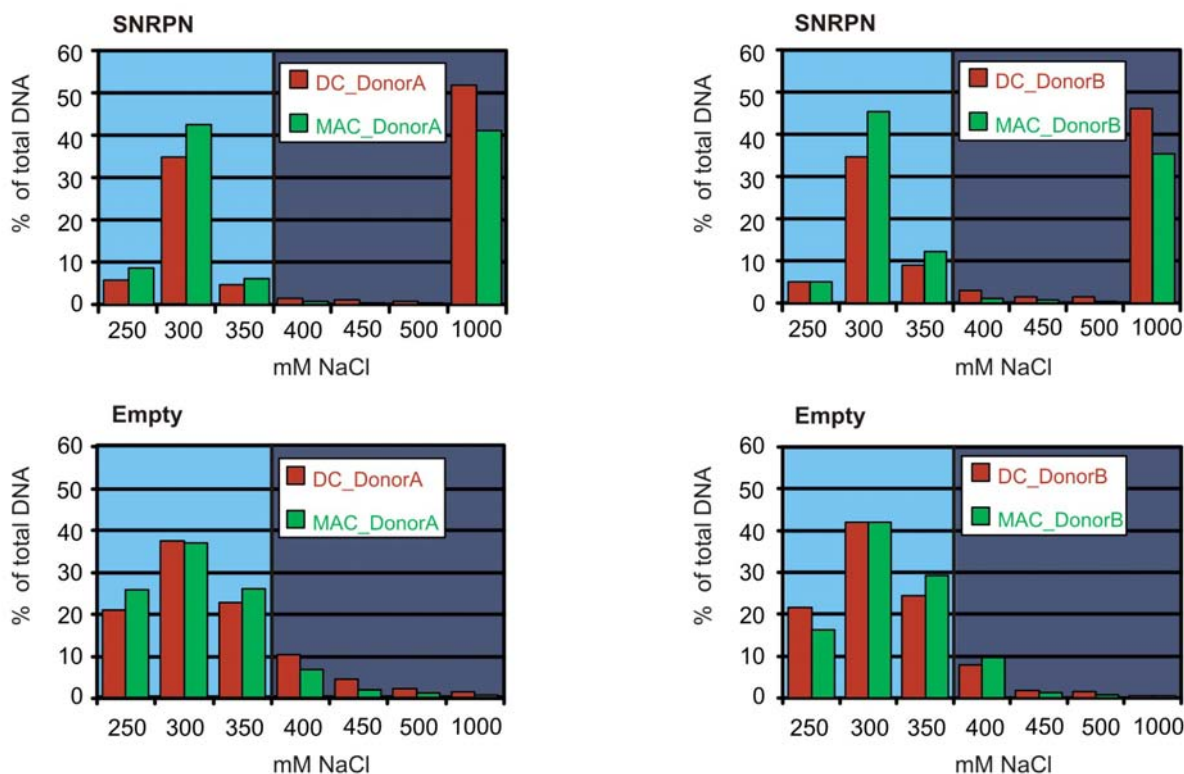
### 5.2.4.1 Global Screening for DMRs Using MCIp Combined to DNA Microarrays

Figure 5-15 represents the schematic work flow of the microarray experiment. Genomic DNA of *in vitro* differentiated macrophages and DCs from two donors was divided into hypermethylated (mCpG) and hypomethylated (CpG) pools via MCIp and subsequent qPCR. While both alleles of the imprinted *SNRPN* eluted in different fractions (the unmethylated one with a low salt buffer, the methylated one with the highest salt concentration), the bulk of the unmethylated CpG empty region is eluted after addition of the 350 mM NaCl buffer (Figure 5-15B). This salt concentration was therefore defined as “cut off” for the separation of both genomes into a CpG and a mCpG pool. Cell type-specific differences in DNA methylation were then identified by comparing co-hybridizations of the two (macrophages and DC) hypermethylated or the two hypomethylated DNA subpopulations on custom designed 244K oligonucleotide arrays. Arrays comprised about 17000 genes, -4000 to + 1000 bp from the transcription start site, with a few regions (including the *CCL13* and *TLR4* loci) tiled over a large genomic interval.

## A MCIp



## B “Cut-off” definition



## C Hybridization of hyper- and hypomethylated DNA pools

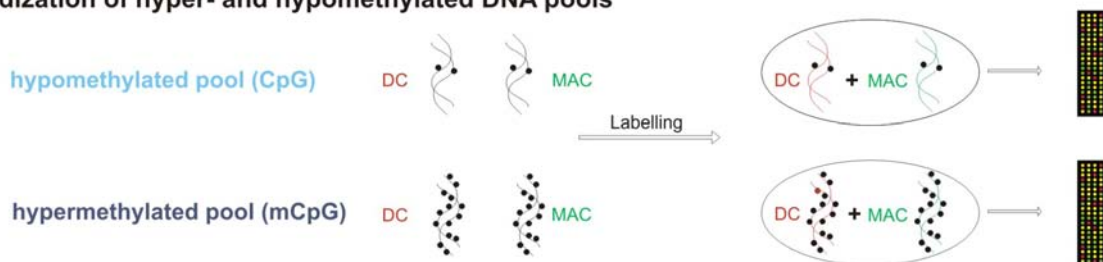


## Figure 5-15 Schematic outline of MCIp for comparative genome-wide methylation analysis

(A) Methyl-CpG-Immunoprecipitation (MCIp). Fragmented (350 – 400 bp) genomic DNA was bound to MBD-Fc-ProteinA-Sepharose for three hours. Each sample was then washed with increasing salt-concentrations to separate highly methylated DNA from unmethylated or weakly methylated DNA. Black circles indicate methylated CpG residues. (B) qPCR revealed a “cut-off” concentration of 350 mM NaCl used for dividing the genome of both donors into an unmethylated (CpG) and a methylated DNA (mCpG) pool. *SNRPN* is an example for an imprinted locus and the *Empty* region does not contain any CpG residue. (C) After purification, samples were labelled and the hypomethylated DC-DNA from DonorA was co-hybridized with the hypomethylated MAC-DNA pool of the same donor. Likewise, hypermethylated DNA from both cell types of the same donor were co-hybridized.

Enriched DNA-fragments from one cell type in the methylated fraction should be depleted in the unmethylated fraction and *vice versa*. Consequently, the signal intensities in CpG pool and mCpG pool hybridizations should behave mirror-inverted and thereby allow the identification of differentially methylated regions (DMR) (Figure 5-16; Figure 5-17 upper panels). In total, microarray analysis revealed 45 regions hypomethylated in dendritic cells compared to macrophages. A complete list is provided below, summarizing microarray and validation data (Table 5-4).

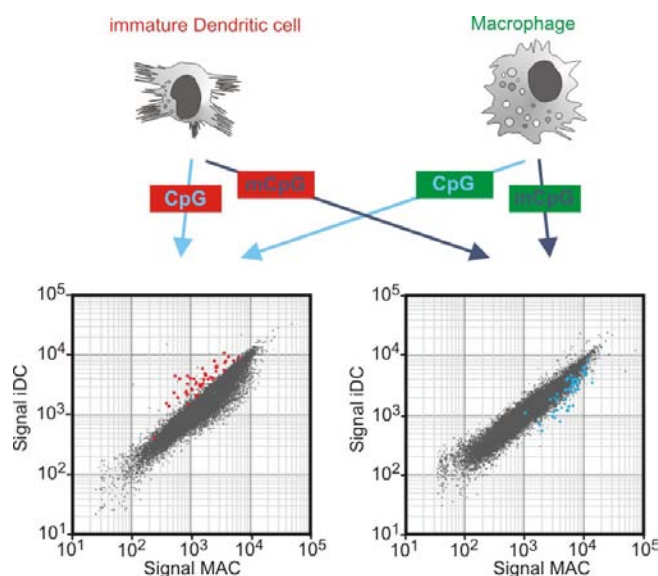


**Figure 5-16 Representative scatter plots of CpG and mCpG pool hybridizations**

The signal intensities of the unmethylated (CpG) DC pool were plotted against the signal intensities of the unmethylated macrophage pool (left side). Signal intensities of the methylated pools (mCpG) were plotted in the same way (scatter plot at the right). Probes enriched in the unmethylated pool of DCs (red spots) were enriched in the methylated pool of MACs (blue spots) and indicated the presence of DMRs. The reciprocal signal intensity ratios served as a preliminary, internal control for the reliability of microarray data. Complete microarray data sets will be submitted with the corresponding publication, which is in preparation.

#### 5.2.4.2 Comparison of Microarray Data with MALDI-TOF MS (EpiTYPER) Data

Validation using mass spectrometry analysis of bisulfite treated DNA (MassARRAY System, Sequenom) was highly consistent (validation rate of 83%) with the microarray data in two independent experiments and with the established positive control *CCL13*. Figure 5-17 shows several examples for the high reproducibility of both approaches. Although the focus laid on demethylation events in DCs, macrophages also exhibited hypomethylated regions (e.g. CD207 CpG6). In order to systematically identify DMRs in macrophages, comparative hybridization analysis between macrophages and monocytes need to be performed.

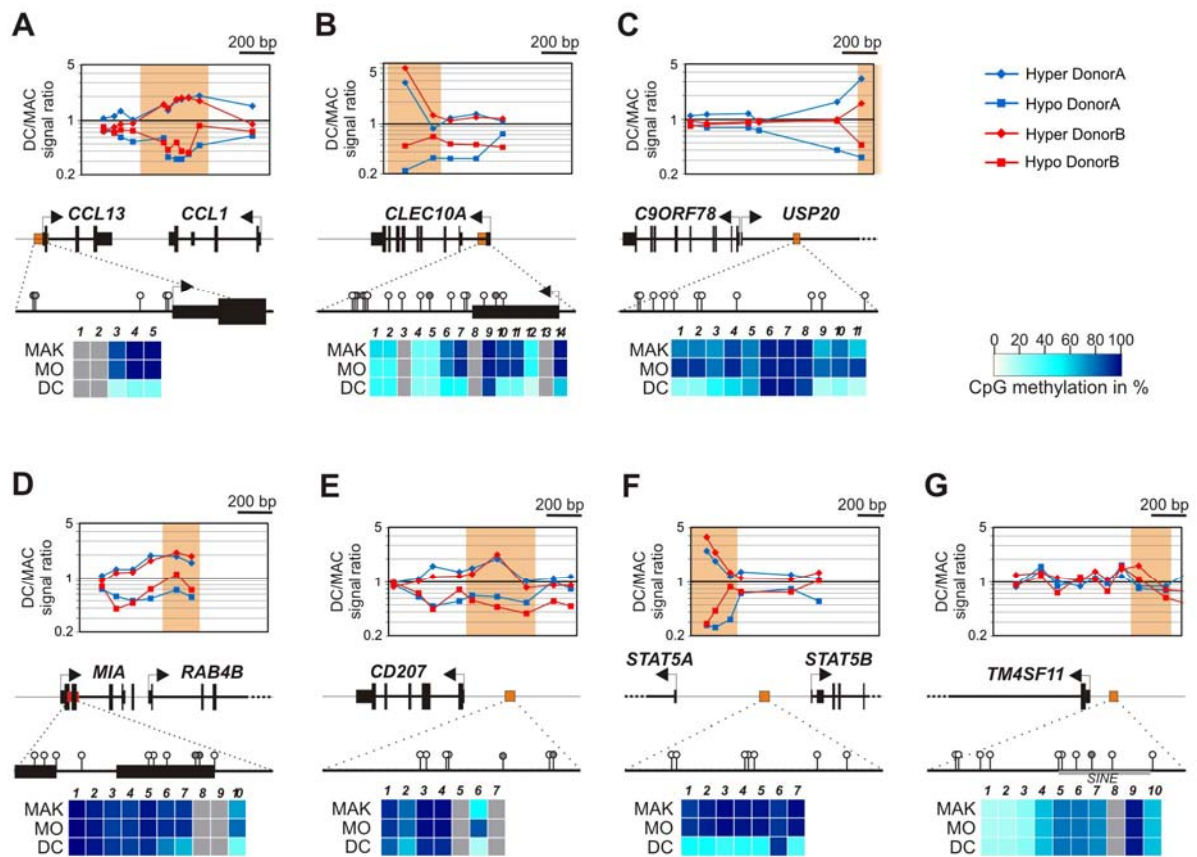


**Figure 5-17 Comparison of hybridization and EpiTYPER data**

(A-G) Diagrams at the top show signal ratios of the microarray probes for both independent experiments (DonorA in blue, DonorB in red) corresponding to their chromosomal localization. Typical DMRs are enriched in the hypomethylated fraction of one cell type and in the hypermethylated region of the other one resulting in a mirror-inverted image. Orange coloured zones indicate those sequence regions validated via bisulfite conversion. Middle panels represent the chromosomal location of DMRs (orange boxes). Regions analysed by MALDI-TOF MS of bisulfite converted DNA are indicated at the bottom. White circles represent detectable CpGs while grey circles or boxes show undetectable CpGs. Heatmaps represent the methylation status of individual CpGs (coloured boxes) averaged from at least 6 analyses of independent donors. (G) Example for a region without DMRs.

Eighteen of the hypomethylated sequences in DCs were controlled using MALDI-TOF MS (matrix-assisted laser desorption/ionization time-of-flight mass spectrometry) of bisulfite converted DNA and EpiTYPER software analysis (for detailed information see also Table 5-4). Validation revealed three false-positive loci resulting in a validation rate of 83%. In addition, 5 loci showing no methylation differences after microarray hybridization were verified with the MassARRAY system but were not considered for further analysis. Remarkably, the demethylation process was not limited to promoter regions as shown for the intergenic region between *STAT5A* and *STAT5B*, the upstream/downstream region of *C9ORF78/Usp20*, or the CpGs downstream the transcription start site (TSS) of *CLEC10A*.

### 5.2.4.3 Characterization of DNA Demethylation Events

In DCs, the existence of active DNA demethylation for at least 14 loci could be confirmed in addition to the initially identified *CCL13* promoter. Now, the time dependence of CpG demethylation was assessed by performing time course experiments. The methylation status of each time point was measured by the MassARRAY system and values of at least four different donors were averaged.

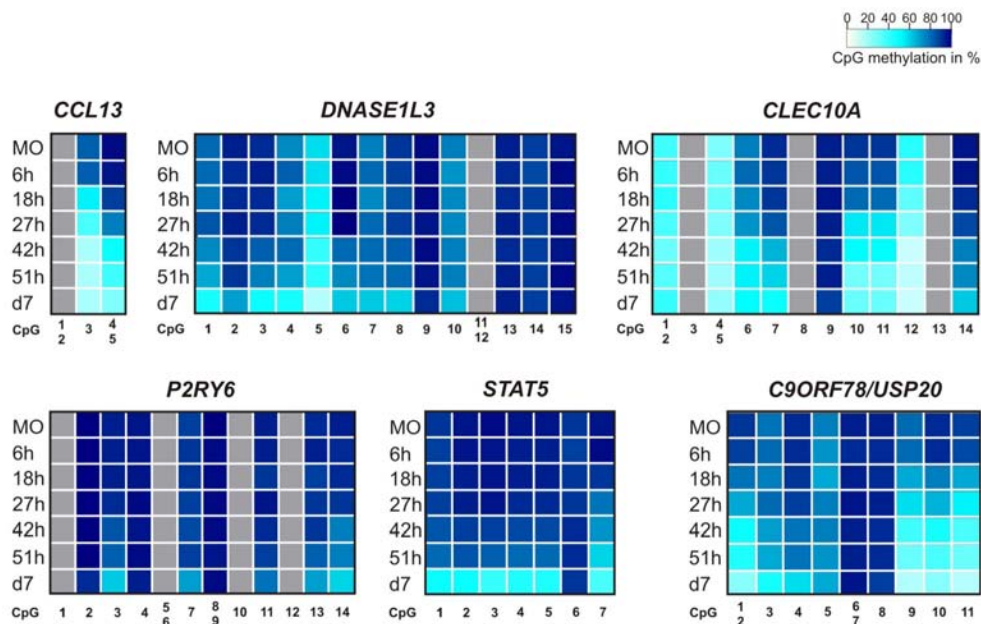


**Figure 5-18 Kinetics of DNA demethylation events**

Mass spectrometry analysis of bisulfite-converted DNA of the indicated culture time points. Heatmaps indicate the methylation content through blue gradations with each box standing for one CpG dinucleotide. Grey boxes represent CpGs not detected by MALDI-TOF MS. Data of 4 to 7 independent experiments were averaged. Indicated CpGs of *CCL13* and *DNASE1L3* are located within their proximal promoters. CpGs of *CLEC10A* and *P2RY6* refer to regions 300 and 500 bp downstream of the TSS and CpGs standing for *STAT5* and *C9ORF78* cover regions far upstream of the TSS or within the *USP20* gene, respectively (see also Figure 5-17 for their chromosomal location).

Heat maps in Figure 5-18 reveal that demethylation processes did not occur synchronously. *STAT5*, *P2RY6* and *DNASE1L3* are examples for late demethylation events, namely between 42 hours and 7 days in culture, whereas *CCL13* and *CLEC10A* demethylation started after 18 h or 27 h of differentiation. Even within one area of demethylation, CpG dinucleotides may be demethylated one after another, providing an explanation why the total demethylation process required more than 24 hours occasionally. For example, demethylation of CpG 3 within the *CCL13* promoter started reproducibly after 18 hours in culture, whereas first demethylation evidence for the following CpG dinucleotides was detected after 27 hours.



The comparison of DNA methylation patterns in various donors showed that the active removal of 5-meC reproducibly takes place at the same sites (exemplary shown for three regions in Figure 5-19). The high reproducibility demonstrated by the heatmaps below makes active CpG demethylation a strictly targeted event instead of being a (random) side effect.

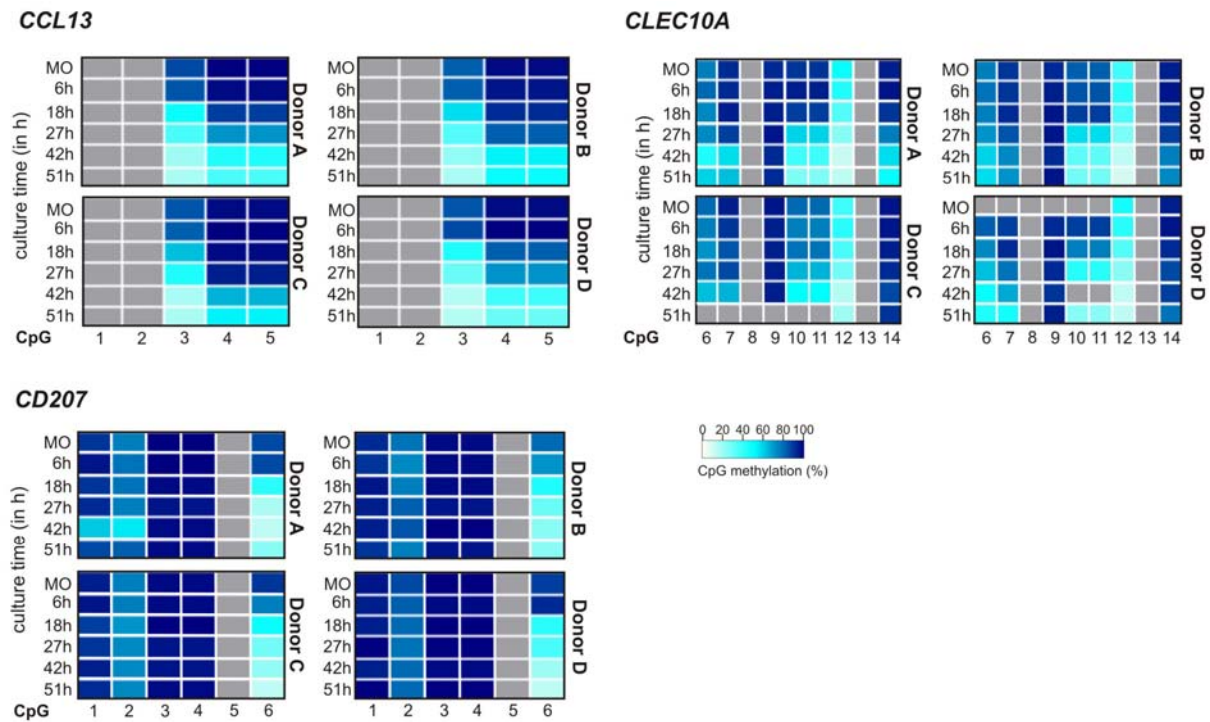


**Figure 5-19 Reproducibility of DNA demethylation events**

Mass spectrometry analysis of bisulfite-converted DNA of the indicated differentiation time points. Heatmaps indicate the methylation content through blue gradations with each box representing one CpG dinucleotide. Grey boxes indicate CpGs that were not detected by MALDI-TOF MS. Data of four donors are shown in isolated heatmaps to demonstrate the high reproducibility between independent experiments.

Table 5-4 summarizes the chromosomal locations along with the corresponding (annotated) genes of all detected and validated DMRs. Note that three loci could not be confirmed and were thus not listed in the following table. Six out of 15 validated DMRs were related to promoter regions whereas the remaining nine ones were located either downstream or far upstream of the TSS of the corresponding genes.

**Table 5-4 Description of detected DMRs; ordered as in Figure 5-20**

Chromosomal location of DMR	Annotated Gene	Offset from TSS	MassArray validation	Alternative Gene	Offset from TSS of the alt. gene
chr14:022422974-022423031	REM2	700		-	
chr6:033151084-033151130	HLA-DPB1	-700	ND	HLA-DPA1	-1700
chr22:036284946-036284994	CDC42EP1	800		-	
chr10:012125841-012125897	UPF2	-800		-	
chr6:161379958-161380005	MAP3K4	-2700		-	
chr11:118457096-118457143	HMBS	-3800		-	
chr7:156648162-156648213	DNAJB6	-2600		-	
chr2:201820275-201820325	CFLAR	300		-	
chr15:070866345-070866389	ADPGK	-3200	YES	-	
chr1:148780880-148780925	S100A10	-1200		-	
chr17:018024022-018024075	ALKBH5	-2500		-	
chr9:129680760-129680817	C9ORF78	-3700	YES	USP20	3500
chr17:037689148-037689197	STAT5A	-4500	YES	STAT5B	-7200
chr4:152374670-152374722	RPS3A	-3700		-	
chr6:030239347-030239393	TRIM15	100	YES	TRIM10	-2700
chr6:030188405-030188462	TRIM31	200		-	
chr12:050585784-050585841	ACVRL1	-1200		-	
chr5:169062431-169062481	DOCK2	-5700		-	
chr2:113588928-113588987	IL1RN	-2900		-	
chr2:070976946-070976999	CD207	-2300	YES	-	
chr8:022464090-022464149	SORBS3	-700		-	
chr20:043421999-043422053	DBNDD2	-3200		-	
chr19:045973172-045973217	MIA	-100	YES	-	
chr1:150560005-150560050	SLC27A3	-1000	YES	-	
chr2:088307570-088307628	FLJ10916	-1400		-	
chr18:000606234-000606293	CLUL1	-500		-	
chr6:112148968-112149027	FYN	-1000		-	
chr1:209173701-209173760	ATF3	-3100		-	
chr15:072516450-072516498	SEMA7A	-3100		-	
chr3:058171761-058171820	DNase1L3	-100	YES	-	
chr21:036427003-036427052	CBR3	-2300	YES	-	

Table 5-4 continued

Chromosomal location of DMR	Annotated Gene	Offset from TSS	MassArray validation	Alternative Gene	Offset from TSS of the alt. gene
chr17:006923912-006923971	CLEC10A	400	YES	-	
chr14:020560610-020560669	NDRG2	-700	YES	-	
chr5:134812435-134812494	C5ORF20	-1500		TIFAB	-3500
chr19:057018722-057018781	FPRL2	-100		-	
chr11:072661646-072661702	P2RY6	750	YES	-	
chr1:021742203-021742254	RAP1GAP	-1100	YES	-	
chr19:007670583-007670633	FCER2	400		-	
chr14:022693817-022693863	SLC7A8	-400	ND	-	
chr17:029707544-029707588	CCL13	-100	YES	-	
chr4:139520655-139520705	SLC7A11	500		-	
chr14:076362022-076362078	C14ORF166B	-500	YES	-	

Gene annotation by the chip manufacturer only refers to that gene, whose promoter is located nearest to the relevant locus. In order to guarantee a complete list of all genes that may be affected by differential methylation, every demethylated locus was searched for alternative genes in its environment using the UCSC genome browser. The distance of each DMR is listed for both, the annotated as well as the alternative (alt.) gene in order to group DMRs for their location.

## 5.2.5 Correlation between Active DNA Demethylation and mRNA Expression

The combination of global DNA methylation and global mRNA expression data sets now allowed a correlation analysis between DNA demethylation and mRNA expression. Expression data was extracted from the whole genome time course data described in Figure 5-11A for all DMR associated genes. About one third of the analysed genes showed strong up-regulation during DC differentiation, whereas transcription activity of a bulk of genes seemed not to be influenced by DNA demethylation (Figure 5-20).

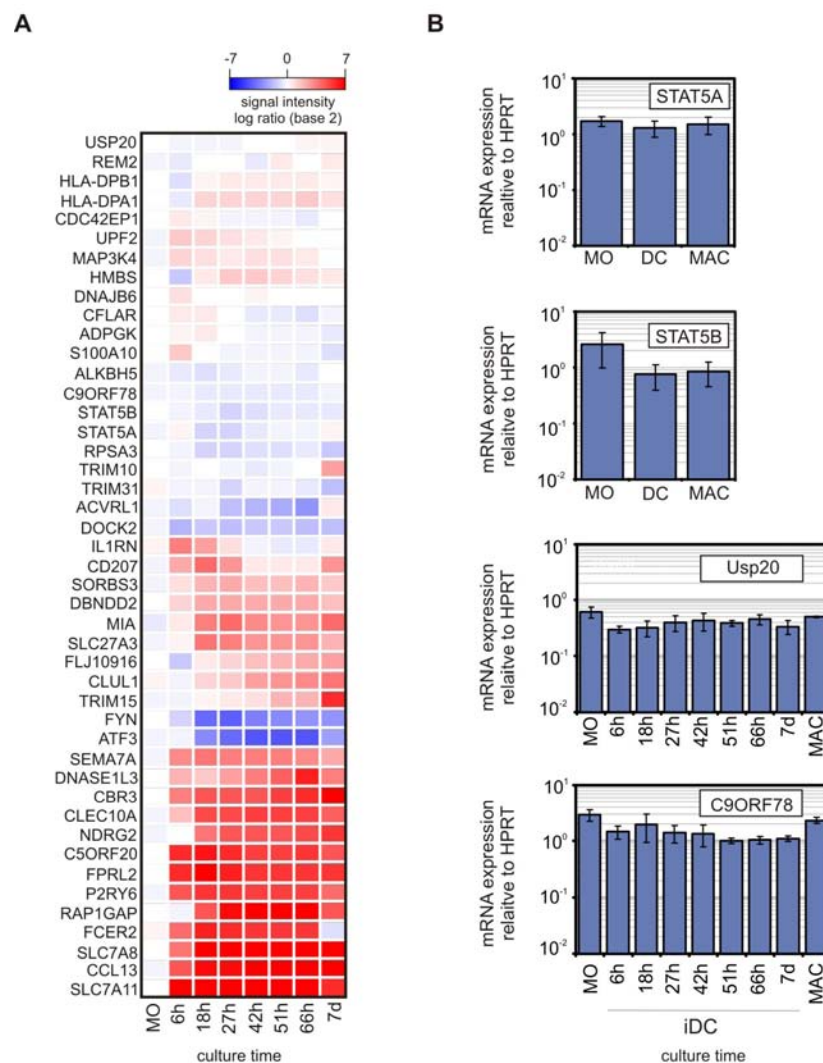


**Figure 5-20 mRNA expression profiles of genes related to DMRs**

(A) The expression levels of genes showing dendritic cell specific CpG demethylation displayed as a heatmap. Blue, white and red represent low, medium and high expression, respectively. Data of two (DC day 7), three (DC 6 – 66 h) or six (MO) independent donors were averaged and normalised to monocytes (MO). (B) Validation of mRNA microarray experiments using RT-qPCR. *STAT5* expression was only controlled in monocytes as well as in seven day old macrophages and dendritic cells. Data were normalised to *HPRT* expression. Values are means and  $\pm$ SD obtained from three independent experiments.

### 5.2.6 Histone Modifications Surrounding DMRs

Because histone modifications provide information about the chromatin accessibility and the gene expression status, the question arises, if there is also a link to active DNA demethylation. By means of reporter constructs, it was demonstrated that histone acetylation and transcription are necessary for active demethylation (D'Alessio et al., 2007; Detich et al., 2003). Promoter regions of active genes are characterized by the acetylation of various histone H3 and H4 residues as well as by histone 3 lysine 4 (H3K4) methylation (Barski et al., 2007; Bernstein et al., 2005; Kim et al., 2005; Pokholok et al., 2005; Schubeler et al., 2004). Here, it is important that methylation of H3K4 occurs in three different forms: mono-, di- and trimethylation (H3K4me1, H3K4me2 or H3K4me3) which are interdependent. Heintzman *et al.* as well as Barski *et al.* identified different chromatin signatures of promoter and enhancer regions, providing new insights into correlations between chromatin modifications and transcriptional regulation (Barski et al., 2007; Heintzman et al., 2007). Despite of several similarities in their histone modification profiles, Heintzman *et al.* distinguished enhancers from promoters by an enrichment of H3K4me1 but missing H3K4me3. Promoter areas, however, were characterized by strong H3K4 trimethylation but marked depletion of H3K4me1. In order to determine the timing of ongoing events and the relevance of activating histone marks during DNA demethylation in dendritic cells, chromatin immunoprecipitations were performed at different differentiation time points. Corresponding to the bisulphite data, seven demethylated sites covering upstream, downstream and promoter regions were selected for real time PCR analysis.

Every analysed activating histone modification was detected quite early within gene promoter regions, although acetylation of histone H3 and H3K4me3 seemed to be slightly delayed (Figure 5-21). Trimethylation of histone 3 lysine 4, a modification usually connected to actively transcribed genes, successively increased with culture time corresponding to the *CCL13* mRNA data shown in Figure 5-9A.

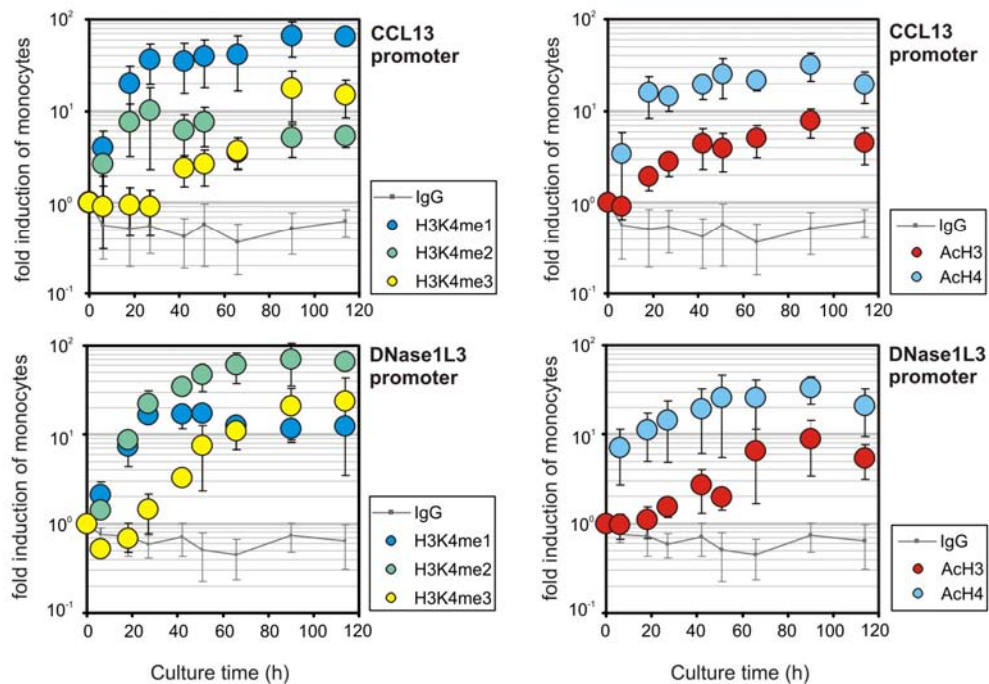


**Figure 5-21 Correlation of histone modifications with CpG demethylation at promoter regions**

Activating histone marks were analysed at differentially methylated promoter regions during dendritic cell differentiation using ChIP. Grey lines represent the background control IgG. DNA enrichment of the indicated time points is normalised to 5% input DNA and shown relative to monocyte (0 h) enrichment. Data represent mean values  $\pm$ SD of at least three independent ChIP experiments.

ChIP primers for the transcriptionally active genes *CLEC10A* and *P2RY6* (see Figure 5-20) cover a region less than 1000 bp downstream their TSSs. Within this area high levels of H3K4me3 were detected whereas H3K4me1 was completely absent (Figure 5-22). H3K4me2 was detected at the *P2RY6* locus but not at *CLEC10A*. This is in line with recently published genome-wide, high resolution data describing a significant dip in H3K4me3 signals between -200 to +50 bp but strong signal peaks at +50, +210 and +360 bp of active genes (Barski et al., 2007). In that study, two major peaks for each modification were detected: -900 and +1000 for H3K4me1, -500 and +700 for H3K4me2 and -300 as well as +100 for H3K4me3.

Signals of mono- and dimethylation downstream the TSS of highly active genes, that were analysed in the context of the present thesis, decreased, probably due to the high levels of trimethylation (Figure 5-22). The H3K4me2 signal at the *CLEC10A* locus seems to flare up only at the beginning, suggesting that the mono- and dimethylated states were not captured due to the rapid and complete methylation of lysine 4.

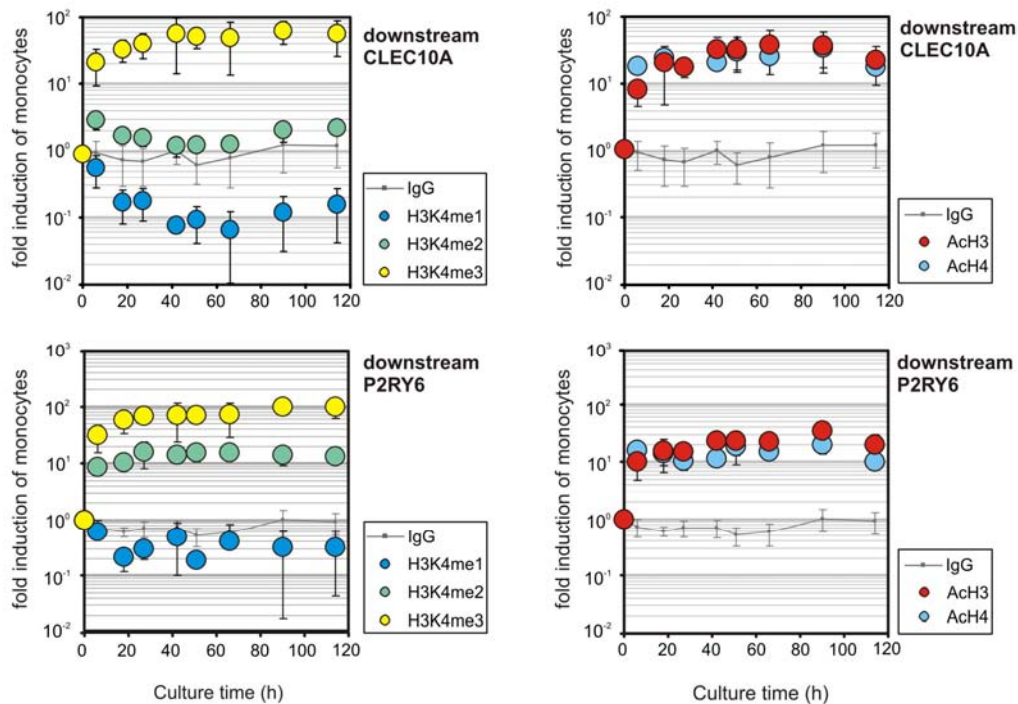


**Figure 5-22 Correlation of histone modifications with CpG demethylation at intragenic regions**

Activating histone marks were analysed at DMRs downstream TSSs during dendritic cell differentiation using ChIP. Grey lines represent the background control IgG. DNA enrichment of the indicated time points is normalised to 5 % input DNA and shown relative to monocyte (0 h) enrichment. Data represent mean values  $\pm$ SD of at least three independent ChIP experiments.

As expected, H3K4 trimethylation was only measured at loci near the transcription start sites (TSS) whereas this mark was undetectable in upstream regions (Figure 5-23). The pattern of histone modifications at the intergenic sites reflected some characteristics of enhancers as described by Heintzman *et al.*. Certainly, to confirm this hypothesis, further experiments like transfection assays have to be done.

Dimethylated H3K4 (H3K4me2) was the most abundant mark compared to the other methylation states because it was detected quite early and at every demethylated site irrespective of the investigated genomic region. Acetylated histone 3 and histone 4 (AcH3 and AcH4) were also found at every demethylated region with AcH3 showing weaker signals except for the downstream regions.

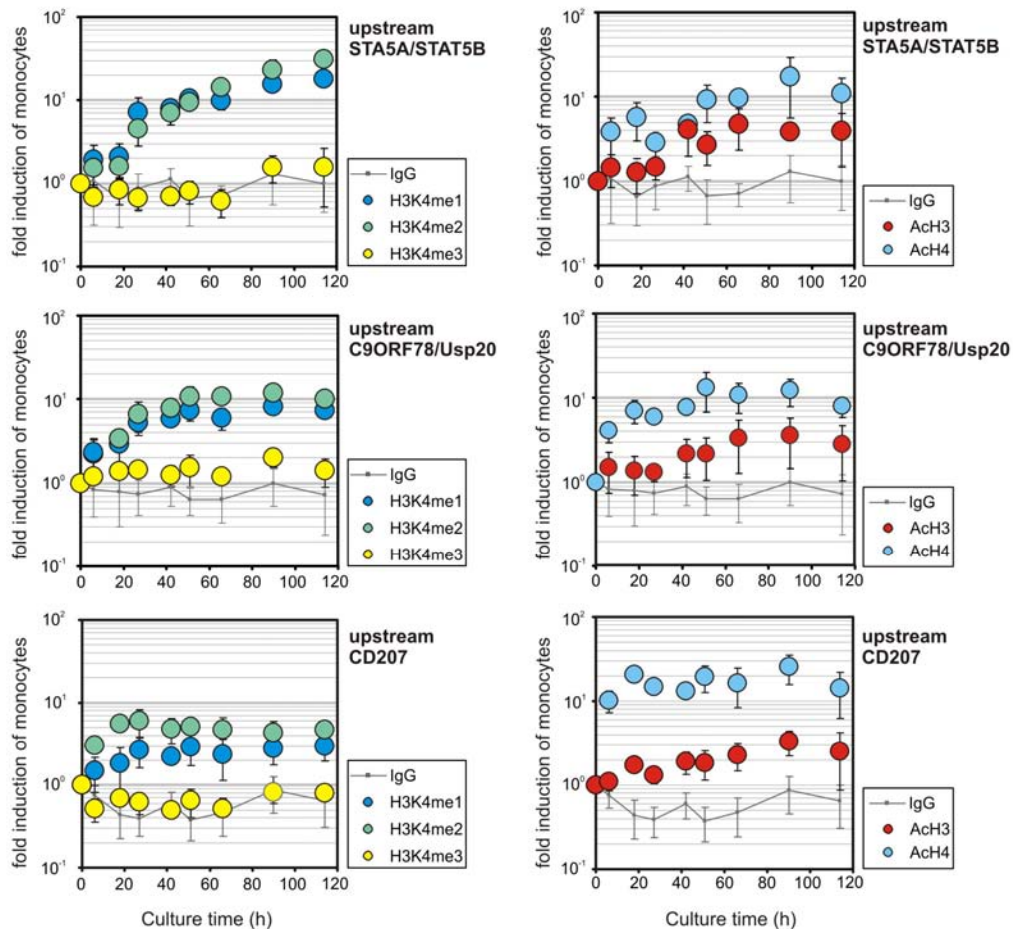


**Figure 5-23 Correlation of histone modifications with CpG demethylation at intergenic regions**

Activating histone marks were analysed at DMRs upstream or upstream/downstream (regarding to the *C9ORF78-Usp20* locus; see also Figure 5-17) from TSSs during dendritic cell differentiation using ChIP. Grey lines represent the background control IgG. Samples were normalised to the 5 % input DNA and evaluated relative to monocytes. Data represent means  $\pm$ SD obtained from at least three independent donors.

Time course experiments analysing DNA methylation patterns and histone modifications demonstrated that CpG demethylation succeeded or occurred simultaneously with alterations in the histone code. Downstream of the *P2RY6* transcription start site, DNA demethylation started after approximately 42 hours in culture. Histone marks were already detected after 6 hours when the locus was still completely methylated. Likewise, histone modifications at the *DNASE1L3* promoter or at the intragenic *CLEC10A* region appeared before first DNA demethylation events were detected. At other loci like the *CCL13* promoter or the intragenic *C9ORF78* region, it was difficult to determine, whether the appearance of histone marks coincided with DNA demethylation or preceded it, on the basis of the present data.



## 5.3 Cell Type-Specific DNA Demethylation

The distribution of H3K4me2 enrichment at lineage-specific hematopoietic promoters reflects the differentiation potential of hematopoietic cell lines (Orford et al., 2008). Furthermore, developmentally poised genes may be identified by defined H3K4 methylation patterns. It is therefore reasonable that the DNA methylation profile, which seems to be correlated with chromatin modifications, also indicates developmentally poised genes.

Lineage-specific transcription factors play key roles in determining cell fates during the differentiation of progenitor cells into mature cell types. Because their tight regulation on the transcription level is likely controlled by epigenetic mechanisms, lineage-restricted transcription factor genes might represent good candidates for the analysis of cell type-specific DNA methylation.

### 5.3.1 Identification of Cell Type-Specific Transcription Factors

The hematopoietic system provides a well-defined model, whose distinct cell-types can be isolated efficiently. Thus, to identify cell type-specific transcription factors, global transcriptome analysis was performed using mRNA of all major mononuclear cell types in human blood (monocytes, B cells, NK cells, and T cells) as well as of monocyte-derived dendritic cells and macrophages. CD34<sup>+</sup> progenitor cells were also included, in order to follow the hematopoietic hierarchy.

After leukapheresis, half of the obtained peripheral blood mononuclear cells (PB-MNCs) were sorted for CD8<sup>+</sup> (T cell), CD4<sup>+</sup>25<sup>+</sup> (regulatory T cell), CD4<sup>+</sup>25<sup>-</sup> (conventional T-cell), CD19<sup>+</sup> (B cell), CD56<sup>+</sup> (natural killer cell) and CD14<sup>+</sup> (monocyte) surface antigen expression using the BD FACSAria by the group of Petra Hoffmann and Matthias Edinger (University Hospital Regensburg, Institute of Hematology and Oncology). Cells were prepared for RNA and DNA isolation immediately after cell sorting to prevent degradation of nucleic acids. The other part of PB-MNCs was elutriated and resulting monocytes were then *in vitro* differentiated into macrophages and DCs until day 7 or directly processed for DNA and RNA isolation, respectively. CD34<sup>+</sup> progenitor cells from two different donors were purchased from Lonza.

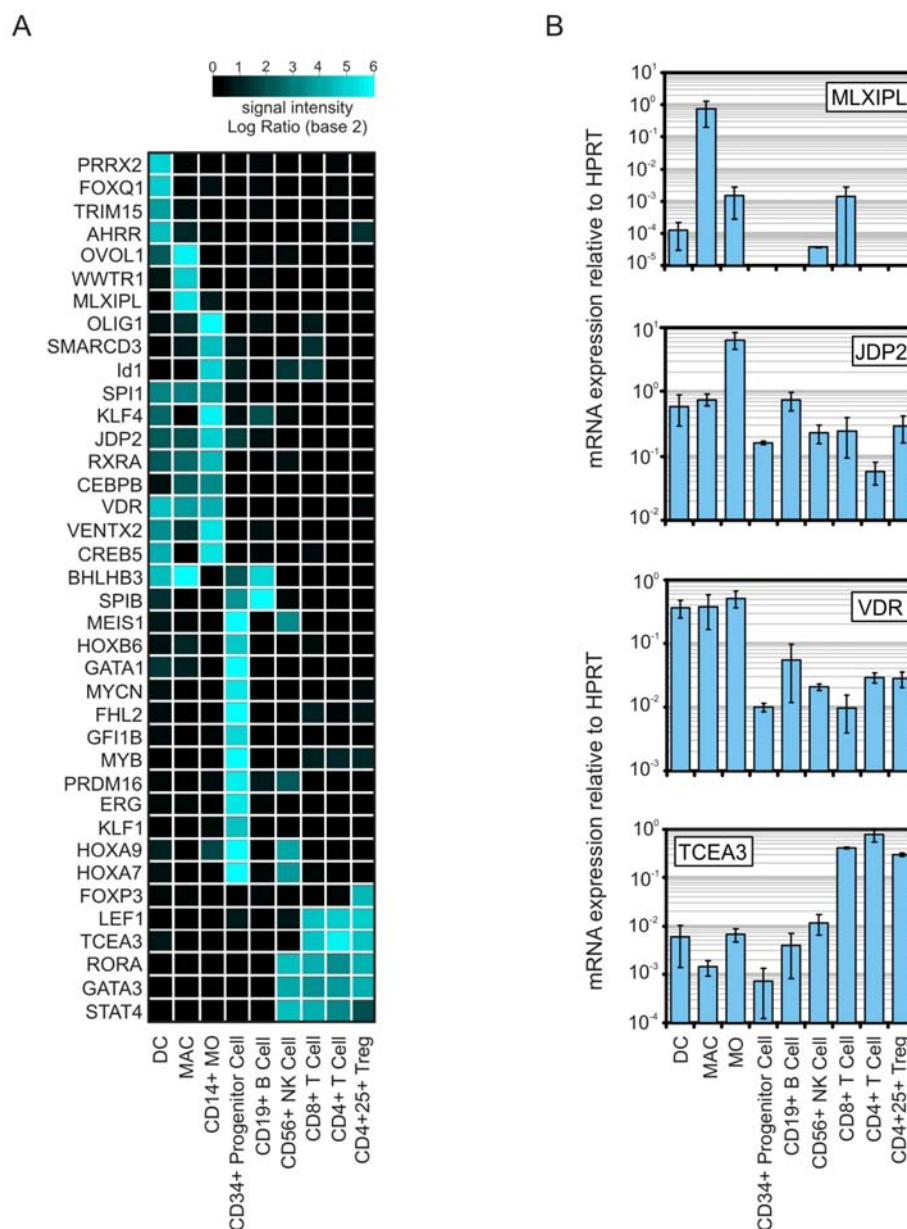


**Figure 5-24 Transcription factor gene expression in human blood cell types**

**(A)** Heat map of transcription factors with lineage-enriched expression in mononuclear blood cell types. Microarray expression data were obtained from two (CD34+ progenitors) to three (all other cell types) independent donors and median normalised. Genes were selected based on an at least ten-fold over-expression in one lineage (e.g. myeloid or lymphoid) or one individual cell type the median of all other types. Low expression signals are illustrated by dark boxes and stronger signals are indicated in bright blue. Complete microarray data sets will be submitted with the corresponding publication, which is in preparation. **(B)** Validation of microarray data using RT-qPCR. Results were normalised to HPRT expression. Data represent mean values of two (CD34+ cells, CD4+25+), three (CD19+, CD4+25-, CD8+ and CD56+ cells) or six (dendritic cells day 7, macrophages day 7, monocytes) different donors measured in duplicates.

Whole genome expression analysis revealed a set of thirty eight transcription factor genes that showed at least 10-fold higher expression in either of the cell lineages (myeloid versus lymphoid) or cell types (Figure 5-24A). Supportive data for lineage restricted expression of most of the identified genes was found in two online reference databases (LSBM RefExA [[www.lsbm.org/site\\_e/database/index.html](http://www.lsbm.org/site_e/database/index.html)] for monocytes and macrophages or BioGPS

[[www.biogps.gnf.org](http://www.biogps.gnf.org)] for white blood cells) as well as in the literature. FOXP3 for example is known to be a specific transcription factor for regulatory T cells (Treg; CD4+CD25+) (Baron et al., 2007; Hoffmann et al., 2009) and SPI1 (also known as PU.1) is absolutely required for myeloid and B cell development (McKercher et al., 1996; Scott et al., 1994; Zhu and Emerson, 2002). A subset of newly identified lineage-specific factors was selected for validation by RT-qPCR. The previously undescribed lineage specific expression of *MLXIPL* in macrophages, *TCEA3* in T cells, *JDP2* in monocytes and *VDR* in myeloid cells was confirmed by RT-qPCR (Figure 5-24B). As the comparison of elutriated and CD14+ sorted monocytes revealed almost identical expression profiles (data not shown), both monocyte-types were considered as one population.

### 5.3.2 Promoter Methylation Profiles of Cell Type-Specific Transcription Factors

After establishing a set of transcription factor genes that were highly enriched in individual blood cell lineages or cell types, the DNA methylation status of their promoter regions was determined. Genomic DNA samples originating from the same donors and the same day as the RNA samples analysed in chapter 5.3.1, were prepared for bisulfite treatment and measurement using the MassARRAY system.

Methylation patterns of the non-CpG island *SPI1* and *SPIB* promoters represented prime examples for lineage or cell type-specific expression, probably regulated by DNA methylation (Figure 5-25). While the *SPIB* promoter region was free of CpG methylation in CD19+ positive B cells, this locus was strongly methylated in all the other cell types analysed. Likewise, the *SPI1* region was consistently methylated in the non-expressing lymphoid cell types and completely unmethylated in progenitor cells as well as in myeloid (monocytes, DC, macrophages) and B cells. The analysed region of the *GFI1B* locus exhibited only slightly higher methylation levels in the lymphoid lineage (CD56+ NK cells, CD4+ and CD8+ T cells). However, CpGs within the SINE element downstream the transcription start site were largely methylated in all cell types. *GFI1B* was induced specifically in CD34+ precursor cells (Figure 5-24) indicating that the DNA methylation status of the promoter region is not pivotal for cell type specific *GFI1B* expression. The CpG-rich regions around the *TCEA3* and the *KLF4* TSS were barely methylated and did not show significant differences between the various cell types.

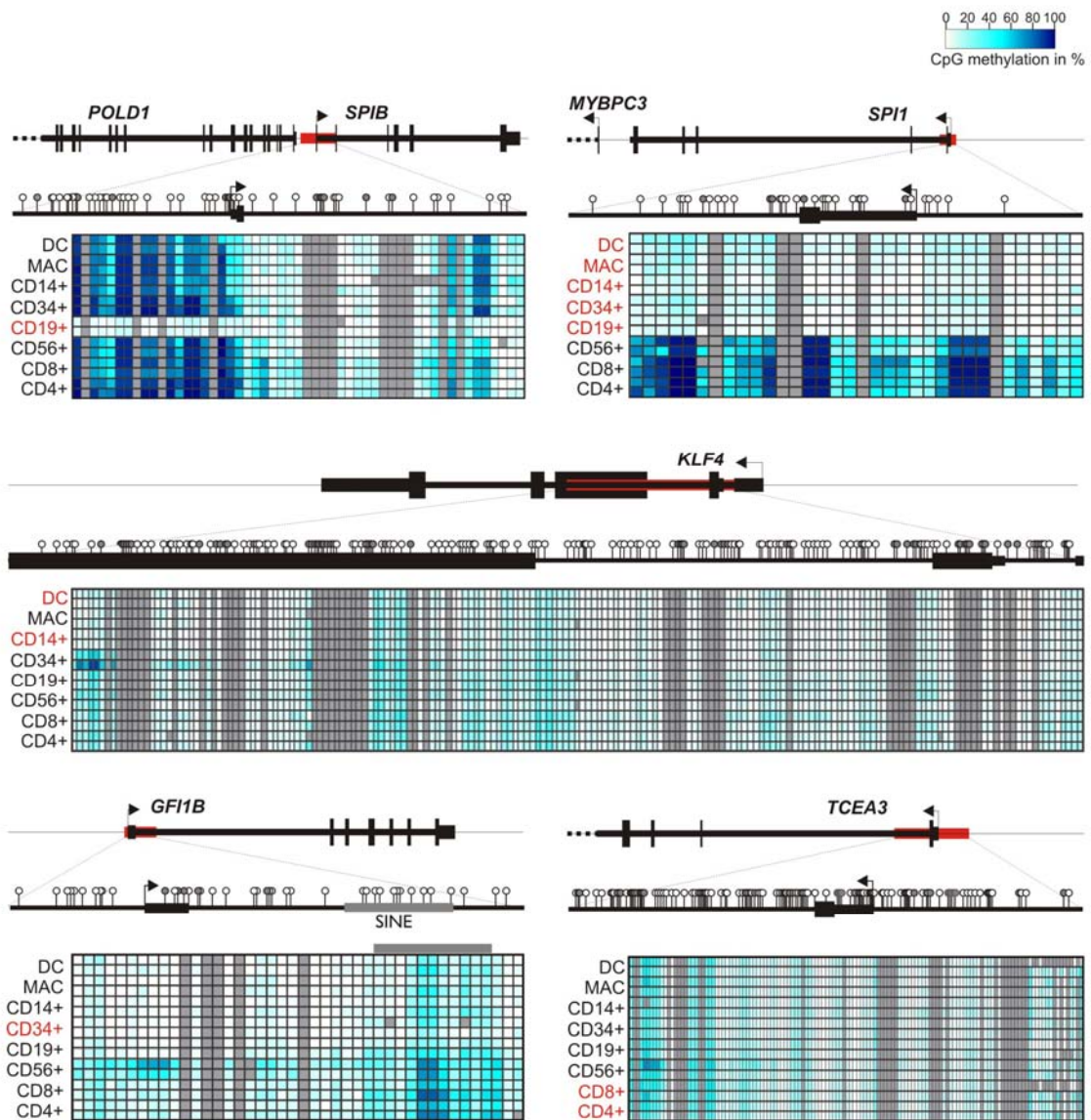


**Figure 5-25 Examples of methylation profiles for lineage enriched transcription factor genes**

gDNA samples of two independent donors were bisulfite treated and prepared for MassARRAY analysis. The upper panel describes the chromosomal location of the analysed regions (indicated in red). White circles stand for detectable CpGs while grey circles could not have been measured by the mass spectrometer. Heat maps at the bottom show the methylation status of each individual CpG of both donors in blue gradations. Grey boxes indicate cytosine residues that were not detected by the MALDI-TOF MS. Cell types expressing the corresponding gene are highlighted in red.

An overview of all promoter regions analysed is given in Table 5-5. Most of the cell type- or lineage-specific transcription factors were associated with CpG island (CGI) promoters which were unmethylated in every cell type. Cell type-specific differences in the methylation profiles were only observed within non-CGI promoter regions.

**Table 5-5 Methylation analysis of cell type-specific transcription factors**

Ordered according to Figure 5-24 with TSS indicating the transcription start site and CGI indicating CpG islands promoters

Gene	Analyzed region, Offset from TSS	CpG density of the associated promoter	# of amplicons	Methylation pattern
<i>PRRX2</i>	-640 to +1760 bp	CGI	10	Variable between donors
<i>FOXQ1</i>	-1500 to +1700 bp	CGI	13	No differences
<i>TRIM15</i>	-160 to +1040 bp	Low	9	Partly DC specific
<i>AHRR</i>	-700 to +1100 bp	Low	11	No differences
<i>OVOL1</i>	-1300 to +1700 bp	CGI	13	No differences
<i>WWTR1</i>	-900 to +1500 bp	CGI	13	No differences
<i>MLXIPL</i>	-300 to +1500 bp	CGI	13	No differences
<i>SMARCD3</i>	-1100 to 800 bp	CGI	11	No differences
<i>ID1</i>	-1300 to +1700 bp	CGI	17	No differences
<i>SPI1</i>	-600 to +1600 bp	Low	12	Hypermethylation in NK and T cells (Figure 5-25)
<i>KLF4</i>	-1100 to +2200 bp	CGI	15	No differences (See Figure 5-25)
<i>CEBPB</i>	-1000 to +1800 bp	CGI	13	No differences
<i>VDR</i>	-1100 to +660 bp	CGI	11	No differences
<i>VENTX2</i>	-2800 to +900 bp	CGI	22	No differences
<i>CREB5</i>	-1100 to +900 bp	Low	11	No differences
<i>BHLHB3</i>	-2000 to +3200 bp	CGI	27	No differences
<i>SPIB</i>	-780 to +1300 bp	Intermediate	14	Hypomethylated in B cells (Figure 5-25)
<i>MEIS1</i>	-2300 to +1600 bp	CGI	21	No differences
<i>GATA1</i>	-1600 to +500 bp	Low	13	No differences
<i>MYCN</i>	-1100 to +2500 bp	CGI	20	No differences
<i>FHL2</i>	-800 to +1000 bp	CGI	12	No differences
<i>GF11B</i>	-400 to +1500 bp	Intermediate	11	Slightly hypermethylated in NK and T cells (Figure 5-25)
<i>MYB</i>	-900 to +2200 bp	CGI	19	No differences
<i>ERG</i>	-450 to +1800 bp	Intermediate, CGI directly downstream TSS	12	No differences
<i>KLF1</i>	-800 to +3000 bp	Intermediate	21	Slightly hypomethylated in CD34+ and myeloid cells
<i>FOXP3</i>	-1000 to +1100 bp	Low	13	Demethylated in regulatory T cells
<i>LEF1</i>	-1000 to +2000 bp	CGI	19	No differences
<i>TCEA3</i>	-800 to +1200 b	CGI	9	No differences (Figure 5-25)
<i>RORA</i>	-800 to +1700 bp	CGI	15	No differences
<i>GATA3</i>	-4600 to +1700 bp	CGI	34	No differences
<i>STAT4</i>	-500 to +1500 bp	Intermediate	12	No differences

However, the finding that the bulk of cell type-specific TFs did not show differences in their promoter methylation pattern does not automatically exclude DNA methylation as important regulator for cell type-specific gene expression. Functionally important differences in CpG methylation may be found at promoter distal sites as described for several other genes such as *FOXP3*, whose activity is controlled by a downstream, methylation-sensitive enhancer (Baron et al., 2007; Floess et al., 2007; Kim and Leonard, 2007). In fact, recent studies, including work of our group (Schmidl et al., 2009), indicate that differentially methylated regions are preferentially found at promoter distal sites and often correlate with enhancers (Decker et al., 2009; Meissner et al., 2008; Schmidl et al., 2009; Yagi et al., 2008).

## 6 Discussion & Perspectives

Methylation of CpG dinucleotides plays a crucial role in numerous biological processes including gene expression, silencing of retrotransposons, genomic imprinting, X-chromosome inactivation and cancer (Bird, 2002; Herman and Baylin, 2003). However, surprisingly little is known about its impact during differentiation of normal somatic cells. The data of the present thesis provide a basis for further investigations on especially CpG-poor DNA stretches, their implication in differentiation-dependent gene regulation and the dynamics of methylation patterns.

### 6.1 Transient Transfection as a Tool to Assess the Effect of DNA Methylation on Gene Expression

One aim of this thesis was to develop a tool for studying the influence of promoter methylation on gene expression. By means of transient transfection assays, the comparison of *in vitro* methylated promoter constructs and their unmethylated counterparts provides insights into the repressive nature of CpG methylation on transcriptional activity. However, *in vitro* methylation of a traditional reporter vector that contains a large number of backbone CpGs significantly suppressed the activity of a CpG-free promoter when methylated (Figure 5-1). The effect of methylated CpGs within the vector backbone was thus sufficient to markedly repress the activity of an intrinsically CpG-free promoter. To avoid those unspecific side-effects, a novel luciferase vector, called pCpGL, was constructed. Due to the lack of backbone CpG dinucleotides, the effects of DNA methylation were entirely limited to the promoter of interest instead of being a consequence of unspecific CpG methylation in the vector backbone (Figure 5-2 and Figure 5-3). In terms of significance and implementation, *in vitro* methylation of pCpGL constructs has significant advantages over the previously used, less specific or time-consuming approaches.

In contrast to the methylation-dependent repression of CpG island promoters, the effect of CpG methylation on CpG-poor promoters is less well established. The novel luciferase reporter vector will enable systematical studies of methylation-dependent effects of both, CpG-rich as well as CpG-poor promoters. However, analyses are not limited to promoter regions. In addition to promoter methylation, the methylation pattern of other regulatory elements such as enhancers seems to interfere with gene expression (Bretschneider et al., 2008; Decker et al., 2009). Combined cloning of a candidate enhancer with a CpG-free

promoter (such as *EF1*) into the pCpGL vector and subsequent transfection of the methylated and unmethylated plasmids, allows the identification of methylation dependent enhancers as shown in a recent publication by our group (Schmidl et al., 2009). The pCpGL vector could not be successfully used to study relevant promoter regions described in this thesis. However, the vector has been applied in numerous other laboratories documented by already released (Dong et al., 2008; Kundakovic et al., 2009) and upcoming publications.

## **6.2 Dynamic Methylation Patterns of CpG-poor DNA Stretches as Important Regulators for Differentiation**

During the recent years, the perception of differential DNA methylation and the dynamics of the methylation patterns has markedly changed. CpG islands (CGI) were previously thought to be almost entirely free of methylation with few exceptions including the second inactive X chromosome of females (Goto and Monk, 1998) or the silent allele of imprinted genes (Li et al., 1993). Recent global methylation analysis of CGIs comprising promoter regions as well as promoter distal sites, however, revealed that 25-30% of CGIs become *de novo* methylated in a tissue-specific manner during development (Straussman et al., 2009). CpG dinucleotides outside CGIs are traditionally considered to be methylated and thereby to silence potential hazardous genetic elements such as retrotransposons (Robertson and Wolffe, 2000; Walsh et al., 1998). However, the methylation status of especially CpG-poor DNA stretches turned out to be dynamic and crucial for cell type- or tissue-specific gene expression (Brunner et al., 2009; Lathrop et al., 2009; Lee et al., 2002; Rouhi et al., 2006). These findings are supported by quantitative methylation analysis of cell type- or lineage-restricted transcription factors performed as part of this thesis. Cell type- or lineage-specific methylation profiles for several of the analysed regulatory factors were only detected at non-CpG island promoters, such as *SPI1* or *SPIB* (Figure 5-25; Table 5-5). Although there is a significant number of methylated CGIs throughout the genome (Illingworth et al., 2008; Straussman et al., 2009), the great majority of CpG island promoters is protected from CpG methylation in normal cells (Bird, 2002; Eckhardt et al., 2006; Weber et al., 2007). This protection possibly results from the presence of special transcription factors like Sp1 (Brandeis et al., 1994) or specific histone marks such as dimethylation of histone 3 lysine 4 (Weber et al., 2007).

Regarding the differentially methylated regions identified in the context of this thesis, the influence of specific methylation patterns on gene expression remains to be proven. Nevertheless, the presented data argue for a regulating role of DNA methylation at CpG-poor



DNA stretches during normal hematopoietic development and emphasize the dynamic potential of DNA methylation.

Although CpG-poor regions seem to be more important targets of dynamic DNA methylation than CGIs, the extent of cell type- or lineage-specific differentially methylated regions throughout the genome has not been completely defined, yet. Likewise, it is unclear how these differences are established during development and differentiation. Whereas the enzymatic transfer of methyl-groups onto unmethylated CpGs is a well characterized process, the removal of methyl cytosines is less well understood. The failure of DNMT1 to methylate the nascent daughter strand of replicating DNA represents a non-enzymatic passive way for removing the methyl mark. This is a comparatively slow process, as maximal 50 % of methylated CpGs are demethylated after one replication cycle (Kress et al., 2001). On the other hand, DNA demethylation may be achieved through a replication-independent, active mechanism, implying the activity of specific enzymes. The existence of such active demethylation mechanisms in humans is still doubted (Ooi and Bestor, 2008), although numerous studies accounted for the occurrence of actively demethylated DNA and identified several candidate factors that may be involved in the demethylating process. Most of these were performed in artificial cell systems like (pharmacologically arrested) cell lines (Kangaspeska et al., 2008; Metivier et al., 2008) or with embryonic cells (Hajkova et al., 2008; Lucarelli et al., 2001), questioning the biological relevance of the observations and providing reasons to argue for a passive mechanism. The unique model system presented in this work allowed the identification and characterization of active DNA demethylation events in untreated post-mitotic primary cells. Differentiation of human peripheral blood monocytes into dendritic cells (DC) and macrophages (MAC) respectively, occurs without proliferation (Figure 5-7), implying that all observed demethylation events have to be active. The reproducible detection of multiple demethylated regions in a post-proliferative cell system (Table 5-4) thus proves the existence of active demethylation events. Likewise, several studies on dividing primary cells or cell lines also argue for the involvement of an active enzymatic mechanism, as the kinetics of the demethylation procedure are too fast to be dependent on cell proliferation. Demethylation of a specific CpG site within the human *IL2* promoter, e.g., occurs within one hour after activation of CD4+ positive T cells (Murayama et al., 2006) and is therefore independent of cell division. Using a rat hepatoma cell line as well as E15 fetal hepatocytes, Kress *et al.* reported DNA demethylation within a glucocorticoid-responsive unit of the *tyrosine aminotransferase (tat)* gene locus upon activation by the glucocorticoid receptor (Kress et al., 2006). Within the time frame of one cycle of cell division, the proportion of unmethylated cytosines at the *tat*-locus reached 85 %, thereby excluding a purely passive demethylation mechanism. The detection of specific DNA

strand breaks next to the methylated cytosine during demethylation suggests the involvement of DNA repair machineries and confirms the dependence on an active process. Given these and other examples (Hajkova et al., 2008; Kersh et al., 2006; Metivier et al., 2008), it is doubted that passive DNA demethylation plays a major role in gene-specific demethylation (Niehrs, 2009). Moreover, it seems counterproductive that regulatory mechanisms which have to adopt rapidly to environmental signals, are based on such a slow and indirect process like passive demethylation. The absence of an active demethylation process would furthermore imply that differentiated, post-mitotic cells would lack CpG demethylation based epigenetic regulation. In other words, those cells would lack a regulatory process, which has been shown to be crucial for priming genes as well as for the induction of mRNA expression.

Earlier studies in our laboratory supported the existence of active DNA demethylation by detecting the first example for differentiation-dependent active demethylation in differentiating monocytes (Heinz S., 2002). The *CCL13* promoter contains three CpG residues within its proximal promoter region that are methylated in monocytes. Two defined residues, -20 as well as -80 bp upstream of the transcription start site, were demethylated during dendritic cell differentiation, accompanied by transcriptional activation. Although the *CCL13* promoter of differentiated macrophages remained methylated, short-time expression was observed after four hours in culture (Heinz S., 2002). RNA expression profiles over seven days of dendritic cell culture demonstrated the continuous, strong up-regulation of *CCL13* (Figure 5-9A), suggesting that CpG demethylation is necessary for strong and constant *CCL13* expression. Using chromatin immunoprecipitations, binding of the interleukin 4 (IL-4) inducible transcription factor STAT6 (signal transducer and activator of transcription 6) to the proximal promoter was detected (Figure 5-9D). Recruitment of STAT6 seemed to occur after initial promoter demethylation and continued over the analysed time period. The two STAT6 binding sites [TTC(N<sub>2-4</sub>)GAA] of the *CCL13* promoter do not contain a CpG residue and are therefore not directly affected by CpG methylation. This argues for a model where several transcription or co-factors act in concert to provide an accessible chromatin state allowing enduring transcription. Possibly, CpG demethylation is a necessary prerequisite for the binding of another (sequence-specific) and methylation-dependent DNA binding factor that in turn recruits STAT6. As STAT6 binding alone is usually not sufficient to stimulate the activation of a specific locus (Hebenstreit et al., 2006), the collaboration of both, the yet not identified factor and STAT6, may keep the chromatin architecture of this region in an active state and promote transcription. Such a stabilizing role of transcription factors has already been shown in other cell models, including e.g. T cells. Following CD4<sup>+</sup> T cell stimulation, a specific CpG residue within the human *IL-2* promoter becomes demethylated (Murayama et

al., 2006). Demethylation is crucial for the binding of the constitutive transcription factor Oct-4, which is responsible for maintaining the presence of activating histone modifications such as acetylation of histone H3. The interplay between demethylation, transcription factor binding and the histone code for long-term transcription of *CCL13*, might be proven by blocking the demethylation process followed by controlling STAT6 binding and the presence of histone modifications. However, as long as the mechanisms that are responsible for active demethylation remain unclear, their inhibition is difficult. Nevertheless, various substances such as DNA polymerase inhibitors that block possibly involved DNA repair mechanisms, have been applied to freshly prepared monocytes for up to three days (Table 5-3). The analysed chemicals were either toxic or did not show any effect either on DNA demethylation or on *CCL13* expression. Transient transfection assays using unmethylated or *in vitro* methylated pCpGL\_*CCL13* promoter constructs, could have confirmed a direct correlation between DNA demethylation and gene expression. However, a cell line that intrinsically expresses the *CCL13* chemokine was not identified. All human (THP-1, HepG2) and murine cell lines (RAW, NIH3T3) tested, failed to transcribe unmethylated *CCL13*-promoter constructs following successful transfection.

To further characterize active DNA demethylation of especially CpG-poor DNA regions, global methylation analysis of differentiating dendritic cells needed to be performed. The recent development of techniques that enrich methylated DNA permitted the investigation of DNA methylation patterns on global platforms such as oligonucleotide tiling arrays or next generation sequencers. Current technologies, including RLGS (restriction landmark genomic scanning), DMH (differential methylation hybridization), Methyl-Seq (sequencing of digested DNA using methylation-sensitive enzymes) and MeDIP (methyl-DNA immunoprecipitation) are particularly suited for the analysis of CpG-dense regions (Brunner et al., 2009; Costello et al., 2009; Mohn et al., 2009; Weber et al., 2005). However, they are not sensitive enough for the systematic detection of differentially methylated CpG-poor DNA stretches. Methyl-Seq, DMH and RLGS are based on the digestion with methylation-sensitive enzymes and are thus limited to the presence of the corresponding recognition sequences. Consequently, those approaches do not cover every occurring CpG residue. For example, only 3.9% of all nonrepeat CpGs in the human genome reside within recognition sites of *Hpa II*, a restriction enzyme that is used for Methyl-Seq and DMH (Fazzari and Grealley, 2004). Moreover, the application of CpG-rich recognition sequences of eight base pairs (Fazzari and Grealley, 2004; Smiraglia and Plass, 2002) and the requirement of several CpG containing recognition sites in close proximity (Brunner et al., 2009) bias those methods towards CpG-islands. MeDIP (also called mDIP) circumvents the described motif bias by detecting methylated DNA with an antibody directed against 5-methylcytidine (Mohn et al.,

2009). However, this approach specifically enriches for methylated fragments and is dependent on the CpG content of the analysed fragments also resulting in a strong bias towards CpG-rich DNA regions (Keshet et al., 2006; Suzuki and Bird, 2008; Weber et al., 2007). Previously, a technique for the fractionation of genomic DNA fragments depending on their CpG density, was established in our laboratory (Gebhard et al., 2006b; Schilling and Rehli, 2007). This approach, called MCIP (methyl CpG Immunoprecipitation), is not dependent on certain sequence motifs and sensitive enough for methylation analysis of CpG-rich as well as CpG-poor DNA stretches. Regarding the objective of the present thesis, MCIP was adapted to identify differentially methylated regions between monocyte-derived macrophages and dendritic cells by separating the genome into hyper- and hypomethylated CpG pools (Figure 5-15). Comparative genome hybridization resulted in the detection of 45 loci specifically demethylated in dendritic cells (Figure 5-16; Table 5-4), partly validated using the bisulfite based MassARRAY approach with a validation rate of 83%. Interestingly, differentially methylated regions (DMR) are not only present within proximal promoters but also, in large part, at promoter-distal sequences (Table 5-4). These data are in line with recent comparative genome-wide methylation analyses performed in our and other groups (Illingworth et al., 2008; Song et al., 2009). E.g. in T cells, it was shown that only approximately 5% of the DMRs are located at proximal promoters (Schmidl et al., 2009). In transient transfection assays, several of the distal DMRs showed methylation-dependent enhancer activity. More global studies in ES cells identified promoter-distal loci as the main sites of changes in the methylation pattern during cell differentiation (Meissner et al., 2008). Investigation of the murine liver revealed that tissue-specific differentially methylated regions are localized a few kilobases away from the TSS and that the methylation status of those regions correlates with transcriptional activation of adjacent genes (Yagi et al., 2008). Hence, the vast majority of dynamic methylation changes is found at promoter distal sites, suggesting that a major function of DNA methylation is to restrict the activity of cell type-specific enhancers.

The evidence for occurring active DNA demethylation events entails the question about the underlying mechanisms and therefore about the identification of enzymes showing convincing activity on 5-methylcytosine. DNA mismatch glycosylases including MBD4 (methyl-CpG binding domain protein 4) and TDG (thymine DNA glycosylase) were shown to be involved in DNA demethylation (Kangaspeska et al., 2008; Metivier et al., 2008; Zhu et al., 2000) but they both have only weak 5-meC base excision activity relative to their activity on thymine (Cortazar et al., 2007; Zhu et al., 2000). Consequently, if those mismatch glycosylases do really mediate DNA demethylation, there must be an initial process providing the appropriate substrate. A study in zebrafish embryos suggests that the 5-meC deaminase

AID (activation induced cytidine deaminase) converts methylated cytosine residues into thymines which finally can be excised by MBD4 (Rai et al., 2008). Another possibility is provided by Tahiliani *et al* suggesting that cytosine demethylation is carried out via the TET1 (ten eleven translocation) dependent formation of 5-hydroxymethylcytosine (hmC) as intermediate (Tahiliani et al., 2009). The existence of hmC was proven in the genome of mouse ES cells, but its universality as well as the affinity of glycosylases or other repair associated enzymes for this intermediate remain to be elucidated.

Although base excision repair mechanisms were shown to mediate active demethylation in flowering plants, their implication in the active removal of mammalian 5-meC has not been definitely proven, yet (Agius et al., 2006; Kapoor et al., 2005; Morales-Ruiz et al., 2006). However, there is emerging evidence that components of the base excision repair (BER) as well as the nucleotide excision repair (NER) machinery are involved in active demethylation of mammalian DNA (Barreto et al., 2007; Ma et al., 2009b; Metivier et al., 2008; Rai et al., 2008). The involvement of DNA repair mechanisms would imply a momentary occurrence of single strand nicks. On the basis of a study that visualized strand breaks during active cytosine demethylation (Kress et al., 2006), these nicks were analysed in differentiating monocytes via ligation mediated PCR of genomic DNA. The low detection limit of this approach, which requires synchronized demethylation events may provide one reason why no sample showed indications for occurring strand breaks (data not shown). Therefore, this approach seems not suitable for the detection of DNA nicks in untreated, differentiating monocytes. Additionally, the presence of stable 5'-phosphate residues at putative DNA nicks has to be guaranteed, as this technique is based on linker ligation to free 5'-phosphate ends. Another approach to assess the role of repair associated factors during active DNA demethylation, might be the identification of possible candidate genes followed by further experiments such as knock-down assays. Genome-wide expression analysis revealed several repair associated genes that are significantly up-regulated during dendritic cell development (Figure 5-13), thus representing potential candidates. Three of those, GADD45a, GADD45b and LIG1, have already been described to be involved in active DNA demethylation. The GADD45 (growth arrest and DNA-damage induced) family proteins were initially identified as stress-inducible factors implicated in cell cycle arrest, DNA repair as well as apoptosis (Fornace, Jr. et al., 1988; Hoffman and Liebermann, 2007) and received increasing interest in the field of DNA demethylation. Several studies propose an important role for GADD45 proteins in linking DNA repair mechanisms with DNA demethylation (Barreto et al., 2007; Ma et al., 2009b; Rai et al., 2008). The ability of Gadd45 to oligomerize may facilitate the coupling of multiple enzymatic steps that are required for BER or NER based DNA demethylation (Ma et al., 2009a). Additionally, Gadd45 proteins are thought to

loosen the chromatin structure and might therefore provide access for demethylating enzymes (Carrier et al., 1999; Ma et al., 2009a). However, especially the *in vivo* implication of Gadd45a is questioned by a study reporting neither global nor locus specific methylation increases in *Gadd45a*-deficient mice (Engel et al., 2009). Similarly, Jin *et al* were unable to confirm an earlier study (Barreto et al., 2007) claiming that Gadd45a has a key role in active DNA demethylation (Jin et al., 2008). The expression profile of *GADD45a* during dendritic cell differentiation potentially supports studies attributing GADD45a a linking role between DNA repair and active demethylation, as *GADD45a* expression is up-regulated during the time frame of active demethylation (Figure 5-13; Figure 5-14). A recently published work argues for a model, in which the TBP (TATA binding protein) associated factor TAF12 recruits GADD45a and the NER machinery to promoters resulting in active DNA demethylation (Schmitz et al., 2009). A general role for TAF12, however, seems unlikely because demethylation events are not limited to promoters (Figure 5-17, Table 5-4), where TAF12 binding is usually detected. Nevertheless, these data further indicate the emerging role of transcription factors for the recruitment of epigenetic modifiers.

Transcription factors are implicated in targeting histone modifying enzymes to their sites of action and may thus additionally recruit demethylating enzymes (Imhof, 2006; Rice et al., 2007; Robert et al., 2004). Nuclear hormone receptors, e.g., represent well documented examples for targeting DNA demethylation (Niehrs, 2009). In order to identify factors that come into consideration for mediating DC specific demethylation, genome-wide expression analysis were performed revealing numerous genes that are highly regulated during dendritic cell development (Figure 5-11). It was questioned whether common recruitment machineries are existent for every demethylated site. A *de novo* motif discovery algorithm was used to identify common sequence motifs within gene promoters that are enriched in the cluster of up- and down-regulated genes. The algorithm revealed three sequence motifs that are significantly enriched within markedly repressed genes. The enriched motifs comprised immunoregulatory sequences that are responsive to interferon stimulation (Figure 5-11B). As IFN $\gamma$  and IL-4 are considered to be mutually counteracting cytokines (Paludan, 1998), the blocking of IFN signalling probably resulted from the IL-4 stimulation at the beginning of cell differentiation. In line with the motif data, gene ontology analysis demonstrated that primarily immune and stress response associated factors were repressed (Figure 5-11C). In contrast, the cluster of highly up-regulated genes did neither exhibit common binding motifs nor clear functional correlations (Figure 5-11B). This suggests that either too many and too distinct factors are involved in their induction, or that common motifs for their regulation might rather be found at enhancer elements. Furthermore, the diversity of functions does not allow any conclusions referring to a regulating role during active DNA demethylation. However, the

slight enrichment of cell cycle factors (Figure 5-11C) might represent a weak link to DNA repair, as several proteins involved in cell cycle progression such as replication and damage checkpoints or polymerases are also implicated in repair processes.

In order to detect the presence of factors that are specifically recruited to a demethylated locus and therefore possibly influence the demethylation event, *in vivo* footprinting of the *CCL13* promoter was performed at various differentiation time points. However, significant differences in transcription factor occupancy between the analysed time points were not detected (data not shown). This might be partly due to the rather long demethylation process (about 24 hours), indicating that demethylation does not occur synchronously in every cell, so that the occupancy of the promoter was below the detection limit of this approach. Chromatin immunoprecipitation (ChIP) experiments are affected by the same limitations. Possible candidate factors recruiting demethylating enzymes or mediating this process presumably occupy the corresponding locus for only a short time frame. As cells were not synchronized, the concentration of factors captured at a certain time point might be below the detection limit. Furthermore, ChIP analyses depend on the availability of well working antibodies. Several candidate factors such as MBD2, TDG or GADD45a were analysed using ChIP but failed to precipitate. Due to the described limitations, it is still open whether those factors are relevant for recruiting or mediating dendritic cell specific DNA demethylation. The detection of a certain DNA binding factor to demethylated loci does not automatically imply its involvement in the demethylating process but may provide a direction for further investigations on active demethylation.

Beside sequence specific transcription factors, histone modifications have been proposed as candidate factors for promoting selective demethylation (Cervoni and Szyf, 2001; Niehrs, 2009). In line with this assumption, the setting of activating histone marks seemed to precede or at least to parallel the active DNA demethylation and possibly prepares the local chromatin for the action of DNA demethylating enzymes (Figure 5-21; Figure 5-22; Figure 5-23). Histone modifications thus represent possible candidates for targeting the demethylation machinery through histone code reading proteins. Irrespective of the genomic localization, all tested demethylated regions shared the presence of activating histone marks such as mono- and dimethylation of H3K4 or acetylation of histones H3 and H4. Given the strict association of CpG demethylation and histone marks, the active DNA demethylation process could be a simple side effect of enzymatic reactions that modify the chromatin structure. E.g. the removal of H3K9me2 methylation can be mediated by the lysine specific demethylase LSD1 through an oxidative process resulting in the production of hydrogen peroxide (Perillo et al., 2008). The main product of the peroxide is 8-oxo-guanine (8-oxo-G) whose accumulation could be inhibited by NAC (N-acetylcysteine), a scavenger of reactive oxygen species. As

8-oxo-G is removed by base excision repair (BER), adjacent 5-MeC might be excised as well and replaced by cytosine, in the course of such an oxidation induced repair pathway. However, such a mechanism would assume at least some randomness in the distribution of demethylation effects. The high reproducibility of demethylation events between various independent donors suggests that the active DNA demethylation mechanism is a strictly targeted process (Figure 5-19) and therefore confutes the argument that active DNA methylation is just a stochastic side effect of other cellular processes. Moreover, the treatment of monocytes with NAC did not result in alterations of the methylation pattern or expression profiles of *CCL13* in differentiating dendritic cells (Table 5-3).

In conclusion, active DNA demethylation during differentiation of dendritic cells may be described as a strictly targeted, highly reproducible process, that is not limited to promoter regions. Only one third of the validated DMRs was detected within promoter regions, whereas the other differentially methylated regions were observed downstream or far upstream the transcription start site. CpG demethylation is accompanied or even preceded by the setting of activating histone marks, leading to a more accessible chromatin structure. A hypothetical view on the chronological order of events at a demethylating locus is given in Figure 6-1. Histone modifying enzymes may be recruited to a specific locus via (sequence specific) DNA binding proteins and alter the chromatin structure. Once the chromatin is more “open”, demethylating enzymes such as components of the DNA repair machineries, can easier access DNA and remove the methyl mark. DNA demethylation leads to further relaxation of chromatin and might be a necessary prerequisite for the stable binding of several transcription factors. As DNA demethylation is not necessarily followed directly by transcriptional induction (Figure 5-20), this process could be important for keeping genes in a primed state by stabilizing the chromatin structure. Priming genes for transcriptional activation guarantees a fast and effective response to an incoming stimulus, as the time consuming process of opening the chromatin has been saved. This model would be in line with several other studies proposing that gene activation occurs sequentially (Bonifer, 2005; Hoogenkamp et al., 2009). Sequence specific DNA binding factors can recruit chromatin modification complexes and thus set the stage for stable complexes that drive transcription (Belikov et al., 2004; Kress et al., 2001; Lin and Hsieh, 2001). However, it remains to be elucidated, whether all factors are capable to transiently interact with their methylated binding sites or, if “pioneer” factors that are able to bind methylated DNA have to act first (Belikov et al., 2004; Bonifer, 2005). Although the chronological order of ongoing events may differ between different studies, transcription factors seem to hold a key role during the dynamic processes of DNA methylation and chromatin remodelling.



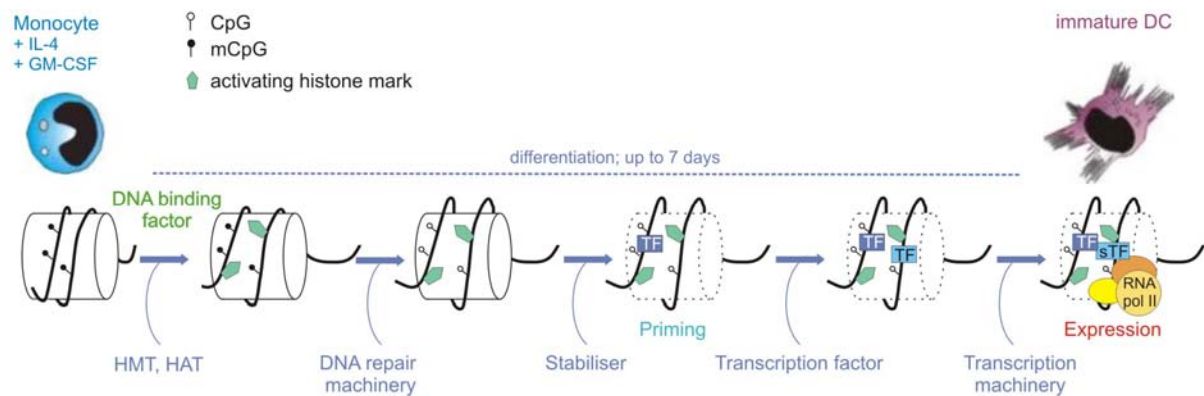


**Figure 6-1 Hypothetical model of successive events accompanying active DNA demethylation during differentiation of dendritic cells**

Monocytes display a compact chromatin structure (white cylinders: histone octamer; black lines with “lollipops”: DNA with CpGs) with methylated cytosine residues (black lollipop). Recruitment of histone acetylases (HAT) and histone methylases (HMT) via DNA binding “pioneer” factors results in the setting of activating histone marks that loosen the chromatin structure. Demethylating enzymes such as components of the DNA repair machinery can now access DNA and remove 5'-methyl cytosines (white lollipops). DNA demethylation results in further relaxation of the chromatin architecture, potentially accompanied by nucleosome loss (indicated by the broken line of the cylinders). The open chromatin structure may now be protected from histone demethylation or histone deacetylation through stabiliser like transcription factors (TF). TFs may either directly induce transcriptional activation or, for the present, just keep the gene in a primed state. Other stimuli like stress signals could then induce the binding of more specific transcription factors (sTF) or accessory factors that induce transcription.

Numerous studies on active DNA demethylation using distinct (mammalian) model systems revealed partly controversial results. It seems that the active demethylation process cannot be reduced to one universal mechanism but is rather operated through different enzymatic reactions adapted to the functional and structural context of the demethylated DNA region. Especially, recruitment actions have to be adjusted to various requirements. Genome-wide demethylation events as observed in mouse primordial germ cells (Hajkova et al., 2008) or in the male pronucleus (Mayer et al., 2000) probably need other recruiting factors than locus specific events. The diversity of involved targeting factors and demethylating enzymes which are adapted to the demands of the corresponding cell system or situation, could explain, why convincing mechanisms of active DNA demethylation are so difficult to define in mammals.

### 6.3 Perspectives

Finally, the mystery about the factors mediating active DNA demethylation, still remains open. Emerging evidence proposes that GADD45-coupled DNA repair mechanisms are adapted to promote the active demethylation of 5-meC. In order to confirm this assumption for the processes occurring in differentiating DCs, siRNA knockdown assays could provide a helpful tool. Considering the transcriptome data (Figure 5-13) in combination with the literature, several candidates such as the *GADD45* genes, DNA polymerases or ligases could be selected systematically and repressed using specific siRNAs. Controlling the methylation pattern of treated versus untreated cells could then give insights into the impact of the corresponding gene in demethylation. However, transfection of monocyte-derived dendritic cells is generally associated with low efficiency and low cell viability (Lenz et al., 2003; Tan et al., 2005). Additionally, differentiating monocytes tend to get activated upon transfection resulting in altered expression profiles, e.g. the rapid down-regulation of *CCL13* (Heinz S., 2002), and incomplete differentiation (Brugger et al., 1991; Stacey et al., 1996). Therefore, before systematic screenings can be applied, an effective transfection assay that avoids dendritic cell activation has to be established. In parallel, it would be interesting to analyse the interaction of DNA binding factors to sites of active demethylation. Adapting the *in vivo* footprinting protocol to our model system – e.g. via more sensitive labelling reactions - may provide insights into the transcription factor occupancy of specific loci. Another possibility to identify factors that target or mediate active demethylation is the adaptation of the present cell model to the murine system. Using knock-out mice such as *Gadd45* deficient ones could help to assess the role of individual genes on active DNA demethylation as well as its association with global gene expression. The identification of DMRs in the murine system would furthermore provide insights into the extent of conserved methylation patterns between humans and mice. However, before such analysis can be performed, it has to be clarified whether differentiation of isolated blood monocytes also occurs without proliferation under similar culture conditions.

Beside the study of the underlying mechanisms mediating active demethylation, the implication of differential methylated regions at promoter distal sites in cell type-specific gene regulation deserves further investigation. The strict association of DNA demethylation and histone marks, that are also found at enhancer elements (Barski et al., 2007; Heintzman et al., 2007) argue for the presence of cis-acting sequences. To identify possible methylation-dependent enhancer activities, transient transfection assays using the novel CpG free pCpGL vector could be useful. Although preliminary experiments using *CCL13*-constructs failed due to the lack of a human DC-like cell line, reporter constructs comprising other gene loci could be more successful.

## 7 Summary

The methylation of CpG dinucleotides represents an epigenetic mark that is crucial for regulating the normal progression of numerous biological processes including development and cell differentiation. During the last decade, it became increasingly clear that methylation patterns are not static but may adapt to various cellular requirements. Regarding normal somatic cells, the dynamic of DNA methylation including its extent throughout the genome as well as its implication in cellular differentiation is largely unknown. In the context of the present thesis, it was demonstrated that several cell type- or cell lineage-specific genes harboured a specific methylation profile. Interestingly, those differences in DNA methylation were mostly confined to regions upstream or downstream of the core promoter and preferentially affected CpG-poor DNA regions. The gene-regulatory relevance of DNA sequences affected by dynamical alterations in the methylation pattern, may be studied by means of transient transfection assays. For this purpose, a novel CpG-free luciferase reporter vector was designed that provides a simple and robust tool for analysing effects of DNA methylation within CpG-poor as well as CpG-rich DNA stretches on gene expression. As particularly the regulated and active removal of methyl-CpG marks still remains controversial, the major aim of the present work was the characterization of this epigenetic phenomenon in a natural setting of post-mitotic cells: the proliferation-independent differentiation of human peripheral blood monocytes into dendritic cells or macrophages, respectively. Using a global, comparative CpG methylation profiling approach that was directed to detect differentially methylated regions in CpG-rich as well as CpG-poor DNA stretches, 45 examples for active demethylation were identified. The validation by a bisulfite conversion-based technique and the characterization of a selected subset revealed that DNA demethylation was not restricted to promoter regions and that the time-course varied for individual CpGs. Irrespective of their location, the removal of methylated cytosines strictly coincided with the appearance of activating histone marks indicating the presence of cis-acting elements. Since demethylation events were highly reproducible between monocyte-derived dendritic cells from distinct donors, the present data suggest that active demethylation is a precisely targeted process. The comparison of the global methylation data with the genome-wide mRNA expression profiles demonstrated that active DNA demethylation is not always directly followed by transcriptional activation. Probably, gene activation is a multilevel process that is dependent on various genetic and epigenetic factors. Thereby, CpG demethylation seems to be a necessary prerequisite for priming the chromatin structure for transcription factor binding.

## Zusammenfassung

Die Methylierung von CpG Dinukleotiden spielt eine entscheidende Rolle bei der Regulierung zahlreicher biologischer Prozesse wie zum Beispiel während der Embryonalentwicklung oder der Differenzierung von Vorläuferzellen. Es wird zunehmend deutlicher, dass DNA-Methylierungsmuster nicht statisch sind, sondern, dass sie sich an verschiedene zelluläre Anforderungen anpassen können. In normalen somatischen Zellen ist jedoch vergleichsweise wenig über die Dynamik von Methylierungsprofilen bekannt. Man weiß weder in welchem Ausmaß solche Veränderungen des Methylierungsstatus auftreten, noch welchen Einfluss diese auf die Differenzierung von gesunden somatischen Zellen haben. Im Rahmen der vorliegenden Dissertation konnte gezeigt werden, dass einige Gene, die in nur einem Zelltyp oder einer Abstammungslinie exprimiert sind, spezifische Methylierungsmuster aufweisen. Interessanterweise waren diese Methylierungsunterschiede hauptsächlich auf CpG-arme Regionen außerhalb von proximalen Promotoren beschränkt. Ob die Regionen, die von dynamischen Methylierungsprofilen betroffen sind, die Genexpression beeinflussen, kann mithilfe von transienten Transfektionsexperimenten geklärt werden. Hierfür wurde ein CpG-freier Luciferase-Reportervektor konstruiert, der eine einfache und zuverlässige Analyse sowohl CpG-armer als auch CpG-reicher DNA-Sequenzen erlaubt.

Da vor allem die regulierte Entfernung der Methylgruppen von Cytosinen noch immer kontrovers diskutiert wird, stand die Charakterisierung dieses epigenetischen Phänomens in einem post-mitotischen Zellsystem (der proliferationsunabhängigen Differenzierung von Monozyten zu Makrophagen beziehungsweise dendritische Zellen) im Mittelpunkt dieser Arbeit. Mittels Methyl-CpG-Immunpräzipitation, die darauf ausgerichtet wurde, global zelltyp-spezifische Methylierungsunterschiede sowohl in CpG-reichen als auch CpG-armen Regionen zu detektieren, wurden 45 Regionen identifiziert, die während der Differenzierung dendritischer Zellen aktiv demethyliert werden. Die Validierung dieser Regionen mit Hilfe von massenspektrometrischen Analysen bisulfit-konvertierter DNA und die Charakterisierung einiger ausgewählter Loci bestätigte, dass DNA Demethylierung nicht nur auf Promotorbereiche beschränkt ist. Des Weiteren konnte gezeigt werden, dass Demethylierungsvorgänge an verschiedenen Loci zwar unterschiedliche Zeitabläufe aufweisen, aber immer mit dem Auftreten von aktivierenden Histonmodifikationen einhergehen. Da aktive Demethylierungsereignisse bei verschiedenen Donoren reproduzierbar nachgewiesen werden konnten, sowohl bezüglich des Zeitfensters als auch der Lokalisation der betroffenen CpGs, handelt es sich hierbei um einen streng zielgerichteten Prozess. Der Vergleich der genomweiten Methylierungsdaten mit globalen mRNA Expressionsprofilen zeigte, dass Demethylierung nicht notwendigerweise mit einer

sofortigen Veränderung der transkriptionellen Aktivität korreliert. Die Aktivierung von Genen scheint eher ein mehrstufiger Prozess zu sein, der von verschiedenen genetischen und epigenetischen Faktoren abhängt. Die aktive Demethylierung ist hierbei vermutlich ein wichtiger Schritt, um die Chromatinstruktur für die Bindung von spezifischen Transkriptionsfaktoren vorzubereiten.

## 8 References

- Abbas, Lichtman, and Pillai (2007). Cellular and molecular immunology.
- Adams,B., Dorfler,P., Aguzzi,A., Kozmik,Z., Urbanek,P., Maurer-Fogy,I., and Busslinger,M. (1992). Pax-5 encodes the transcription factor BSAP and is expressed in B lymphocytes, the developing CNS, and adult testis. *Genes Dev.* 6, 1589-1607.
- Agius,F., Kapoor,A., and Zhu,J.K. (2006). Role of the Arabidopsis DNA glycosylase/lyase ROS1 in active DNA demethylation. *Proc. Natl. Acad. Sci. U. S. A.* 103, 11796-11801.
- Akashi,K. (2005). Lineage promiscuity and plasticity in hematopoietic development. *Ann. N. Y. Acad. Sci.* 1044:125-31., 125-131.
- Andreesen,R., Picht,J., and Lohr,G.W. (1983). Primary cultures of human blood-born macrophages grown on hydrophobic teflon membranes. *J. Immunol. Methods.* 56, 295-304.
- Ballestar,E. and Wolffe,A.P. (2001). Methyl-CpG-binding proteins. Targeting specific gene repression. *Eur. J. Biochem.* 268, 1-6.
- Baron,U., Floess,S., Wieczorek,G., Baumann,K., Grutzkau,A., Dong,J., Thiel,A., Boeld,T.J., Hoffmann,P., Edinger,M., Turbachova,I., Hamann,A., Olek,S., and Huehn,J. (2007). DNA demethylation in the human FOXP3 locus discriminates regulatory T cells from activated FOXP3(+) conventional T cells. *Eur. J. Immunol.* 37, 2378-2389.
- Barreto,G., Schafer,A., Marhold,J., Stach,D., Swaminathan,S.K., Handa,V., Doderlein,G., Maltry,N., Wu,W., Lyko,F., and Niehrs,C. (2007). Gadd45a promotes epigenetic gene activation by repair-mediated DNA demethylation. *Nature.* 445, 671-675.
- Barski,A., Cuddapah,S., Cui,K., Roh,T.Y., Schones,D.E., Wang,Z., Wei,G., Chepelev,I., and Zhao,K. (2007). High-resolution profiling of histone methylations in the human genome. *Cell.* 129, 823-837.
- Belikov,S., Holmqvist,P.H., Astrand,C., and Wrangé,O. (2004). Nuclear factor 1 and octamer transcription factor 1 binding preset the chromatin structure of the mouse mammary tumor virus promoter for hormone induction. *J. Biol. Chem.* 279, 49857-49867.
- Berger,S.L. (2007). The complex language of chromatin regulation during transcription. *Nature.* 447, 407-412.
- Bernstein,B.E., Kamal,M., Lindblad-Toh,K., Bekiranov,S., Bailey,D.K., Huebert,D.J., McMahon,S., Karlsson,E.K., Kulbokas,E.J., III, Gingeras,T.R., Schreiber,S.L., and Lander,E.S. (2005). Genomic maps and comparative analysis of histone modifications in human and mouse. *Cell.* 120, 169-181.
- Bernstein,B.E., Meissner,A., and Lander,E.S. (2007). The mammalian epigenome. *Cell.* 128, 669-681.
- Bernstein,E. and Allis,C.D. (2005). RNA meets chromatin. *Genes Dev.* 19, 1635-1655.
- Bestor,T., Laudano,A., Mattaliano,R., and Ingram,V. (1988). Cloning and sequencing of a cDNA encoding DNA methyltransferase of mouse cells. The carboxyl-terminal domain of the mammalian enzymes is related to bacterial restriction methyltransferases. *J. Mol. Biol.* 203, 971-983.
- Bestor,T.H. (2000). The DNA methyltransferases of mammals. *Hum. Mol. Genet.* 9, 2395-2402.
- Bhattacharya,S.K., Ramchandani,S., Cervoni,N., and Szyf,M. (1999). A mammalian protein with specific demethylase activity for mCpG DNA. *Nature.* 397, 579-583.
- Bird,A. (2002). DNA methylation patterns and epigenetic memory. *Genes Dev.* 16, 6-21.

- Bird,A.P. and Wolffe,A.P. (1999). Methylation-induced repression—belts, braces, and chromatin. *Cell*. **99**, 451-454.
- Bonifer,C. (2005). Epigenetic plasticity of hematopoietic cells. *Cell Cycle*. **4**, 211-214.
- Bonifer,C., Lefevre,P., and Tagoh,H. (2006). The regulation of chromatin and DNA-methylation patterns in blood cell development. *Curr. Top. Microbiol. Immunol.* **310:1-12.**, 1-12.
- Bottardi,S., Ghiam,A.F., Bergeron,F., and Milot,E. (2007). Lineage-specific transcription factors in multipotent hematopoietic progenitors: a little bit goes a long way. *Cell Cycle*. **6**, 1035-1039.
- Boyer,L.A., Plath,K., Zeitlinger,J., Brambrink,T., Medeiros,L.A., Lee,T.I., Levine,S.S., Wernig,M., Tajonar,A., Ray,M.K., Bell,G.W., Otte,A.P., Vidal,M., Gifford,D.K., Young,R.A., and Jaenisch,R. (2006). Polycomb complexes repress developmental regulators in murine embryonic stem cells. *Nature*. **441**, 349-353.
- Brandeis,M., Frank,D., Keshet,I., Siegfried,Z., Mendelsohn,M., Nemes,A., Temper,V., Razin,A., and Cedar,H. (1994). Sp1 elements protect a CpG island from de novo methylation. *Nature*. **371**, 435-438.
- Bretschneider,N., Sara,K., Seifert,M., Reid,G., Gannon,F., and Denger,S. (2008). E2-mediated cathepsin D (CTSD) activation involves looping of distal enhancer elements. *Mol. Oncol.* **2**, 182-190.
- Brugger,W., Reinhardt,D., Galanos,C., and Andreesen,R. (1991). Inhibition of in vitro differentiation of human monocytes to macrophages by lipopolysaccharides (LPS): phenotypic and functional analysis. *Int. Immunol.* **3**, 221-227.
- Brunner,A.L., Johnson,D.S., Kim,S.W., Valouev,A., Reddy,T.E., Neff,N.F., Anton,E., Medina,C., Nguyen,L., Chiao,E., Oyolu,C.B., Schroth,G.P., Absher,D.M., Baker,J.C., and Myers,R.M. (2009). Distinct DNA methylation patterns characterize differentiated human embryonic stem cells and developing human fetal liver. *Genome Res.* **19**, 1044-1056.
- Carrier,F., Georgel,P.T., Pourquier,P., Blake,M., Kontny,H.U., Antinore,M.J., Gariboldi,M., Myers,T.G., Weinstein,J.N., Pommier,Y., and Fornace,A.J., Jr. (1999). Gadd45, a p53-responsive stress protein, modifies DNA accessibility on damaged chromatin. *Mol. Cell Biol.* **19**, 1673-1685.
- Cervoni,N. and Szyf,M. (2001). Demethylase activity is directed by histone acetylation. *J. Biol. Chem.* **276**, 40778-40787.
- Clouaire,T. and Stancheva,I. (2008). Methyl-CpG binding proteins: specialized transcriptional repressors or structural components of chromatin? *Cell Mol. Life Sci.* **65**, 1509-1522.
- Conti,L. and Gessani,S. (2008). GM-CSF in the generation of dendritic cells from human blood monocyte precursors: recent advances. *Immunobiology.* **213**, 859-870.
- Cortazar,D., Kunz,C., Saito,Y., Steinacher,R., and Schar,P. (2007). The enigmatic thymine DNA glycosylase. *DNA Repair (Amst).* **6**, 489-504.
- Costello,J.F., Hong,C., Plass,C., and Smiraglia,D.J. (2009). Restriction landmark genomic scanning: analysis of CpG islands in genomes by 2D gel electrophoresis. *Methods Mol. Biol.* **507:131-48.**, 131-148.
- Costello,J.F. and Plass,C. (2001). Methylation matters. *J. Med. Genet.* **38**, 285-303.
- D'Alessio,A.C., Weaver,I.C., and Szyf,M. (2007). Acetylation-induced transcription is required for active DNA demethylation in methylation-silenced genes. *Mol. Cell Biol.* **27**, 7462-7474.
- Daniel,J.A., Pray-Grant,M.G., and Grant,P.A. (2005). Effector proteins for methylated histones: an expanding family. *Cell Cycle*. **4**, 919-926.

- de Bruin,R.A. and Wittenberg,C. (2009). All eukaryotes: before turning off G1-S transcription, please check your DNA. *Cell Cycle*. **8**, 214-217.
- De Smedt,T., Pajak,B., Muraille,E., Lespagnard,L., Heinen,E., De Baetselier,P., Urbain,J., Leo,O., and Moser,M. (1996). Regulation of dendritic cell numbers and maturation by lipopolysaccharide in vivo. *J. Exp. Med.* **184**, 1413-1424.
- de,I.C., X, Lois,S., Sanchez-Molina,S., and Martinez-Balbas,M.A. (2005). Do protein motifs read the histone code? *Bioessays*. **27**, 164-175.
- Decker,T., Pasca,d.M., McManus,S., Sun,Q., Bonifer,C., Tagoh,H., and Busslinger,M. (2009). Stepwise activation of enhancer and promoter regions of the B cell commitment gene Pax5 in early lymphopoiesis. *Immunity*. **30**, 508-520.
- Detich,N., Bovenzi,V., and Szyf,M. (2003). Valproate induces replication-independent active DNA demethylation. *J. Biol. Chem.* **278**, 27586-27592.
- DiNardo,D.N., Butcher,D.T., Robinson,D.P., Archer,T.K., and Rodenhiser,D.I. (2001). Functional analysis of CpG methylation in the BRCA1 promoter region. *Oncogene*. **20**, 5331-5340.
- Dong,E., Nelson,M., Grayson,D.R., Costa,E., and Guidotti,A. (2008). Clozapine and sulpiride but not haloperidol or olanzapine activate brain DNA demethylation. *Proc. Natl. Acad. Sci. U. S. A.* **105**, 13614-13619.
- Eckhardt,F., Lewin,J., Cortese,R., Rakyan,V.K., Attwood,J., Burger,M., Burton,J., Cox,T.V., Davies,R., Down,T.A., Haefliger,C., Horton,R., Howe,K., Jackson,D.K., Kunde,J., Koenig,C., Liddle,J., Niblett,D., Otto,T., Pettett,R., Seemann,S., Thompson,C., West,T., Rogers,J., Olek,A., Berlin,K., and Beck,S. (2006). DNA methylation profiling of human chromosomes 6, 20 and 22. *Nat. Genet.* **38**, 1378-1385.
- Ehrich,M., Nelson,M.R., Stanssens,P., Zabeau,M., Liloglou,T., Xinarianos,G., Cantor,C.R., Field,J.K., and van den,B.D. (2005). Quantitative high-throughput analysis of DNA methylation patterns by base-specific cleavage and mass spectrometry. *Proc. Natl. Acad. Sci. U. S. A.* **102**, 15785-15790.
- Engel,N., Tront,J.S., Erinle,T., Nguyen,N., Latham,K.E., Sapienza,C., Hoffman,B., and Liebermann,D.A. (2009). Conserved DNA methylation in Gadd45a(-/-) mice. *Epigenetics*. **4**.
- Esteller,M. (2007). Epigenetic gene silencing in cancer: the DNA hypermethylome. *Hum. Mol. Genet.* **16 Spec No 1:R50-9.**, R50-R59.
- Esteller,M., Fraga,M.F., Paz,M.F., Campo,E., Colomer,D., Novo,F.J., Calasanz,M.J., Galm,O., Guo,M., Benitez,J., and Herman,J.G. (2002). Cancer epigenetics and methylation. *Science*. **297**, 1807-1808.
- Fazzari,M.J. and Grealay,J.M. (2004). Epigenomics: beyond CpG islands. *Nat. Rev. Genet.* **5**, 446-455.
- Fischle,W., Wang,Y., and Allis,C.D. (2003). Histone and chromatin cross-talk. *Curr. Opin. Cell Biol.* **15**, 172-183.
- Floess,S., Freyer,J., Siewert,C., Baron,U., Olek,S., Polansky,J., Schlawe,K., Chang,H.D., Bopp,T., Schmitt,E., Klein-Hessling,S., Serfling,E., Hamann,A., and Huehn,J. (2007). Epigenetic control of the foxp3 locus in regulatory T cells. *PLoS. Biol.* **5**, e38.
- Fornace,A.J., Jr., Alamo,I., Jr., and Hollander,M.C. (1988). DNA damage-inducible transcripts in mammalian cells. *Proc. Natl. Acad. Sci. U. S. A.* **85**, 8800-8804.
- Fromme,J.C. and Verdine,G.L. (2004). Base excision repair. *Adv. Protein Chem.* **69:1-41.**, 1-41.
- Frommer,M., McDonald,L.E., Millar,D.S., Collis,C.M., Watt,F., Grigg,G.W., Molloy,P.L., and Paul,C.L. (1992). A genomic sequencing protocol that yields a positive display of 5-methylcytosine residues in individual DNA strands. *Proc. Natl. Acad. Sci. U. S. A.* **89**, 1827-1831.



- Fuks,F. (2005). DNA methylation and histone modifications: teaming up to silence genes. *Curr. Opin. Genet. Dev.* 15, 490-495.
- Fuks,F., Hurd,P.J., Wolf,D., Nan,X., Bird,A.P., and Kouzarides,T. (2003). The methyl-CpG-binding protein MeCP2 links DNA methylation to histone methylation. *J. Biol. Chem.* 278, 4035-4040.
- Gebhard,C., Schwarzfischer,L., Pham,T.H., Andreesen,R., Mackensen,A., and Rehli,M. (2006a). Rapid and sensitive detection of CpG-methylation using methyl-binding (MB)-PCR. *Nucleic Acids Res.* 34, e82.
- Gebhard,C., Schwarzfischer,L., Pham,T.H., Schilling,E., Klug,M., Andreesen,R., and Rehli,M. (2006b). Genome-wide profiling of CpG methylation identifies novel targets of aberrant hypermethylation in myeloid leukemia. *Cancer Res.* 66, 6118-6128.
- Gehring,M., Reik,W., and Henikoff,S. (2009). DNA demethylation by DNA repair. *Trends Genet.* 25, 82-90.
- Georgopoulos,K., Winandy,S., and Avitahl,N. (1997). The role of the Ikaros gene in lymphocyte development and homeostasis. *Annu. Rev. Immunol.* 15:155-76., 155-176.
- Goto,T. and Monk,M. (1998). Regulation of X-chromosome inactivation in development in mice and humans. *Microbiol. Mol. Biol. Rev.* 62, 362-378.
- Graw,R.G., Jr., Herzig,G.P., Eisel,R.J., and Perry,S. (1971). Leukocyte and platelet collection from normal donors with the continuous flow blood cell separator. *Transfusion.* 11, 94-101.
- Guo,M., Akiyama,Y., House,M.G., Hooker,C.M., Heath,E., Gabrielson,E., Yang,S.C., Han,Y., Baylin,S.B., Herman,J.G., and Brock,M.V. (2004). Hypermethylation of the GATA genes in lung cancer. *Clin. Cancer Res.* 10, 7917-7924.
- Guo,Y., Pakneshan,P., Gladu,J., Slack,A., Szyf,M., and Rabbani,S.A. (2002). Regulation of DNA methylation in human breast cancer. Effect on the urokinase-type plasminogen activator gene production and tumor invasion. *J. Biol. Chem.* 277, 41571-41579.
- Hajkova,P., Ancelin,K., Waldmann,T., Lacoste,N., Lange,U.C., Cesari,F., Lee,C., Almouzni,G., Schneider,R., and Surani,M.A. (2008). Chromatin dynamics during epigenetic reprogramming in the mouse germ line. *Nature.* 452, 877-881.
- Hakem,R. (2008). DNA-damage repair; the good, the bad, and the ugly. *EMBO J.* 27, 589-605.
- Hebbar,P.B. and Archer,T.K. (2003). Chromatin remodeling by nuclear receptors. *Chromosoma.* 111, 495-504.
- Hebenstreit,D., Wirnsberger,G., Horejs-Hoeck,J., and Duschl,A. (2006). Signaling mechanisms, interaction partners, and target genes of STAT6. *Cytokine Growth Factor Rev.* 17, 173-188.
- Heintzman,N.D., Stuart,R.K., Hon,G., Fu,Y., Ching,C.W., Hawkins,R.D., Barrera,L.O., Van Calcar,S., Qu,C., Ching,K.A., Wang,W., Weng,Z., Green,R.D., Crawford,G.E., and Ren,B. (2007). Distinct and predictive chromatin signatures of transcriptional promoters and enhancers in the human genome. *Nat. Genet.* 39, 311-318.
- Heinz S. Identification and Characterization of Genes with Specific Expression in Dendritic Cells. 2002. Ref Type: Thesis/Dissertation
- Herman,J.G. and Baylin,S.B. (2003). Gene silencing in cancer in association with promoter hypermethylation. *N. Engl. J. Med.* 349, 2042-2054.
- Hoffman,B. and Liebermann,D.A. (2007). Role of gadd45 in myeloid cells in response to hematopoietic stress. *Blood Cells Mol. Dis.* 39, 344-347.

- Hoffmann,P., Boeld,T.J., Eder,R., Huehn,J., Floess,S., Wieczorek,G., Olek,S., Dietmaier,W., Andreesen,R., and Edinger,M. (2009). Loss of FOXP3 expression in natural human CD4+CD25+ regulatory T cells upon repetitive in vitro stimulation. *Eur. J. Immunol.* **39**, 1088-1097.
- Hoogenkamp,M., Lichtinger,M., Krysinska,H., Lancrin,C., Clarke,D., Williamson,A., Mazzarella,L., Ingram,R., Jorgensen,H., Fisher,A., Tenen,D.G., Kouskoff,V., Lacaud,G., and Bonifer,C. (2009). Early chromatin unfolding by RUNX1 - a molecular explanation for differential requirements during specification versus maintenance of the hematopoietic gene expression program. *Blood*.
- Hubscher,U., Maga,G., and Spadari,S. (2002). Eukaryotic DNA polymerases. *Annu. Rev. Biochem.* **71**:133-63. *Epub*;%2001 Nov 9., 133-163.
- Hume,D.A. (2008). Macrophages as APC and the dendritic cell myth. *J. Immunol.* **181**, 5829-5835.
- Illingworth,R., Kerr,A., Desousa,D., Jorgensen,H., Ellis,P., Stalker,J., Jackson,D., Clee,C., Plumb,R., Rogers,J., Humphray,S., Cox,T., Langford,C., and Bird,A. (2008). A novel CpG island set identifies tissue-specific methylation at developmental gene loci. *PLoS. Biol.* **6**, e22.
- Imhof,A. (2006). Epigenetic regulators and histone modification. *Brief. Funct. Genomic. Proteomic.* **5**, 222-227.
- Ivascu,C., Wasserkort,R., Lesche,R., Dong,J., Stein,H., Thiel,A., and Eckhardt,F. (2007). DNA methylation profiling of transcription factor genes in normal lymphocyte development and lymphomas. *Int. J. Biochem. Cell Biol.* **39**, 1523-1538.
- Jin,S.G., Guo,C., and Pfeifer,G.P. (2008). GADD45A does not promote DNA demethylation. *PLoS. Genet.* **4**, e1000013.
- Johnson,W.D., Jr., Mei,B., and Cohn,Z.A. (1977). The separation, long-term cultivation, and maturation of the human monocyte. *J. Exp. Med.* **146**, 1613-1626.
- Jones,P.L., Veenstra,G.J., Wade,P.A., Vermaak,D., Kass,S.U., Landsberger,N., Strouboulis,J., and Wolffe,A.P. (1998). Methylated DNA and MeCP2 recruit histone deacetylase to repress transcription. *Nat. Genet.* **19**, 187-191.
- Jost,J.P. (1993). Nuclear extracts of chicken embryos promote an active demethylation of DNA by excision repair of 5-methyldeoxycytidine. *Proc. Natl. Acad. Sci. U. S. A.* **90**, 4684-4688.
- Jost,J.P., Siegmann,M., Sun,L., and Leung,R. (1995). Mechanisms of DNA demethylation in chicken embryos. Purification and properties of a 5-methylcytosine-DNA glycosylase. *J. Biol. Chem.* **270**, 9734-9739.
- Kangaspeska,S., Stride,B., Metivier,R., Polycarpou-Schwarz,M., Ibberson,D., Carmouche,R.P., Benes,V., Gannon,F., and Reid,G. (2008). Transient cyclical methylation of promoter DNA. *Nature.* **452**, 112-115.
- Kapoor,A., Agius,F., and Zhu,J.K. (2005). Preventing transcriptional gene silencing by active DNA demethylation. *FEBS Lett.* **579**, 5889-5898.
- Kass,S.U., Pruss,D., and Wolffe,A.P. (1997). How does DNA methylation repress transcription? *Trends Genet.* **13**, 444-449.
- Kawahara,T.L., Michishita,E., Adler,A.S., Damian,M., Berber,E., Lin,M., McCord,R.A., Ongaigui,K.C., Boxer,L.D., Chang,H.Y., and Chua,K.F. (2009). SIRT6 links histone H3 lysine 9 deacetylation to NF-kappaB-dependent gene expression and organismal life span. *Cell.* **136**, 62-74.
- Kersh,E.N., Fitzpatrick,D.R., Murali-Krishna,K., Shires,J., Speck,S.H., Boss,J.M., and Ahmed,R. (2006). Rapid demethylation of the IFN-gamma gene occurs in memory but not naive CD8 T cells. *J. Immunol.* **176**, 4083-4093.

- Keshet,I., Schlesinger,Y., Farkash,S., Rand,E., Hecht,M., Segal,E., Pikarski,E., Young,R.A., Niveleau,A., Cedar,H., and Simon,I. (2006). Evidence for an instructive mechanism of de novo methylation in cancer cells. *Nat. Genet.* **38**, 149-153.
- Kim,H.P. and Leonard,W.J. (2007). CREB/ATF-dependent T cell receptor-induced FoxP3 gene expression: a role for DNA methylation. *J. Exp. Med.* **204**, 1543-1551.
- Kim,T.H., Barrera,L.O., Zheng,M., Qu,C., Singer,M.A., Richmond,T.A., Wu,Y., Green,R.D., and Ren,B. (2005). A high-resolution map of active promoters in the human genome. *Nature.* **436**, 876-880.
- Klose,R.J. and Bird,A.P. (2006). Genomic DNA methylation: the mark and its mediators. *Trends Biochem. Sci.* **31**, 89-97.
- Kornberg,R.D. (1974). Chromatin structure: a repeating unit of histones and DNA. *Science.* **184**, 868-871.
- Kornberg,R.D. and Lorch,Y. (1999). Twenty-five years of the nucleosome, fundamental particle of the eukaryote chromosome. *Cell.* **98**, 285-294.
- Kouzarides,T. (2007). Chromatin modifications and their function. *Cell.* **128**, 693-705.
- Kress,C., Thomassin,H., and Grange,T. (2001). Local DNA demethylation in vertebrates: how could it be performed and targeted? *FEBS Lett.* **494**, 135-140.
- Kress,C., Thomassin,H., and Grange,T. (2006). Active cytosine demethylation triggered by a nuclear receptor involves DNA strand breaks. *Proc. Natl. Acad. Sci. U. S. A.* **103**, 11112-11117.
- Kundakovic,M., Chen,Y., Guidotti,A., and Grayson,D.R. (2009). The reelin and GAD67 promoters are activated by epigenetic drugs that facilitate the disruption of local repressor complexes. *Mol. Pharmacol.* **75**, 342-354.
- Larsson,J. and Karlsson,S. (2005). The role of Smad signaling in hematopoiesis. *Oncogene.* **24**, 5676-5692.
- Lathrop,M.J., Hsu,M., Richardson,C.A., Olivier,E.N., Qiu,C., Bouhassira,E.E., Fiering,S., and Lowrey,C.H. (2009). Developmentally regulated extended domains of DNA hypomethylation encompass highly transcribed genes of the human beta-globin locus. *Exp. Hematol.* **37**, 807-813.
- Lee,D.U., Agarwal,S., and Rao,A. (2002). Th2 lineage commitment and efficient IL-4 production involves extended demethylation of the IL-4 gene. *Immunity.* **16**, 649-660.
- Lee,J.S. and Shilatifard,A. (2007). A site to remember: H3K36 methylation a mark for histone deacetylation. *Mutat. Res.* **618**, 130-134.
- Lee,T.I., Jenner,R.G., Boyer,L.A., Guenther,M.G., Levine,S.S., Kumar,R.M., Chevalier,B., Johnstone,S.E., Cole,M.F., Isono,K., Koseki,H., Fuchikami,T., Abe,K., Murray,H.L., Zucker,J.P., Yuan,B., Bell,G.W., Herbolsheimer,E., Hannett,N.M., Sun,K., Odom,D.T., Otte,A.P., Volkert,T.L., Bartel,D.P., Melton,D.A., Gifford,D.K., Jaenisch,R., and Young,R.A. (2006). Control of developmental regulators by Polycomb in human embryonic stem cells. *Cell.* **125**, 301-313.
- Lenz,P., Bacot,S.M., Frazier-Jessen,M.R., and Feldman,G.M. (2003). Nucleoporation of dendritic cells: efficient gene transfer by electroporation into human monocyte-derived dendritic cells. *FEBS Lett.* **538**, 149-154.
- LeRoy,G., Rickards,B., and Flint,S.J. (2008). The double bromodomain proteins Brd2 and Brd3 couple histone acetylation to transcription. *Mol. Cell.* **30**, 51-60.
- Li,E., Beard,C., and Jaenisch,R. (1993). Role for DNA methylation in genomic imprinting. *Nature.* **366**, 362-365.

- Li,X. and Zhao,X. (2008). Epigenetic regulation of mammalian stem cells. *Stem Cells Dev.* 17, 1043-1052.
- Lin,I.G. and Hsieh,C.L. (2001). Chromosomal DNA demethylation specified by protein binding. *EMBO Rep.* 2, 108-112.
- Liu,K., Victora,G.D., Schwickert,T.A., Guernonprez,P., Meredith,M.M., Yao,K., Chu,F.F., Randolph,G.J., Rudensky,A.Y., and Nussenzweig,M. (2009). In vivo analysis of dendritic cell development and homeostasis. *Science.* 324, 392-397.
- Lomberk,G., Wallrath,L., and Urrutia,R. (2006). The Heterochromatin Protein 1 family. *Genome Biol.* 7, 228.
- Lu,Q. and Richardson,B. (2004). Methods for Analyzing the Role of DNA Methylation and Chromatin Structure in Regulating T Lymphocyte Gene Expression. *Biol. Proced. Online.* 6:189-203. *Epub;2004 Sep 16.*, 189-203.
- Lucarelli,M., Fuso,A., Strom,R., and Scarpa,S. (2001). The dynamics of myogenin site-specific demethylation is strongly correlated with its expression and with muscle differentiation. *J. Biol. Chem.* 276, 7500-7506.
- Lunyak,V.V., Burgess,R., Prefontaine,G.G., Nelson,C., Sze,S.H., Chenoweth,J., Schwartz,P., Pevzner,P.A., Glass,C., Mandel,G., and Rosenfeld,M.G. (2002). Corepressor-dependent silencing of chromosomal regions encoding neuronal genes. *Science.* 298, 1747-1752.
- Ma,D.K., Guo,J.U., Ming,G.L., and Song,H. (2009a). DNA excision repair proteins and Gadd45 as molecular players for active DNA demethylation. *Cell Cycle.* 8, 1526-1531.
- Ma,D.K., Jang,M.H., Guo,J.U., Kitabatake,Y., Chang,M.L., Pow-Anpongkul,N., Flavell,R.A., Lu,B., Ming,G.L., and Song,H. (2009b). Neuronal activity-induced Gadd45b promotes epigenetic DNA demethylation and adult neurogenesis. *Science.* 323, 1074-1077.
- Maxam,A.M. and Gilbert,W. (1980). Sequencing end-labeled DNA with base-specific chemical cleavages. *Methods Enzymol.* 65, 499-560.
- Mayer,W., Niveleau,A., Walter,J., Fundele,R., and Haaf,T. (2000). Demethylation of the zygotic paternal genome. *Nature.* 403, 501-502.
- McKercher,S.R., Torbett,B.E., Anderson,K.L., Henkel,G.W., Vestal,D.J., Baribault,H., Klemsz,M., Feeney,A.J., Wu,G.E., Paige,C.J., and Maki,R.A. (1996). Targeted disruption of the PU.1 gene results in multiple hematopoietic abnormalities. *EMBO J.* 15, 5647-5658.
- Meierhoff,G., Krause,S.W., and Andreesen,R. (1998). Comparative analysis of dendritic cells derived from blood monocytes or CD34+ hematopoietic progenitor cells. *Immunobiology.* 198, 501-513.
- Meissner,A., Mikkelsen,T.S., Gu,H., Wernig,M., Hanna,J., Sivachenko,A., Zhang,X., Bernstein,B.E., Nusbaum,C., Jaffe,D.B., Gnirke,A., Jaenisch,R., and Lander,E.S. (2008). Genome-scale DNA methylation maps of pluripotent and differentiated cells. *Nature.* 454, 766-770.
- Metivier,R., Gallais,R., Tiffoche,C., Le Peron,C., Jurkowska,R.Z., Carmouche,R.P., Ibberson,D., Barath,P., Demay,F., Reid,G., Benes,V., Jeltsch,A., Gannon,F., and Salbert,G. (2008). Cyclical DNA methylation of a transcriptionally active promoter. *Nature.* 452, 45-50.
- Metivier,R., Penot,G., Hubner,M.R., Reid,G., Brand,H., Kos,M., and Gannon,F. (2003). Estrogen receptor-alpha directs ordered, cyclical, and combinatorial recruitment of cofactors on a natural target promoter. *Cell.* 115, 751-763.
- Mohn,F. and Schubeler,D. (2009). Genetics and epigenetics: stability and plasticity during cellular differentiation. *Trends Genet.* 25, 129-136.

- Mohn,F., Weber,M., Schubeler,D., and Roloff,T.C. (2009). Methylated DNA immunoprecipitation (MeDIP). *Methods Mol. Biol.* 507:55-64., 55-64.
- Morales-Ruiz,T., Ortega-Galisteo,A.P., Ponferrada-Marin,M.I., Martinez-Macias,M.I., Ariza,R.R., and Roldan-Arjona,T. (2006). DEMETER and REPRESSOR OF SILENCING 1 encode 5-methylcytosine DNA glycosylases. *Proc. Natl. Acad. Sci. U. S. A.* 103, 6853-6858.
- Mullis,K., Faloona,F., Scharf,S., Saiki,R., Horn,G., and Erlich,H. (1986). Specific enzymatic amplification of DNA in vitro: the polymerase chain reaction. *Cold Spring Harb. Symp. Quant. Biol.* 51 Pt 1:263-73., 263-273.
- Murayama,A., Sakura,K., Nakama,M., Yasuzawa-Tanaka,K., Fujita,E., Tateishi,Y., Wang,Y., Ushijima,T., Baba,T., Shibuya,K., Shibuya,A., Kawabe,Y., and Yanagisawa,J. (2006). A specific CpG site demethylation in the human interleukin 2 gene promoter is an epigenetic memory. *EMBO J.* 25, 1081-1092.
- Nan,X., Ng,H.H., Johnson,C.A., Laherty,C.D., Turner,B.M., Eisenman,R.N., and Bird,A. (1998). Transcriptional repression by the methyl-CpG-binding protein MeCP2 involves a histone deacetylase complex. *Nature.* 393, 386-389.
- Ng,H.H., Zhang,Y., Hendrich,B., Johnson,C.A., Turner,B.M., Erdjument-Bromage,H., Tempst,P., Reinberg,D., and Bird,A. (1999). MBD2 is a transcriptional repressor belonging to the MeCP1 histone deacetylase complex. *Nat. Genet.* 23, 58-61.
- Niehrs,C. (2009). Active DNA demethylation and DNA repair. *Differentiation.* 77, 1-11.
- Okano,M., Bell,D.W., Haber,D.A., and Li,E. (1999). DNA methyltransferases Dnmt3a and Dnmt3b are essential for de novo methylation and mammalian development. *Cell.* 99, 247-257.
- Okano,M., Xie,S., and Li,E. (1998). Cloning and characterization of a family of novel mammalian DNA (cytosine-5) methyltransferases. *Nat. Genet.* 19, 219-220.
- Ooi,S.K. and Bestor,T.H. (2008). The colorful history of active DNA demethylation. *Cell.* 133, 1145-1148.
- Orford,K., Kharchenko,P., Lai,W., Dao,M.C., Worhunsy,D.J., Ferro,A., Janzen,V., Park,P.J., and Scadden,D.T. (2008). Differential H3K4 methylation identifies developmentally poised hematopoietic genes. *Dev. Cell.* 14, 798-809.
- Orkin,S.H. (2000). Diversification of haematopoietic stem cells to specific lineages. *Nat. Rev. Genet.* 1, 57-64.
- Paludan,S.R. (1998). Interleukin-4 and interferon-gamma: the quintessence of a mutual antagonistic relationship. *Scand. J. Immunol.* 48, 459-468.
- Parsons,J.L., Preston,B.D., O'Connor,T.R., and Dianov,G.L. (2007). DNA polymerase delta-dependent repair of DNA single strand breaks containing 3'-end proximal lesions. *Nucleic Acids Res.* 35, 1054-1063.
- Perillo,B., Ombra,M.N., Bertoni,A., Cuzzo,C., Sacchetti,S., Sasso,A., Chiariotti,L., Malorni,A., Abbondanza,C., and Avvedimento,E.V. (2008). DNA oxidation as triggered by H3K9me2 demethylation drives estrogen-induced gene expression. *Science.* 319, 202-206.
- Plass,C. and Soloway,P.D. (2002). DNA methylation, imprinting and cancer. *Eur. J. Hum. Genet.* 10, 6-16.
- Plath,K., Fang,J., Mlynarczyk-Evans,S.K., Cao,R., Worringer,K.A., Wang,H., de la Cruz,C.C., Otte,A.P., Panning,B., and Zhang,Y. (2003). Role of histone H3 lysine 27 methylation in X inactivation. *Science.* 300, 131-135.

- Pokholok,D.K., Harbison,C.T., Levine,S., Cole,M., Hannett,N.M., Lee,T.I., Bell,G.W., Walker,K., Rolfe,P.A., Herbolzheimer,E., Zeitlinger,J., Lewitter,F., Gifford,D.K., and Young,R.A. (2005). Genome-wide map of nucleosome acetylation and methylation in yeast. *Cell*. *122*, 517-527.
- Probst,A.V., Dunleavy,E., and Almouzni,G. (2009). Epigenetic inheritance during the cell cycle. *Nat. Rev. Mol. Cell Biol.* *10*, 192-206.
- Quirion,M.R., Gregory,G.D., Umetsu,S.E., Winandy,S., and Brown,M.A. (2009). Cutting edge: Ikaros is a regulator of Th2 cell differentiation. *J. Immunol.* *182*, 741-745.
- Rai,K., Huggins,I.J., James,S.R., Karpf,A.R., Jones,D.A., and Cairns,B.R. (2008). DNA demethylation in zebrafish involves the coupling of a deaminase, a glycosylase, and gadd45. *Cell*. *135*, 1201-1212.
- Randolph,G.J., Beaulieu,S., Lebecque,S., Steinman,R.M., and Muller,W.A. (1998). Differentiation of monocytes into dendritic cells in a model of transendothelial trafficking. *Science*. *282*, 480-483.
- Rehli,M., Niller,H.H., Ammon,C., Langmann,S., Schwarzfischer,L., Andreesen,R., and Krause,S.W. (2003). Transcriptional regulation of CHI3L1, a marker gene for late stages of macrophage differentiation. *J. Biol. Chem.* *278*, 44058-44067.
- Reiner,S.L. (2005). Epigenetic control in the immune response. *Hum. Mol. Genet.* *14 Spec No 1*:R41-6., R41-R46.
- Ricardo,S.D., van Goor,H., and Eddy,A.A. (2008). Macrophage diversity in renal injury and repair. *J. Clin. Invest.* *118*, 3522-3530.
- Rice,K.L., Hormaeche,I., and Licht,J.D. (2007). Epigenetic regulation of normal and malignant hematopoiesis. *Oncogene*. *26*, 6697-6714.
- Riggs,A., Martienssen,R., and Russo,V. (1996). Epigenetic Mechanisms of Gene Regulation.
- Rinn,J.L., Kertesz,M., Wang,J.K., Squazzo,S.L., Xu,X., Bruggmann,S.A., Goodnough,L.H., Helms,J.A., Farnham,P.J., Segal,E., and Chang,H.Y. (2007). Functional demarcation of active and silent chromatin domains in human HOX loci by noncoding RNAs. *Cell*. *129*, 1311-1323.
- Robert,F., Pokholok,D.K., Hannett,N.M., Rinaldi,N.J., Chandy,M., Rolfe,A., Workman,J.L., Gifford,D.K., and Young,R.A. (2004). Global position and recruitment of HATs and HDACs in the yeast genome. *Mol. Cell*. *16*, 199-209.
- Robertson,K.D. and Wolffe,A.P. (2000). DNA methylation in health and disease. *Nat. Rev. Genet.* *1*, 11-19.
- Roh,T.Y., Cuddapah,S., Cui,K., and Zhao,K. (2006). The genomic landscape of histone modifications in human T cells. *Proc. Natl. Acad. Sci. U. S. A.* *103*, 15782-15787.
- Rouhi,A., Gagnier,L., Takei,F., and Mager,D.L. (2006). Evidence for epigenetic maintenance of Ly49a monoallelic gene expression. *J. Immunol.* *176*, 2991-2999.
- Sallusto,F. and Lanzavecchia,A. (1994). Efficient presentation of soluble antigen by cultured human dendritic cells is maintained by granulocyte/macrophage colony-stimulating factor plus interleukin 4 and downregulated by tumor necrosis factor alpha. *J. Exp. Med.* *179*, 1109-1118.
- Sanderson,R.J., Shepperdson,R.T., Vatter,A.E., and Talmage,D.W. (1977). Isolation and enumeration of peripheral blood monocytes. *J. Immunol.* *118*, 1409-1414.
- Schilling,E. and Rehli,M. (2007). Global, comparative analysis of tissue-specific promoter CpG methylation. *Genomics*. *90*, 314-323.

- Schmidl,C., Klug,M., Boeld,T.J., Andreesen,R., Hoffmann,P., Edinger,M., and Rehli,M. (2009). Lineage-specific DNA methylation in T cells correlates with histone methylation and enhancer activity. *Genome Res.*
- Schmitz,K.M., Schmitt,N., Hoffmann-Rohrer,U., Schafer,A., Grummt,I., and Mayer,C. (2009). TAF12 Recruits Gadd45a and the Nucleotide Excision Repair Complex to the Promoter of rRNA Genes Leading to Active DNA Demethylation. *Mol. Cell.* 33, 344-353.
- Schreiber,S.L. and Bernstein,B.E. (2002). Signaling network model of chromatin. *Cell.* 111, 771-778.
- Schubeler,D., MacAlpine,D.M., Scalzo,D., Wirbelauer,C., Kooperberg,C., van Leeuwen,F., Gottschling,D.E., O'Neill,L.P., Turner,B.M., Delrow,J., Bell,S.P., and Groudine,M. (2004). The histone modification pattern of active genes revealed through genome-wide chromatin analysis of a higher eukaryote. *Genes Dev.* 18, 1263-1271.
- Scott,E.W., Simon,M.C., Anastasi,J., and Singh,H. (1994). Requirement of transcription factor PU.1 in the development of multiple hematopoietic lineages. *Science.* 265, 1573-1577.
- Seta,N. and Kuwana,M. (2007). Human circulating monocytes as multipotential progenitors. *Keio J. Med.* 56, 41-47.
- Sims,R.J., III, Millhouse,S., Chen,C.F., Lewis,B.A., Erdjument-Bromage,H., Tempst,P., Manley,J.L., and Reinberg,D. (2007). Recognition of trimethylated histone H3 lysine 4 facilitates the recruitment of transcription postinitiation factors and pre-mRNA splicing. *Mol. Cell.* 28, 665-676.
- Smiraglia,D.J. and Plass,C. (2002). The study of aberrant methylation in cancer via restriction landmark genomic scanning. *Oncogene.* 21, 5414-5426.
- Song,F., Mahmood,S., Ghosh,S., Liang,P., Smiraglia,D.J., Nagase,H., and Held,W.A. (2009). Tissue specific differentially methylated regions (TDMR): Changes in DNA methylation during development. *Genomics.* 93, 130-139.
- Stacey,K.J., Sweet,M.J., and Hume,D.A. (1996). Macrophages ingest and are activated by bacterial DNA. *J. Immunol.* 157, 2116-2122.
- Steinman,R.M. and Cohn,Z.A. (1973). Identification of a novel cell type in peripheral lymphoid organs of mice. I. Morphology, quantitation, tissue distribution. *J. Exp. Med.* 137, 1142-1162.
- Strahl,B.D. and Allis,C.D. (2000). The language of covalent histone modifications. *Nature.* 403, 41-45.
- Straussman,R., Nejman,D., Roberts,D., Steinfeld,I., Blum,B., Benvenisty,N., Simon,I., Yakhini,Z., and Cedar,H. (2009). Developmental programming of CpG island methylation profiles in the human genome. *Nat. Struct. Mol. Biol.* 16, 564-571.
- Suzuki,M.M. and Bird,A. (2008). DNA methylation landscapes: provocative insights from epigenomics. *Nat. Rev. Genet.* 9, 465-476.
- Swisher,J.F., Rand,E., Cedar,H., and Marie,P.A. (1998). Analysis of putative RNase sensitivity and protease insensitivity of demethylation activity in extracts from rat myoblasts. *Nucleic Acids Res.* 26, 5573-5580.
- Szyf,M. (2009). Epigenetics, DNA methylation, and chromatin modifying drugs. *Annu. Rev. Pharmacol. Toxicol.* 49:243-63., 243-263.
- Tagoh,H., Cockerill,P.N., and Bonifer,C. (2006). In vivo genomic footprinting using LM-PCR methods. *Methods Mol. Biol.* 325:285-314., 285-314.
- Tahiliani,M., Koh,K.P., Shen,Y., Pastor,W.A., Bandukwala,H., Brudno,Y., Agarwal,S., Iyer,L.M., Liu,D.R., Aravind,L., and Rao,A. (2009). Conversion of 5-Methylcytosine to 5-Hydroxymethylcytosine in Mammalian DNA by the MLL Fusion Partner TET1. *Science.*

- Tan, P.H., Beutelspacher, S.C., Wang, Y.H., McClure, M.O., Ritter, M.A., Lombardi, G., and George, A.J. (2005). Immunolipoplexes: an efficient, nonviral alternative for transfection of human dendritic cells with potential for clinical vaccination. *Mol. Ther.* *11*, 790-800.
- Taverna, S.D., Li, H., Ruthenburg, A.J., Allis, C.D., and Patel, D.J. (2007). How chromatin-binding modules interpret histone modifications: lessons from professional pocket pickers. *Nat. Struct. Mol. Biol.* *14*, 1025-1040.
- Urbanek, P., Wang, Z.Q., Fetka, I., Wagner, E.F., and Busslinger, M. (1994). Complete block of early B cell differentiation and altered patterning of the posterior midbrain in mice lacking Pax5/BSAP. *Cell.* *79*, 901-912.
- van Furth, R. and Cohn, Z.A. (1968). The origin and kinetics of mononuclear phagocytes. *J. Exp. Med.* *128*, 415-435.
- Varol, C., Yona, S., and Jung, S. (2009). Origins and tissue-context-dependent fates of blood monocytes. *Immunol. Cell Biol.* *87*, 30-38.
- Wagner, S., Hess, M.A., Ormonde-Hanson, P., Malandro, J., Hu, H., Chen, M., Kehrer, R., Frodsham, M., Schumacher, C., Beluch, M., Honer, C., Skolnick, M., Ballinger, D., and Bowen, B.R. (2000). A broad role for the zinc finger protein ZNF202 in human lipid metabolism. *J. Biol. Chem.* *275*, 15685-15690.
- Walsh, C.P., Chaillet, J.R., and Bestor, T.H. (1998). Transcription of IAP endogenous retroviruses is constrained by cytosine methylation. *Nat. Genet.* *20*, 116-117.
- Wang, Z., Zang, C., Rosenfeld, J.A., Schones, D.E., Barski, A., Cuddapah, S., Cui, K., Roh, T.Y., Peng, W., Zhang, M.Q., and Zhao, K. (2008). Combinatorial patterns of histone acetylations and methylations in the human genome. *Nat. Genet.* *40*, 897-903.
- Weber, M., Davies, J.J., Wittig, D., Oakeley, E.J., Haase, M., Lam, W.L., and Schubeler, D. (2005). Chromosome-wide and promoter-specific analyses identify sites of differential DNA methylation in normal and transformed human cells. *Nat. Genet.* *37*, 853-862.
- Weber, M., Hellmann, I., Stadler, M.B., Ramos, L., Paabo, S., Rebhan, M., and Schubeler, D. (2007). Distribution, silencing potential and evolutionary impact of promoter DNA methylation in the human genome. *Nat. Genet.* *39*, 457-466.
- Wei, K., Clark, A.B., Wong, E., Kane, M.F., Mazur, D.J., Parris, T., Kolas, N.K., Russell, R., Hou, H., Jr., Kneitz, B., Yang, G., Kunkel, T.A., Kolodner, R.D., Cohen, P.E., and Edelman, W. (2003). Inactivation of Exonuclease 1 in mice results in DNA mismatch repair defects, increased cancer susceptibility, and male and female sterility. *Genes Dev.* *17*, 603-614.
- Weiss, A., Keshet, I., Razin, A., and Cedar, H. (1996). DNA demethylation in vitro: involvement of RNA. *Cell.* *86*, 709-718.
- Weissmann, F. and Lyko, F. (2003). Cooperative interactions between epigenetic modifications and their function in the regulation of chromosome architecture. *Bioessays.* *25*, 792-797.
- Yagi, S., Hirabayashi, K., Sato, S., Li, W., Takahashi, Y., Hirakawa, T., Wu, G., Hattori, N., Hattori, N., Ohgane, J., Tanaka, S., Liu, X.S., and Shiohara, K. (2008). DNA methylation profile of tissue-dependent and differentially methylated regions (T-DMRs) in mouse promoter regions demonstrating tissue-specific gene expression. *Genome Res.* *18*, 1969-1978.
- Yoder, J.A., Soman, N.S., Verdine, G.L., and Bestor, T.H. (1997). DNA (cytosine-5)-methyltransferases in mouse cells and tissues. Studies with a mechanism-based probe. *J. Mol. Biol.* *270*, 385-395.
- Yu, L., Liu, C., Vandeusen, J., Becknell, B., Dai, Z., Wu, Y.Z., Raval, A., Liu, T.H., Ding, W., Mao, C., Liu, S., Smith, L.T., Lee, S., Rassenti, L., Marcucci, G., Byrd, J., Caligiuri, M.A., and Plass, C. (2005). Global assessment of promoter methylation in a mouse model of cancer identifies ID4 as a putative tumor-suppressor gene in human leukemia. *Nat. Genet.* *37*, 265-274.



Zhu,B., Zheng,Y., Hess,D., Angliker,H., Schwarz,S., Siegmann,M., Thiry,S., and Jost,J.P. (2000). 5-methylcytosine-DNA glycosylase activity is present in a cloned G/T mismatch DNA glycosylase associated with the chicken embryo DNA demethylation complex. *Proc. Natl. Acad. Sci. U. S. A.* 97, 5135-5139.

Zhu,J. and Emerson,S.G. (2002). Hematopoietic cytokines, transcription factors and lineage commitment. *Oncogene.* 21, 3295-3313.

## 9 Abbreviations

5meC	5-methyl Cytosine
APC	Antigen Presenting Cell
bp	base pair
BER	Base excision repair
BM	Bone marrow
BSA	Bovine Serum Albumine
cDNA	complementary DNA
CGI	CpG island
ChIP	Chromatin immunoprecipitation
CpG	Cytosine-Guanine dinucleotide
DC	Dendritic Cell
Dd	Double Distilled
DEPC	Diethyl Pyrocarbonate
DMEM	Dulbecco's Modified Eagle Medium
DMR	Differential Methylated Region
DMS	Dimethyl sulfate
DMSO	Dimethyl Sulfoxide
DNMT	DNA methyl transferase
dNTP	deoxy-Nucleotide Triphosphate
ECL	Enhanced Chemiluminescence
EDTA	Ethylenediaminetetraacetic Acid
ES cell	Embryonic stem cell
EtOH	Ethanol
FACS	Fluorescence activated cell sorting
FCS	Fetal Calf Serum
FITC	Flourescein isothiocyanate
HSC	Hematopoietic stem cell
GM-CSF	Granulocyte-Macrophage Colony Stimulating Factor
H3K4me1	Histone 3 Lysine 4 monomethylation
H3K4me2	Histone 3 Lysine 4 dimethylation
H3K4me3	Histone 3 Lysine 4 trimethylation
HAT	Histone acetyl-Transferase
HDAC	Histone Deacetylase
HMT	Histone methyl-Transferase
iDC	immature Dendritic Cell
IL	Interleukin
LB	Luria Bertani

LM-PCR	Ligation mediated polymerase chain reaction
LPS	Lipopolysaccharid
MAC	Macrophage
MALDI-TOF MS	Matrix-assisted Laser Desorption/ionization Time-of-Flight Mass spectrometry
MBD	Methyl-CpG-Binding-Domain
MCIp	methyl-CpG Immunoprecipitation
MO	Monocyte
MOPS	3-(N-Morpholino) Propanesulfonic acid
MPS	Mononuclear Phagocyte System
mRNA	messenger RNA
MvA	Signal log ratio vs. average log intensity
NaOAc	Sodium Acetate
NER	Nucleotide excision repair
NK cell	Natural killer cell
NP-40	Nonidet P-40
O/N	Over night
PB-MNCs	Peripheral Blood Mononuclear Cells
PBS	Phosphate Buffered Saline
PE	Phycoerythrin
PEG	Polyethyleneglycol
PCR	polymerase chain reaction
qPCR	quantitative PCR
rpm	rounds per minute
RT	Room Temperature
RT-qPCR	quantitative reverse transcription PCR
SDS	Sodium Dodecyl Sulfate
TAE	Tris Acetate /EDTA electrophoresis buffer
TE	Tris-EDTA
TEMED	N,N,N',N',-Tetramethylenediamine
TNF	Tumor Necrosis Factor
Treg	regulatory T Cell
TSS	Trasncription Start Site
UCSC	University of California, Santa Cruz

## Publications

### **Lineage-specific DNA methylation in T cells correlates with histone methylation and enhancer activity**

Schmidl C, Klug M, Boeld TJ, Andreesen R, Hoffmann P, Edinger M, Rehli M  
Genome Res. 2009 Jul;19(7):1165-74. Epub 2009 Jun 3.

### **Functional analysis of promoter CpG methylation using a CpG-free luciferase reporter vector**

Klug M, Rehli M  
Epigenetics. 2006 Jul-Sep;1(3):127-30. Epub 2006 Aug 28

### **Dap12 expression in activated microglia from retinoschisin-deficient retina and its PU.1-dependent promoter regulation**

Weigelt K, Ernst W, Walczak Y, Ebert S, Loenhardt T, Klug M, Rehli M, Weber BH, Langmann T.  
J Leukoc Biol. 2007 Dec;82(6):1564-74. Epub 2007 Sep 7

### **CCAAT enhancer-binding protein beta regulates constitutive gene expression during late stages of monocyte to macrophage differentiation**

Pham TH, Langmann S, Schwarzfischer L, EL Chartouni C, Lichtinger M, Klug M, Krause SW, Rehli M  
J Biol Chem. 2007 Jul 27;282(30):21924-33. Epub 2007 May 31

### **Genome-wide profiling of CpG methylation identifies novel targets of aberrant hypermethylation in myeloid leukemia**

Gebhard C, Schwarzfischer L, Pham TH, Schilling E, Klug M, Andreesen R, Rehli M  
Cancer Res. 2006 Jun 15;66(12):6118-28

## Eidesstattliche Erklärung

Ich erkläre hiermit an Eides statt, dass ich die vorliegende Arbeit ohne unzulässige Hilfe Dritter und ohne Benutzung anderer als der angegebenen Hilfsmittel angefertigt habe. Die aus anderen Quellen direkt oder indirekt übernommenen Daten und Konzepte sind unter Angabe des Literaturzitats gekennzeichnet.

Weitere Personen waren an der inhaltlich-materiellen Herstellung der vorliegenden Arbeit nicht beteiligt. Insbesondere habe ich hierfür nicht die entgeltliche Hilfe eines Promotionsberaters oder anderer Personen in Anspruch genommen. Niemand hat von mir weder unmittelbar noch mittelbar geldwerte Leistungen für Arbeiten erhalten, die in Zusammenhang mit dem Inhalt der vorgelegten Dissertation stehen.

Die Arbeit wurde bisher weder im In- noch Ausland in gleicher oder ähnlicher Form einer anderen Prüfungsbehörde vorgelegt.

-----  
-----  
(Maja Klug)



## Vielen, vielen Dank an...

... **Prof. Dr. Reinhard Andreesen** für die Chance, meine Doktorarbeit in seiner Abteilung durchführen zu dürfen, für eine sehr angenehme Atmosphäre in der Abteilung und für richtig schöne Weihnachtsfeiern, Betriebsausflüge und die Retreats in Hirschberg.

... **Prof. Dr. Herbert Tschochner** für die Bereitschaft, diese Arbeit zu betreuen und zu begutachten, für sein Interesse an meinem Thema sowie das sehr gute Klima in seinem Team.

... **PD Dr. Michael Rehli** für das Thema und die Betreuung meiner Arbeit, für die Möglichkeit, sehr viel lernen zu können, für seine einzigartige Geduld und seine Fähigkeit, Ruhe zu verbreiten, sowie für die Unterstützung beim Schokoladen-Vernichtungskommando und den 5-kg-Ritter-Sport-Vorrat.

... **Claudia**, mein Judo-Ass und treues Mitglied der « Schoki-for-ever » Fraktion, für ihre Hilfsbereitschaft zu jeder Tages- und Nachtzeit und inspirierende Kongressbesuche. Ohne Dich hätte ich so Manches nicht geschafft!

 „...and you're singing this song, thinking this is the life...“ 

... **Lucia**, die Perle der AG-Rehli, für ihre uneingeschränkte, tatkräftige Unterstützung und das Beherbergen unserer Schokorationen.

... **Dagmar** für ihren tollen Einsatz, **Carol**, mi guapa soporte especialmente en el curso español, für grandiose Sushi-Abende und für das Word-PDF-Notfall-Management, **Hang**, für geniale Frühlingsrollen, **Moni** für ihre beruhigende Aura, **Tobi** für einmalige, John-Travolta-gleiche Tanzeinlagen, **Chris** für ausgefallene Milchschnittenvariationen, **Sabine** für ihre Hilfe und an **Eddy** für die Kaffeepausenbereitschaft zu jeder Zeit.

... **Ireen** und **Julia**: schön, dass Ihr jetzt auch zu unserer AG gehört.

... die Carreras-Crew, mit **Prof. Marina Kreutz**, **Ute**, **Eva**, **Monika**, **Kaste**, **Martina**, **Sandra**, **Gabi**, **Alice**, **Alexandra** und **Katrin** für ihre Hilfe, den wissenschaftlichen Input sowie für viele schöne und lustige Momente und eine Notfall-Schokoschublade.

...die **AG Edinger/Hoffmann** - besonders an **Rüdiger**- für die Cell Sorting Experimente bis spät in die Nacht hinein und die passenden Schauergeschichten im Nebel.

...**Kristina** und **Julia** für den Seelenbeistand, Hallo-wach-Kaffees, Frustrationsgetränke und die Trostsokolade sowie to **Altug** for the funny late-night-shows at McDonalds.

... **Juliane** für ihre Organisationsbereitschaft und ein Wiedersehen mit Jordan Catalano, **Kristin** für ihr liebes und lustiges Wesen, **Jochen**, **Steffen** und **Al** für spaßige Stunden im Praktikum, **Anna**, meine Leidensgenossin in der Endphase, für den Versuch, die Ungerechtigkeiten dieser Welt zu bekämpfen, **Andi** für seine Monozyten und an **alle anderen Bewohner des House of the Ribosome** für Kaffee, Kuchen, Bier, Pizza und Wodka-Martinis.

... **Annina**, meine treue Wegbegleiterin durch 9 Jahre voller Hochs und Tiefs, für extravagante Glühweinabende und die „Pension Seitz“. Gut, dass Du Dich für Regensburg entschieden hast.

... **Frank**, für seine unbeschreibliche Geduld, für Diskussionen über die Wertung der Biologie gegenüber der Physik und für die Fähigkeit, mich vieles aus einem anderen Blickwinkel und damit lockerer sehen zu lassen. Danke, dass Du mich in den letzten 3 Monaten ertragen hast!

... **meine Eltern**, für das Ertragen meiner Launen, fürs Zuhören und Aufbauen, dafür, dass sie an mich geglaubt haben, immer für mich da sind und für einen Ort, an den ich immer wieder zurückkommen kann, sowie an **meinen Lieblings-Bruder** für die stetige Erinnerung an den Verbleib seiner Steuergelder und dafür, dass er mich immer wieder auch in stressigen Situationen zum Lachen bringen kann.